Documentation of the Santa Clara Valley Regional Ground-Water/Surface-Water Flow Model, Santa Clara County, California

By R.T. Hanson, Zhen Li, and C.C. Faunt

In cooperation with the
Santa Clara Valley Water District

Scientific Investigations Report 2004-5231

U.S. Department of the Interior
U.S. Geological Survey

U.S. Department of the Interior
Gale A. Norton, Secretary

U.S. Geological Survey
Charles G. Groat, Director

U.S. Geological Survey, Reston, Virginia: 2004
For sale by U.S. Geological Survey, Information Services
Box 25286, Denver Federal Center
Denver, CO 80225-0286

For more information about the USGS and its products:
Telephone: 1-888-ASK-USGS
World Wide Web: http://www.usgs.gov/

Suggested citation:
Hanson, R.T., Li, Zhen, and Faunt, C.C., 2004, Documentation of the Santa Clara Valley regional ground-water/surface-water flow model, Santa Clara County, California: U.S. Geological Survey Scientific Investigations Report 2004–5231, 75 p.

Contents

Figures

Animations

Tables

Conversion Factors, Vertical Datum, and Abbreviations

CONVERSION FACTORS

Multiply	By	To obtain
acre	0.4047	hectometer
acre-foot (acre-ft)	0.001233	cubic hectometer
acre-foot per year (acre-ft/yr)	0.001233	cubic hectometer per year
foot (ft)	0.3048	meter
cubic foot per second (ft^3/s)	0.02832	cubic meter per second
square foot per day (ft^2/d)	0.09290	square meter per day
inch (in.)	25.4	millimeter
mile (mi)	1.609	kilometer
square mile (mi^2)	2.590	square kilometer
pound	0.4545	kilogram

Temperature in degrees Celsius (^oC) may be converted to degrees Fahrenheit (^oF) as follows:

$$^oF=1.8\ ^oC+32.$$

VERTICAL DATUM

Sea level: In this report, "sea level" refers to the National Geodetic Vertical Datum of 1929 (NGVD of 1929)—a geodetic datum *derived* from a general adjustment of the first-order level nets of both the United States and Canada, formerly called Sea Level Datum of 1929.

ABBREVIATIONS

CCOC	Coyote Creek Outdoor Classroom (site)
cm	centimeter
ET	evapotranspiration
ft bls	feet below land surface
g/cm^3	grams per cubic centimeter
GHB	general-head boundary
HFB	Horizontal Flow Barrier (package)
HK	horizontal hydraulic conductivity
IBS	Interbed Storage (package)
InSAR	interferometric synthetic aperture radar
K	hydraulic conductivity
km/s	kilometers per second
$km-g/s-cm^3$	kilometers-grams per second-centimeter cubed
LPF	Layer-Property Flow (package)
m	meter

MF2K	MODFLOW-2000
MNW	Multi-Node Well (package)
PDO	Pacific Decadal Oscillation
RMS	root-mean-square
SCVM	Santa Clara Valley model
STPK	Santana Park (site)
STR	Streamflow Routing (package)
VK	vertical hydraulic conductivity

Organizations

CDWR	California Department of Water Resources
SCVWD	Santa Clara Valley Water District
USGS	U.S. Geological Survey

Well-Numbering System

Wells are identified and numbered according to their location in the rectangular system for the subdivision of public lands. Identification consists of the township number, north or south; the range number, east or west; and the section number. Each section is divided into sixteen 40-acre tracts lettered consecutively (except I and O), beginning with “A” in the northeast corner of the section and progressing in a sinusoidal manner to “R” in the southeast corner. Within the 40-acre tract, wells are sequentially numbered in the order they are inventoried. The final letter refers to the base line and meridian. In California, there are three base lines and meridians; Humboldt (H), Mount Diablo (M), and San Bernardino (S). All wells in the study area are referenced to the Mount Diablo base line and meridian (M). Well numbers consist of 16 characters and follow the format 007S001E016C008M. In this report, well numbers are abbreviated and written 7S/1E-16C8. Wells in the same township and range are referred to only by their section designation, 16C8. The following diagram shows how the number for well 7S/1E-16C8 is derived.

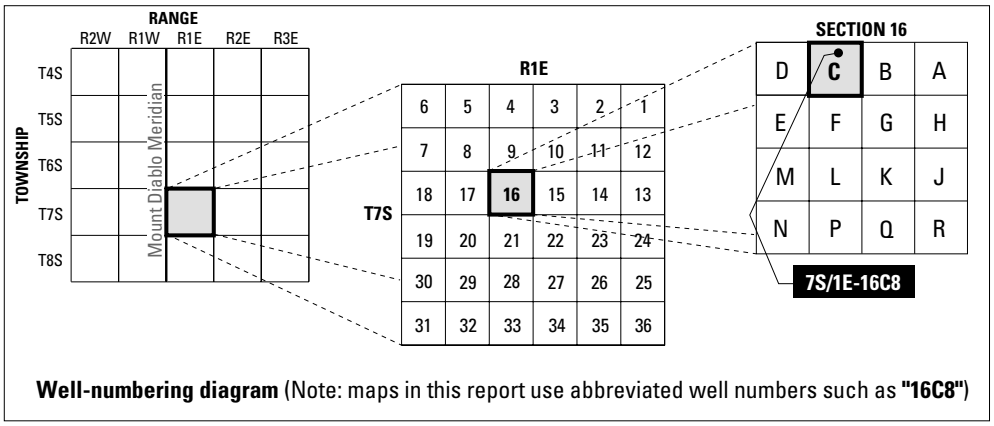

Well-numbering diagram (Note: maps in this report use abbreviated well numbers such as **"16C8"**)

Documentation of the Santa Clara Valley Regional Ground-Water/Surface-Water Flow Model, Santa Clara County, California

By R.T. Hanson, Zhen Li, and C.C. Faunt

Abstract

The Santa Clara Valley is a long, narrow trough extending about 35 miles southeast from the southern end of San Francisco Bay where the regional alluvial-aquifer system has been a major source of water. Intensive agricultural and urban development throughout the 20th century and related ground-water development resulted in ground-water-level declines of more than 200 feet and land subsidence of as much as 12.7 feet between the early 1900s and the mid-1960s. Since the 1960s, Santa Clara Valley Water District has imported surface water to meet growing demands and reduce dependence on ground-water supplies. This importation of water has resulted in a sustained recovery of the ground-water flow system. To help support effective management of the ground-water resources, a regional ground-water/surface-water flow model was developed. This model simulates the flow of ground water and surface water, changes in ground-water storage, and related effects such as land subsidence.

A numerical ground-water/surface-water flow model of the Santa Clara Valley subbasin of the Santa Clara Valley was developed as part of a cooperative investigation with the Santa Clara Valley Water District. The model better defines the geohydrologic framework of the regional flow system and better delineates the supply and demand components that affect the inflows to and outflows from the regional ground-water flow system. Development of the model includes revisions to the previous ground-water flow model that upgraded the temporal and spatial discretization, added source-specific inflows and outflows, simulated additional flow features such as land subsidence and multi-aquifer wellbore flow, and extended the period of simulation through September 1999. The transient-state model was calibrated to historical surface-water and ground-water data for the period 1970–99 and to historical subsidence for the period 1983–99.

The regional ground-water flow system consists of multiple aquifers that are grouped into upper- and lower-aquifer systems. Ground-water inflow occurs as natural recharge in the form of streamflow infiltration and areal infiltration of precipitation along stream channels, artificial recharge from infiltration of imported water at recharge ponds and along selected stream channels, and leakage along selected transmission pipelines. Ground-water outflow occurs as evapotranspiration, stream base flow, discharge through pumpage from wells, and subsurface flow to the San Francisco Bay.

The geohydrologic framework of the regional ground-water flow system was represented as six model layers. The hydraulic properties were redefined on the basis of cell-based lithologic properties that were delineated in terms of aggregate thicknesses of coarse-grained, fine-grained, and mixed textural categories. The regional aquifer systems also are dissected by several laterally extensive faults that may form at least partial barriers to the lateral flow of ground water. The spatial extent of the ground-water flow model was extended and refined to cover the entire Santa Clara Valley, including the Evergreen subregion. The temporal discretization was refined and the period of simulation was extended to 1970–99.

The model was upgraded to MODFLOW-2000 (MF2K) and was calibrated to fit historical ground-water levels, streamflow, and land subsidence for the period 1970–99. The revised model slightly overestimates measured water levels with an root-mean-square error of −7.34 feet. The streamflow generally shows a good match on gaged creeks and rivers for flows greater than 1.2 cubic feet per second. The revised model also fits the measured deformation at the borehole extensometer site located near San Jose within 16 to 27 percent and the extensometer site near Sunnyvale within 3 percent of the maximum measured seasonal deformation for the deepest extensometers.

The total ground-water inflow and outflow of about 225,500 acre-feet per year (acre-ft/yr) for the period 1970–89 and of about 205,300 acre-feet per year for the period 1970–99 is comparable with that of the previous model, 207,200 acre-ft/yr for the period 1970–89. Overall the simulated net change in storage increased by about 189,500 acre-ft/yr for the entire period of simulation, which represents about one and a half years of the 1970–99 average pumping. The changes in ground-water flow and storage generally reflect the major climate cycles and the additional importation of water by Santa Clara Valley Water District, with the basin in recovery since the drought of the late 1980s and early 1990s. The average total recharge rate, from natural and artificial recharge and from streamflow infiltration for the revised model for the entire simulation period 1970–99, was about 157,100 acre-ft/yr, which represents about 59 percent of the inflow to the ground-water flow system. The average rate of artificial recharge of about 77,600 acre-ft/yr represents about 30 percent of the inflow to the ground-water flow system. The average pumpage for the entire 29.75-year simulation period is about 133,400 acre-ft/yr and represents about 69 percent of the outflow from the ground-water flow system. Most of the simulated recharge infiltrates and flows through the uppermost layers (i.e. model layers 1 and 3) of the aquifer system. Most of the water that flows to the deeper model layers is occurring through wellbores, with wellbore flow representing 19 percent of the total ground-water inflow between model layers.

Introduction

The Santa Clara Valley is a long narrow trough extending about 35 mi southeast from the southern end of San Francisco Bay (fig. 1). In the first half of the 20th century, the valley was intensively cultivated for fruit and truck crops. Subsequent development has included urbanization and industrialization, and the area is now commonly known as “Silicon Valley.” The area underwent extensive ground-water development from the early 1900s through the mid 1960s. This development caused ground-water-level declines of more than 200 ft and induced regional subsidence of as much as 12.7 ft from the early 1900s to the mid-1960s (Poland, 1971; Poland and Ireland, 1988). As with other coastal aquifer systems, the possibility exists for the combined effects of land subsidence and seawater intrusion with large water-level declines (Tolman and Poland, 1940; Iwamura, 1980). The San Francisco Water Department started delivering imported water to several north county cities in the early 1950s. In the 1960s the Santa Clara Valley Water District (SCVWD) began importing surface water into the valley to help meet growing demands for water and to reduce the area's dependence on ground water. Imported water is treated and delivered to ponds used to artificially recharge the aquifer system. The combination of reduced ground-water pumpage and artificial recharge has caused ground-water levels to recover to near their predevelopment levels and this, in turn, has arrested the land subsidence in the area. Currently, the water purveyors in the Santa Clara Valley, in conjunction with SCVWD, would like to meet the water demand in the basin, while limiting any potential for additional land subsidence. A detailed ground-water/surface-water model is needed to assess successful management strategies that will minimize land subsidence while maximizing a reliable water supply to meet growing demands from water users.

To protect the quantity and quality of the ground-water supplies and reduce the adverse effects of subsidence, the SCVWD already operates a comprehensive water-management program. The program includes artificial recharge, an in-lieu replacement program in which imported water is provided to pumpers to supplant ground-water use, and promotion of conservation techniques.

In order to evaluate how these activities can be conducted most effectively, it is necessary to compile and collect data to describe the geohydrologic and geochemical framework of the Santa Clara Valley, develop appropriate modeling tools to help understand the ground-water system, and provide a tool for evaluating alternative management strategies.

Purpose and Scope

The purpose of this study was to acquire a better understanding of the hydrogeologic system in the Santa Clara Valley and to develop a tool to help analyze the changes in storage and the potential problems affecting water-resources management for this coastal aquifer system. The study included development of a ground-water/surface-water flow model that simulates the historical development for the period 1970–99 and related tools to help analyze simulation results. The purpose of this report is to describe the components of the regional ground-water/surface-water flow model that was constructed by the U.S. Geological Survey (USGS) in cooperation with the Santa Clara Valley Water District.

Approach

The regional model of ground-water/surface-water flow that simulates the hydrologic system was developed to help SCVWD evaluate the natural and human-induced controls on the regional water resources (fig. 1). This study revises and updates the Santa Clara Valley Model (SCVM) from the previous ground-water flow model (CH2M Hill, 1991) by incorporating new knowledge gained from recent studies, new hydrologic data, and new simulation techniques.

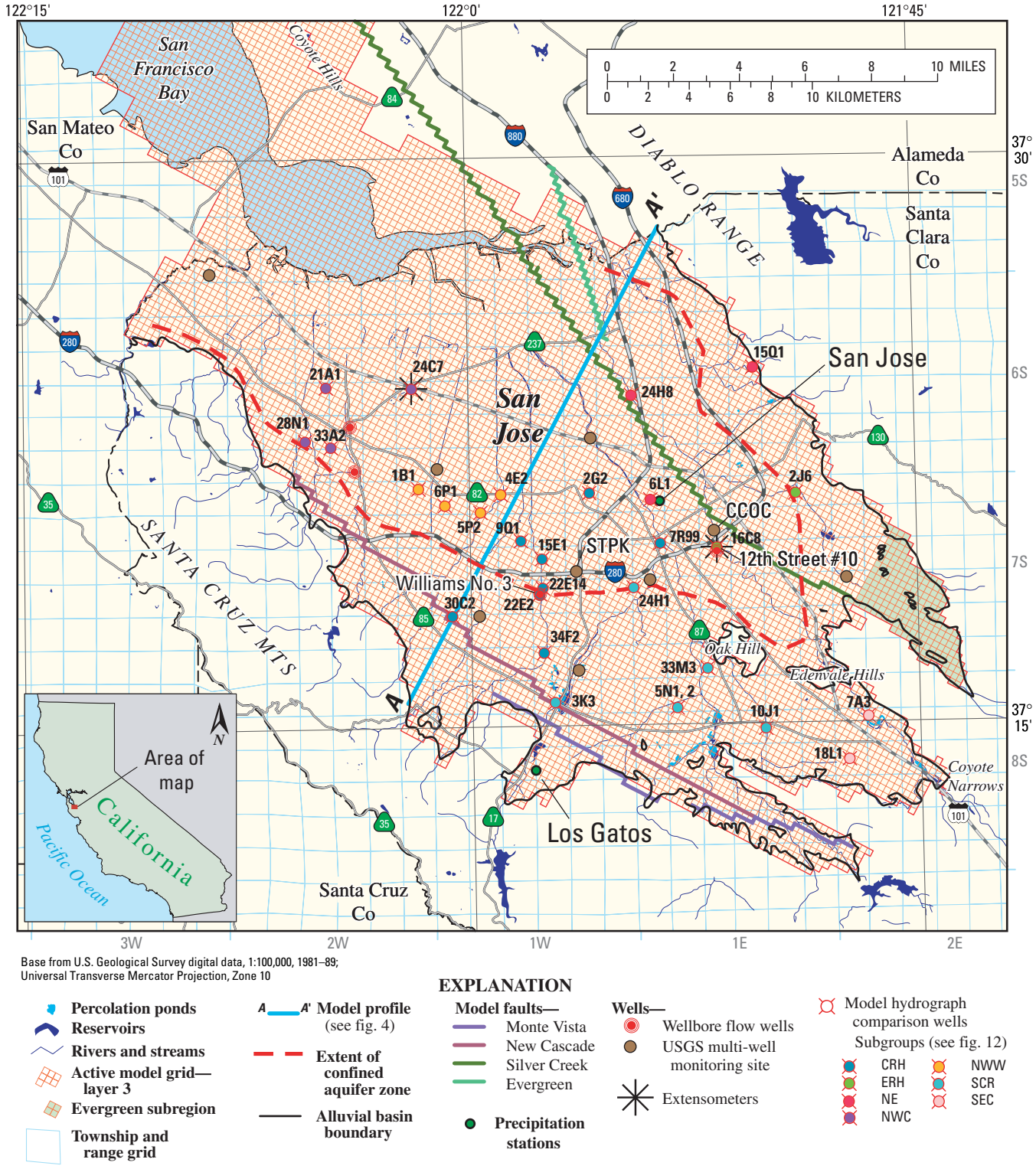

Figure 1. Santa Clara Valley model area and model grid and selected water-level and compaction comparison sites, Santa Clara Valley, California.

The previous model represented a compilation of previous hydrologic studies of the basin (California Department of Water Resources, 1967; Johnson and Dreiss, 1989; Iwamura, 1995) and databases (Majumdar and others, 1977; CH2M Hill, 1992a; Jaimes, 1998). The revised SCVM modifies the previous model with improved simulation techniques, and includes information derived from additional and subsequent studies of the ground-water resources (Muir and Coplen, 1981; Wilson, 1993; Metzger, 2002) and the geohydrologic framework (Poland and Ireland, 1988; Koltermann and Gorelick, 1992; Leighton and others, 1994; Fio and Leighton, 1995).

A major revision to the modeling technique was the separation and re-estimation of major inflow and outflow components, which were combined in the previous model. In addition, several new model packages explicitly account for subsidence, streamflow routing, faults as horizontal flow barriers, multi-aquifer well pumpage for separation of intraborehole flow from interlayer flow, and inflow and outflow with general-head boundaries at the coastal boundary along the San Francisco Bay. The previous regional model (CH2M Hill, 1991) simulated a six-layer regional aquifer system within the Santa Clara Valley subbasin of the Santa Clara Valley (herein simply referred to as the Santa Clara Valley) with an areal extent of about 23 mi long and 14 mi wide (fig. 1). The previous model simulated ground-water flow for the period 1970–89 with constant-head boundaries at the inflow and outflow locations; a composite net-recharge composed of artificial recharge, natural areal and streamflow infiltration, transmission-pipe losses, and potential evapotranspiration; and a fixed vertical distribution of ground-water pumpage that spanned up to four layers for multi-aquifer wells.

All hydraulic properties were transformed from zone-based estimates to lithologic cell-based estimates. The ground-water model used for simulation was upgraded from MODFLOW-88 (McDonald and Harbaugh, 1988) to MF2K (Harbaugh and McDonald, 1996; Harbaugh and others, 2000b). The revised model simulates artificial recharge plus transmission-line losses, natural areal recharge, streamflow routing and infiltration, and evapotranspiration separately. In addition, the constant-head boundaries were replaced with general-head boundaries at the Bay, and the simulation of subsidence, faults as horizontal-flow boundaries, and multi-aquifer well pumpage were added to the model. Finally, seasonal stress periods were reduced to monthly periods and the simulation period was extended to 1999. The spatial discretization was revised to a uniform grid of 1,000-ft^2 cells, and the areal extent of the model was expanded to include the Evergreen subarea in the southeastern part of Santa Clara Valley. These features allow the exploration of conjunctive-use and related ground-water development/replenishment strategies that affect the management of the water resources by SCVWD and better facilitate the evaluation of water-resources with respect to subsidence, recharge, and sustainability.

Description of Study Area

The Santa Clara Valley is a 240-mi^2 coastal watershed that borders the southern San Francisco Bay and principally drains parts of Santa Clara and San Mateo Counties (fig. 1). Most of the basin is characterized by gently sloping topography of coalescing alluvial fans that combine to form the valley floor and coastal tidal lowlands.

The onshore ground-water basin is bounded by the Santa Cruz Mountains on the west, the Diablo Range and the Coyote Hills to the northeast, and small hills such as Oak Hill, and the Edenvale Hills to the southeast near Coyote Narrows (fig. 1). Mountain peaks in the Santa Cruz Mountains on the west exceed 2,600 ft in altitude, and peaks in the Diablo Range on the east exceed 4,200 ft. The sloping offshore plain and underlying aquifers extend beneath the Bay. However, the location of the northwest boundary and the extent of the ground-water basin offshore beneath the Bay and its connection with adjacent areas such as the Niles Cone or Fremont ground-water areas remains uncertain. In general, ground-water flow in the Santa Clara Valley can be characterized as a convergent regional flow system within a basin bounded by mountains and hills on three sides. Recharge to the ground-water flow system starts along the mountain fronts and flows toward the center of the basin and toward the southern San Francisco Bay. Much of the predevelopment flow paths has been modified by pumping centers characterized by groups of wells that have resulted in subregional cones of depression and related flow paths. Discharge from the ground-water flow system occurs as pumpage, underflow, base flow to streams, and evapotranspiration.

The Santa Clara Valley is a regional ground-water basin that has been divided into two onshore subregions that represent the confined and unconfined parts of the aquifer systems (fig. 1). The basin contains extensive alluvial-aquifer systems that are bounded by faults and bedrock mountains (fig. 1). The area has undergone extensive ground-water development in the shallow upper aquifers (locally referred to as the "upper aquifers"), which are composed of Recent, Holocene-age, and Pleistocene-age fluvial deposits and marine estuarine deposits (locally referred to as the "Bay Mud" and "Old Bay Mud") (fig. 2). Extensive ground-water development also has occurred below these deposits in the Pleistocene and Pliocene-age fluvial deposits that are locally referred to as the "lower aquifers" (fig. 2). The alluvial deposits that form the regional aquifer systems are unconformably underlain by Pliocene-age deposits of the Santa Clara Formation, Tertiary-age sediments that include the Miocene-age parts of the Monterey Formation, and Tertiary-age serpentinites (fig. 2). These underlying deposits form the relatively impermeable base of the regional aquifer systems. The alluvial aquifer systems are composed of a complex sequence of layers of fluvial sand and gravel and fluvial fine-grained silt and clay (California Department of Water Resources, 1967; Wagner and others, 1990; Wentworth, 1993, 1997; Wentworth and others, 1998; Knudsen and others, 2000).

The surface-water system in the Santa Clara Valley includes the natural streamflow network, seven reservoirs, and a system of aqueducts, pipelines, and storm drains. The major streams discharge directly to the San Francisco Bay through the tidal lowlands along the southern end of San Francisco Bay. Other creeks, such as San Francisquito Creek that forms the northwestern boundary of the Santa Clara Valley Water District, drain directly into the San Francisco Bay. The reservoirs discharge directly into several of the major tributaries and creeks. The aqueducts and pipelines are used to transport imported water directly to treatment plants where the water is treated and then delivered to artificial-recharge facilities. The storm-drain channels drain additional runoff from the valley floor to the San Francisco Bay.

Climate

The climate of the basin is mediterranean and 89 percent of the rainfall occurs between November and April, which is typical of the California coastal areas. Average annual precipitation is about 14.5 in. at the City of San Jose (1883–2002), about 23 in. near Los Gatos (1964–2001) in the intermediate altitudes of the Santa Clara Valley, and more than 50 in. in the surrounding mountains (fig. 3). The average daily mean temperature ranges from 27.9°C (82.2°F) in San Jose during the middle of summer to below freezing in the bordering mountains during the winter.

The climate is seasonally variable and has been variable throughout the period of record in the past century. The cumulative departure rainfall at San Jose, during the past century indicates a persistent set of multi-year wet and dry periods—some that are relatively long (10 to 21 years) and some periods that are shorter (2 to 9 years) (fig. 3). These wet and dry periods also are related to major droughts and floods (California History Center, 1981). Although wet years may occur in dry periods and dry years in wet periods, the historical climate (fig. 3) generally can be categorized into six climate cycles that represent 13 wet and dry periods that were determined from the cumulative departure of annual precipitation at San Jose as:

Cycle	Wet	Dry
1	—	1874–87
2	1888–96	1897–1903
3	1904–16	1917–36
3	1937–44	1945–65
4	1966–75	1976–77
5	1978–83	1984–91
6	1992–98	1999–2002

Land and Water Use

Prior to the 1900s, most land in the Santa Clara Valley was used for grazing cattle and dry-land farming. In the early 1900s, agriculture was the chief economic activity. As in most coastal basins in California, urbanization since the late 1940s resulted in the transfer of agricultural lands to residential and commercial uses. Since 1915 the population of the valley has grown from less than 100,000 to more than 1.7 million in 2000, with a 12.4 percent increase between 1990 and 2000 in Santa Clara County (U.S. Census Bureau, 2003). Water use has changed from predominantly agricultural prior to the 1960s to almost completely urban and industrial water use since the mid-1960s. About 12.7 ft of land subsidence and more than 200 ft of ground-water-level decline occurred from ground-water development from the early 1900s to the mid-1960s. To mitigate the effects of ground-water depletion, surface water was imported for direct use starting in the 1950s and for artificial recharge in the mid-1960s. Owing to the proximity to the San Francisco metropolitan area and the continued growth of the technology industries, growth may continue with an expanding urban and industrial economy. An excellent summary of the early development of water resources in Santa Clara County is given by the California History Center (1981).

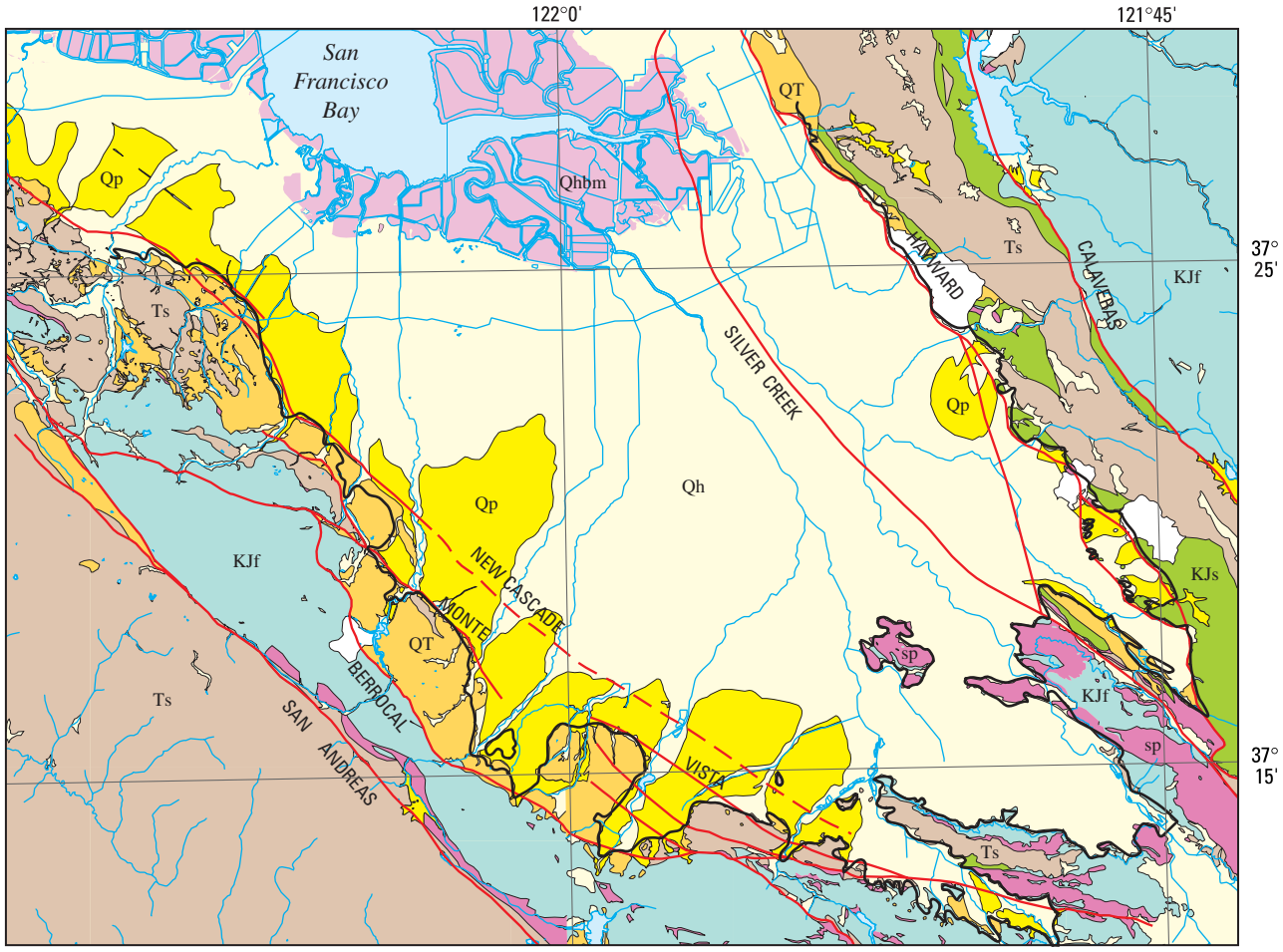

Figure 2. Geologic outcrops, major structural features, and depth to bedrock estimated from gravity for the Santa Clara Valley, California.

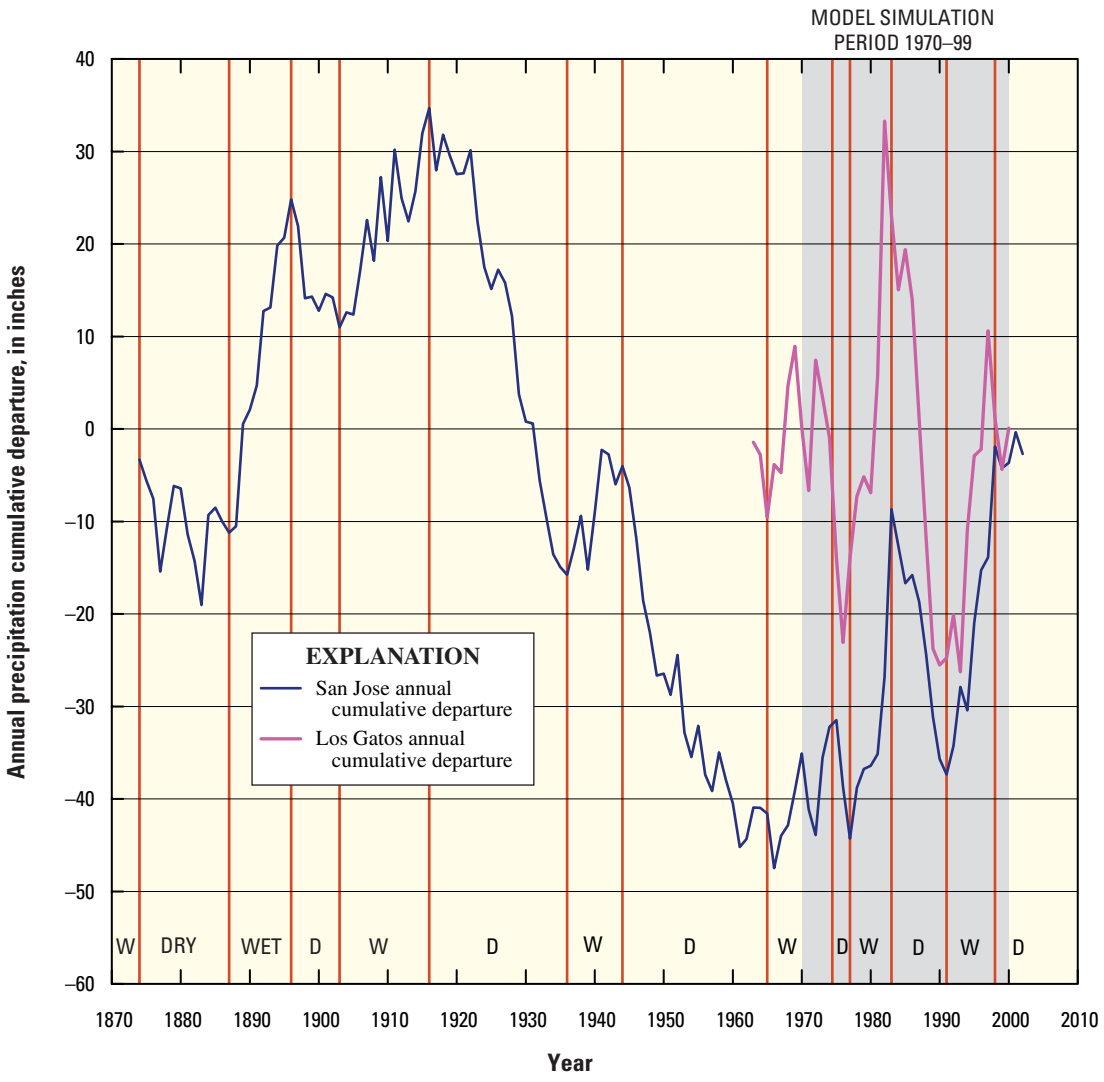

Figure 3. Cumulative departure for precipitation at San Jose and Los Gatos, California.

Acknowledgments

This study could not have been accomplished without the assistance of personnel from the Santa Clara Valley Water District. In particular Mark Merritt, Vanessa Reymers, Roger Pierno, and Bezhad Ahmadi are especially acknowledged for assistance with compilation of data needed to assemble the ground-water/surface-water flow model. We thank USGS hydrologists Keith Halford for his major contributions to the multi-node well package, Steve Predmore for his contribution to ARC-GIS algorithms for creating the streamflow network for MODFLOW, and Peter Martin for his technical guidance. In addition, we acknowledge the valuable guidance of USGS geologists/geophysicists Carl Wentworth and Bob Jachens for their contribution to characterizing the basin stratigraphy and structure.

Conceptual Model

Regional ground-water flow within the multiple aquifers of the Santa Clara Valley is the result of natural and artificial inflows and outflows. Ground water flows from the edges of the elliptical basin along the mountain fronts, where a combination of natural and artificial recharge enters the aquifers, to the pumping centers in the central part of the basin and to the Bay as underflow.

Ground-water inflow occurs as recharge, subsurface flow along the northern coastal boundary of the southern San Francisco Bay, and water derived from aquifer and interbed storage. Ground-water recharge includes areally distributed infiltration of precipitation in excess of runoff and evaporation, streamflow infiltration, artificial recharge, and losses from water-transmission lines. Ground-water outflow occurs as evapotranspiration, stream base flow, discharge through pumpage from wells, and subsurface flow to the San Francisco Bay.

Geohydrologic Framework

For the purposes of the regional flow model, the regional ground-water flow systems are subdivided into upper-aquifer and lower-aquifer systems. The upper-aquifer system is composed of the Shallow aquifer, which is coincident with Holocene-age deposits, and the mid to late Pleistocene-age deposits. The upper-aquifer system contains some water that recently (less than 50 years before present) entered the ground-water system as recharge and some water that has entered the system as much as 2,500 years before present (Hanson and others, 2002a). The lower aquifer system is composed of sediments of early Pleistocene or Pliocene age and contains water that entered the ground-water system more than 10,000 years before present (Hanson and others, 2002a). The presence of the Santa Clara Formation in the alluvial deposits of the Santa Clara Valley remains uncertain. The Santa Clara Formation was not initially identified in many deeper wells (Tolman and Poland, 1940) and has not been encountered in the recently completed multi-well monitoring sites completed by the USGS in cooperation with SCVWD. Therefore, the depth of the alluvial aquifer system and the depth of the effective ground-water flow system remain uncertain in some parts of the valley. The further delineation of the sequence stratigraphy and related hydrostratigraphy is part of ongoing USGS studies (Jachens and others, 2001). The regional aquifer system is underlain and surrounded by the relatively impermeable bedrock.

The ground-water flow system also is affected by the presence of faults that may potentially act as hydrologic flow barriers and by lithofacies that may represent regions of enhanced or reduced permeability. The faults identified as part of this study include the Silver Creek and Evergreen Faults in the eastern part of the valley and the Monte Vista and New Cascade Faults in the western part of the valley. In addition to these features, coarse-grained facies subparallel to and beneath selected stream channels potentially provide enhanced permeability, and fine-grained facies beneath other selected stream channels reduce permeability.

Simulation of Ground-Water Flow

A numerical ground-water flow model of the two regional aquifer systems in the Santa Clara Valley was developed to simulate transient conditions for the historical period of January 1970–September 1999. Model simulations provide a means to determine hydrologic conditions and aquifer response to changes in inflow and outflow through time over several climate cycles. Simulations were made using the three-dimensional finite-difference ground-water flow model, MODFLOW-2000 (MF2K) (Harbaugh and others, 2000a, b). Additional packages were used in conjunction with the ground-water flow model to simulate the routing of streamflow (Prudic, 1989), land subsidence (Leake and Prudic, 1991), faults as horizontal barriers to ground-water flow (Hsieh and Freckleton, 1993), multi-aquifer (multi-node) wells (Halford and Hanson, 2002), and estimation of hydrologic time-series for ground-water levels, streamflow, and deformation (Hanson and Leake, 1998).

The revised Santa Clara Valley model (SCVM) was calibrated with transient simulation that spans 30 years (1970–99), over a period of systematic hydrologic data collection including reported pumpage. The steady-state simulation was not included because initial heads were used from the previous model, which was calibrated to a mean initial condition that generally represents those in 1970 on the basis of measured 1970 water levels (CH2M Hill, 1992b). Calibration of the SCVM included matching ground-water levels, streamflow, aquifer-system deformation, and selected wellbore flow during 1970–99. The SCVM separates the supply components (recharge and intrawellbore flow to the aquifers) and demand components (pumpage, changes in storage, stream base flow, evapotranspiration, and potential outflow at the Bay). This model structure facilitates the analysis and assessment of water-resources management alternatives and related changes in storage. The model also facilitates the analysis of the effect that implementation of selected alternatives and geologic controls might have on recharge, coastal landward flow (seawater intrusion), land subsidence, ground-water movement, and overall resource management under climatically varying conditions that affect supply and demand.

Model Framework

The SCVM is an extension and refinement of the previously developed regional models and local one-dimensional deformation models. The orientation, areal extent, spatial and temporal discretization, model boundaries, and zonation of hydraulic properties constitute the framework of the numerical ground-water flow model developed for this study.

Previous Models

The first models of the Santa Clara Valley divided the system into three model layers: an uppermost unconfined, a middle confining, and a lower confined layer (California Department of Water Resources, 1975; Reichard and Bredehoeft, 1984). The previous regional model (CH2M Hill, 1991) simulated a six-layer regional aquifer system that was similar in structure, with an upper unconfined layer, a middle confining layer and a lower confined system that is split into four layers; the lowest layer is below the depth of most historical ground-water pumping (figs. 1, 4). The previous model covered the entire Santa Clara Valley except for the Evergreen subregion and had variable grid spacing with the smallest cells of 1,000 by 1,000 ft located near San Jose (CH2M Hill, 1991). This previous regional model simulated ground-water flow using MODFLOW-88 (McDonald and Harbaugh, 1988) for the period 1970–89.

The simulation of subsidence was previously investigated (Reichard and Bredehoeft, 1984; Poland and Ireland, 1988; Wilson, 1993) and was assessed by SCVWD at selected well sites throughout the basin by the use of separate one-dimensional deformation models (Helm, 1975, 1977, 1978; Poland and Ireland, 1988) that used water-level time-series derived from the regional ground-water flow model to drive the simulation of one-dimensional deformation. This previous approach to the simulation of ground-water/surface-water flow and subsidence decoupled the processes and did not allow for the interchange of mass flow. Combining the simulations in one regional model couples ground water released from or taken into storage related to aquifer-system deformation (i.e. compression as elastic deformation and compaction as inelastic deformation) and ground-water flow.

Spatial Discretization

The model grid of the SCVM is identical to the previous models (CH2M Hill, 1991), covers the entire alluvial aquifer system of the Santa Clara Valley, including the Evergreen subregion, and extends offshore into the southern San Francisco Bay in the northwest corner of all layers (fig. 1). The orientation of N 27.8°W and extent of the model grid was retained from the previous model (CH2M Hill, 1991). The SCVM contains a uniform grid with a cell size of 1,000 by 1,000 ft for a total of 106 rows and 172 columns (fig. 1). In a manner similar to that of the previous model (CH2M Hill, 1991), the SCVM contains six layers (fig. 4), five for the upper-aquifer system and one for the lower-aquifer system. The six model layers differ in areal extent throughout the model domain and the largest areal extent is in model layer 3 (fig. 4). The top of the upper layer was realigned with the land surface throughout the upper layer (layer 1) and portions of layer 3 where the upper two layers are inactive. The bottom of the uppermost layer and the tops of the other five layers are coincident with the layer boundaries estimated for the previous model, except for the Evergreen subregion. These model-layer boundaries were generally aligned with the predominant altitudes of screened intervals in the water-supply wells. The bottom of the lowest layer remains relatively uncertain, but it is generally coincident with the bottom of the Pliocene-Pleistocene alluvial deposits throughout most of the model area. In some areas the bottom of the lowest layer is coincident with relatively impermeable bedrock.

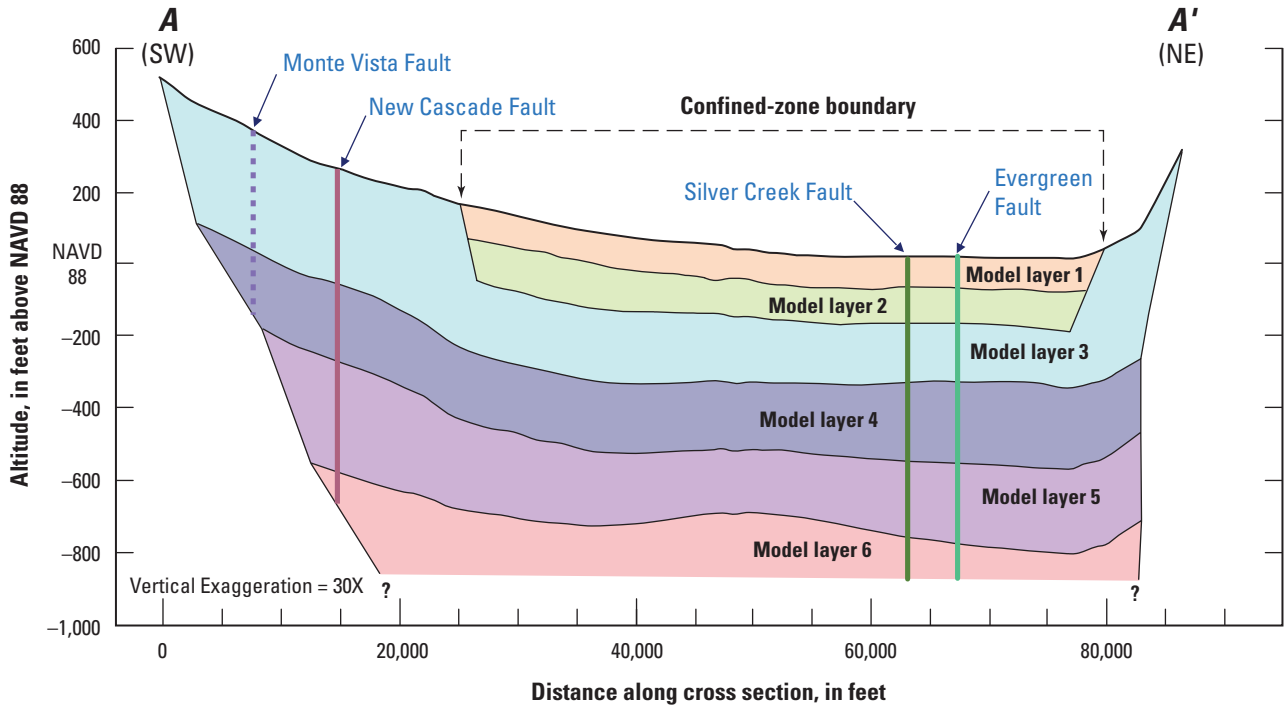

Figure 4. Extent of model layers of the previous regional model (CH2M Hill, 1991) and the revised model.

The upper part of the upper-aquifer system represented by model layer 1 is composed of the Shallow aquifer consisting of Holocene-age and late-Pleistocene-age deposits and has an areal extent of about 122 mi^2. The second layer represents the group of fine-grained deposits that includes the "Bay Mud" and "Old-Bay Mud" and is coincident in areal extent with layer 1. The upper-aquifer system has its largest areal extent in model layer 3 (fig. 1) with an active flow region of about 323 mi^2, of which about 30 percent is offshore. The lower parts of the upper-aquifer system are represented by model layers 4 and 5 and have an active flow region of 258 mi^2 and 240 mi^2, respectively; about 30 per cent of layer 4 and 32 percent of layer 5 are offshore. The lower-aquifer system is represented by model layer 6, which has an active flow region of 213 mi^2, 36 percent of which is offshore.

Temporal Discretization

The previous model simulated the historical period using a 14-year calibration period, 1970–83, and a six-year "verification" period, 1984–89. Trial-and-error calibration was achieved through adjustments to inflows, outflows, and hydraulic properties to match selected ground-water-level hydrographs at selected wells (locations shown in fig. 1). The temporal discretization of the previous model was seasonal stress periods using variable time steps (CH2M Hill, 1991). Therefore, all specified inflows and outflows such as recharge and pumpage were held constant, using average values for periods of three months. In the SCVM the stress periods were reduced to monthly periods and weekly time steps. The monthly time periods are short enough to maintain some degree of separation in the variability present in ground-water pumpage, natural recharge, and artificial recharge, and are long enough to encompass the recession periods of most streamflow events.

Model Boundaries

The perimeter of the active flow region within the revised model represents the approximate limit of the ground-water flow system. The outer boundary is represented by a combination of no-flow, specified flow, and head-dependent boundaries (fig.5). The landward model cells along the outer boundary of all active cells in all model layers are represented as a no-flow boundary. No-flow boundaries occur where there is no flow of water between the active flow-region model cells and the adjacent areas. The bottom of the lower layer is also represented as a no-flow boundary and is coincident with older consolidated deposits of Tertiary age or bedrock comprising the Great Valley Sequence, the ophiolite sequence, or the Franciscan Formation of Mesozoic age (Stanley and others, 2002). These no-flow boundaries represent the contact with non-water-bearing rocks. The runoff from the surrounding mountain fronts results in ungaged streamflow that forms recharge that enters along stream channels in the uppermost layer that is treated as specified inflows and is described later in this section. Evapotranspiration is treated as a sink and is a head-dependent boundary along all of the major stream channels (fig. 5) and is discussed later in this section of the report.

The offshore boundary in all layers is represented as a source-sink boundary that has been located at the northwestern edge of the model grid and represents coastal flow or underflow using water-bearing units that continue beneath San Francisco Bay (California Department of Water Resources, 1967). This boundary is represented in the model as a general-head boundary that simulates an inflow (source) of water from outside the model area or a discharge (sink) of water from the boundary model cells to outside the model area. The offshore boundary is described later in this report in the "Coastal Flow" section.

Hydraulic Properties

The intrinsic hydraulic properties for the aquifers used in the revised model include horizontal and vertical hydraulic conductivity and specific storage (fig. 6). Average values of hydraulic properties are assigned at the center of each cell. Estimates of hydraulic properties are based, in part, on cell-by-cell estimates of fractions of thickness for beds predominantly composed of coarse-grained, fine-grained, or mixed deposits. The product of these fractions and a base value (table 1) result in cell-by-cell hydraulic property values. The fractional thicknesses are referred to as multiplier values (fig.6). All layers have different cell-by-cell multiplier values except layer 2 which had constant hydraulic properties (fig. 6). These cell-based estimates were derived from hundreds of indexed lithologies from drillers' and geologists' logs (Leighton and others, 1994, fig. 3). The lithologies were grouped in four major categories representing incompressible fine-grained, compressible fine-grained, mixed, and coarse-grained deposits. The thicknesses for each category were summed at each well and linearly interpolated to each cell within the equivalent depth intervals of the model layers as defined from the previous model. This approach is similar to that used in previous model studies that have used textural facies to distribute regional estimates of hydraulic properties (Zimmerman and others, 1991; Hanson and others, 2002a). The relation of textural properties to sedimentary facies was previously demonstrated for the Santa Clara Valley by numerous researchers (Koltermann and Gorelick, 1992; Fio and Leighton, 1995; Johnson, 1995a, b; Johnson and Dreiss, 1999) and represents a reasonable basis for estimating spatially distributed hydraulic properties.

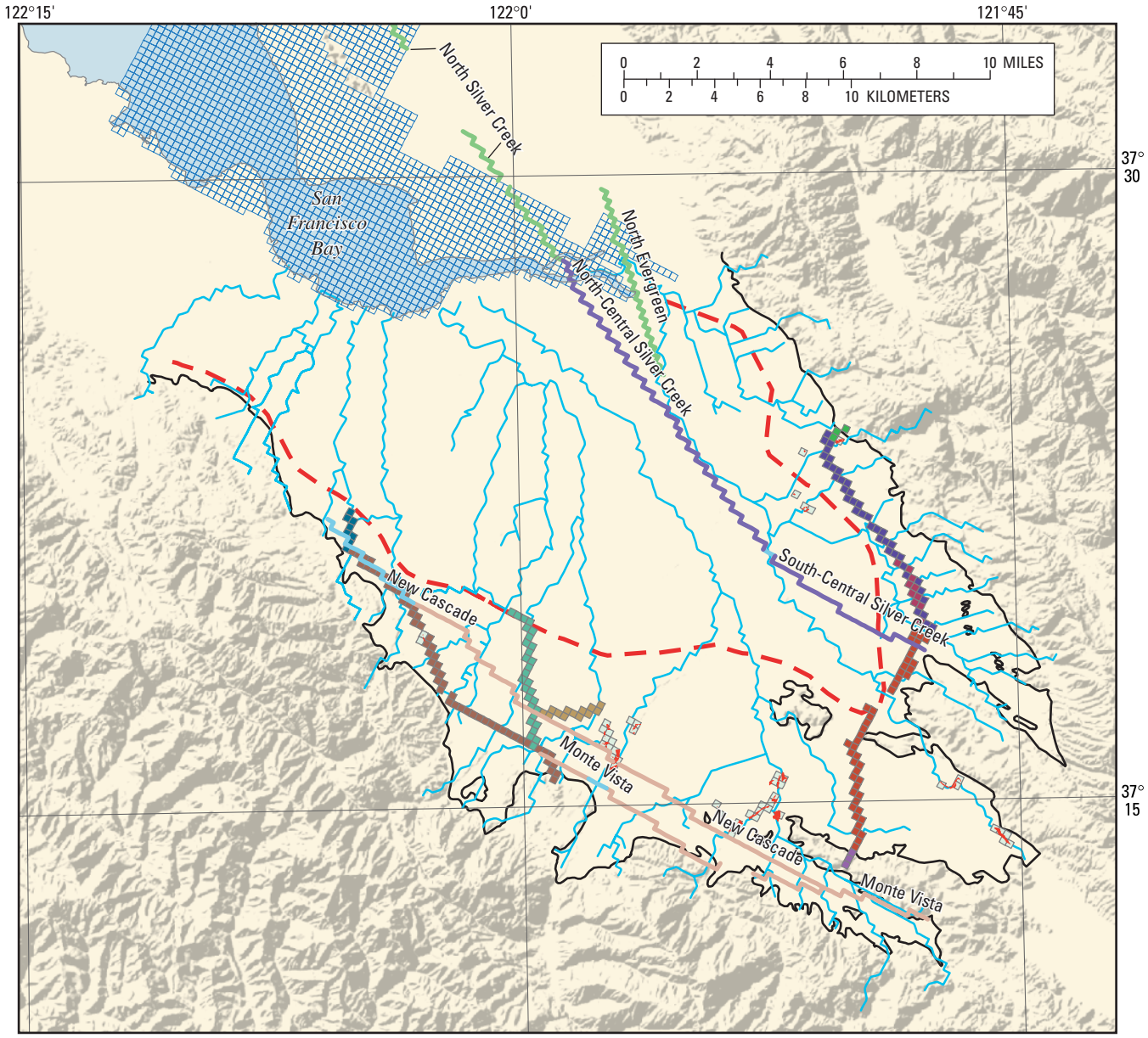

Base from U.S. Geological Survey digital elevation data, 1:250,000, 1987, and digital data, 1:100,000, 1981–89; Universal Transverse Mercator Projection, Zone 10. Shaded relief base from 1:250,000-scale Digital Elevation Model; simulated sun illumination from northwest at 30 degrees above the horizon

EXPLANATION

Water-supply transmission pipes (Model layers 1 & 3)

- Campbell Distributary
- Evergreen Pipeline
- Mountain View Distributary
- Parallel East Pipeline
- Penetencia Delivery Main
- Santa Clara Distributary
- Santa Teresa Tunnel
- Snell Pipeline
- Sunnyvale Distributary
- West Pipeline

Horizontal flow barrier characteristics, in feet per day (See table 2 for model layer assignments)

- 0.0001
- 0.001
- 0.01
- 0.1

- **Recharge ponds**
- **Model pond cell**
- **General-head boundary cell (GHB)**
- **Extent of confined aquifer zone**
- **Alluvial basin boundary**
- **Streams**

Figure 5. Ground-water flow model grid and selected inflows and outflows for the Santa Clara Valley model, Santa Clara Valley, California.

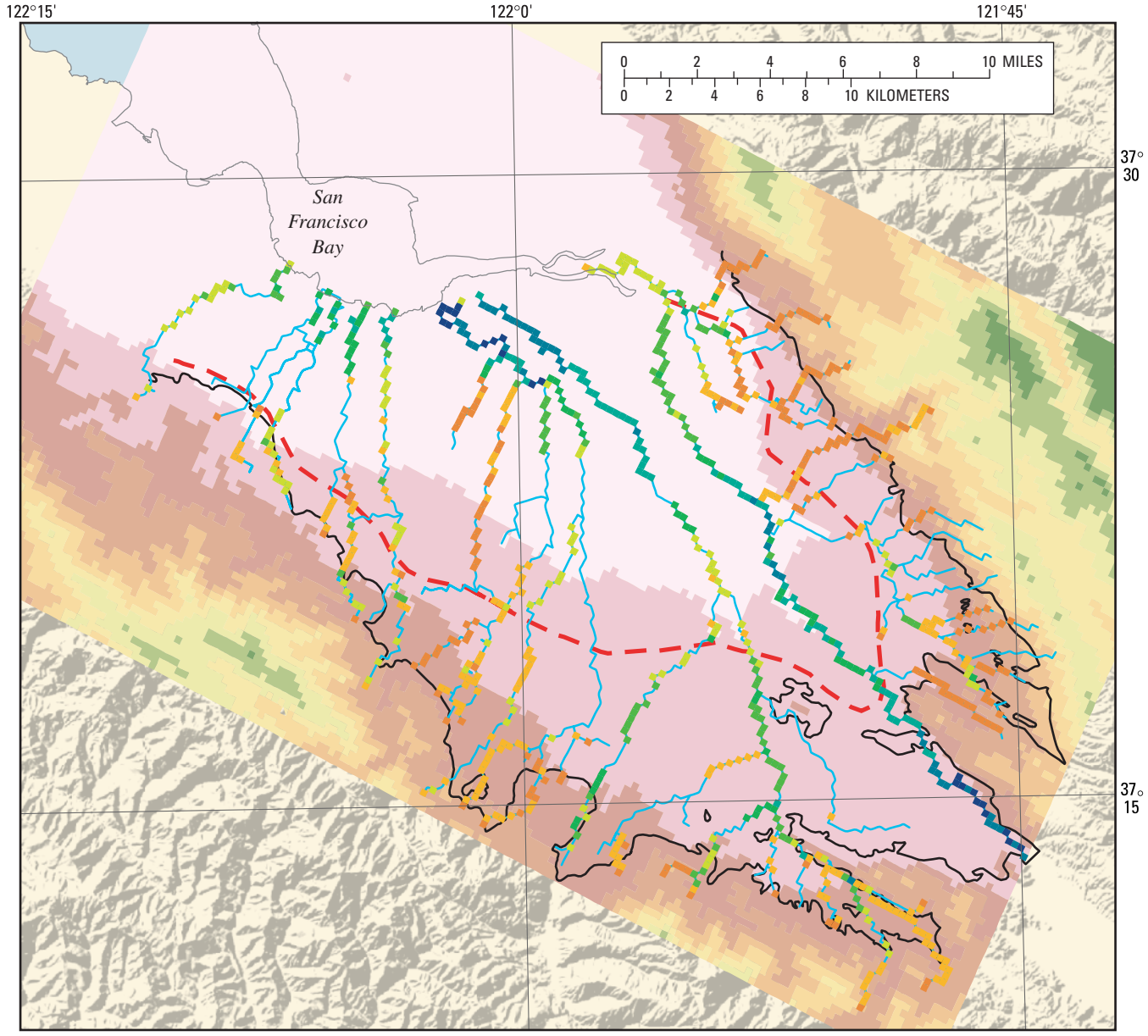

Base from U.S. Geological Survey digital elevation data, 1:250,000, 1987, and digital data, 1:100,000, 1981–89; Universal Transverse Mercator Projection, Zone 10. Shaded relief base from 1:250,000-scale Digital Elevation Model; simulated sun illumination from northwest at 30 degrees above the horizon

EXPLANATION

Elevation, in feet above NAVD 88

–6 to 95	1,041 to 1,385
96 to 259	1,386 to 1,739
260 to 465	1,740 to 2,136
466 to 728	2,137 to 2,618
729 to 1,040	2,619 to 3,517

Evapotranspiration rate, in feet per day x 10^{-3} (Model layers 1 & 3)

0.000 to 0.023	0.402 to 0.728
0.024 to 0.075	0.729 to 1.146
0.076 to 0.148	1.147 to 1.935
0.149 to 0.232	1.936 to 3.414
0.233 to 0.399	3.415 to 9.001

Streams

Extent of confined aquifer zone

Alluvial basin boundary

Figure 5. —Continued.

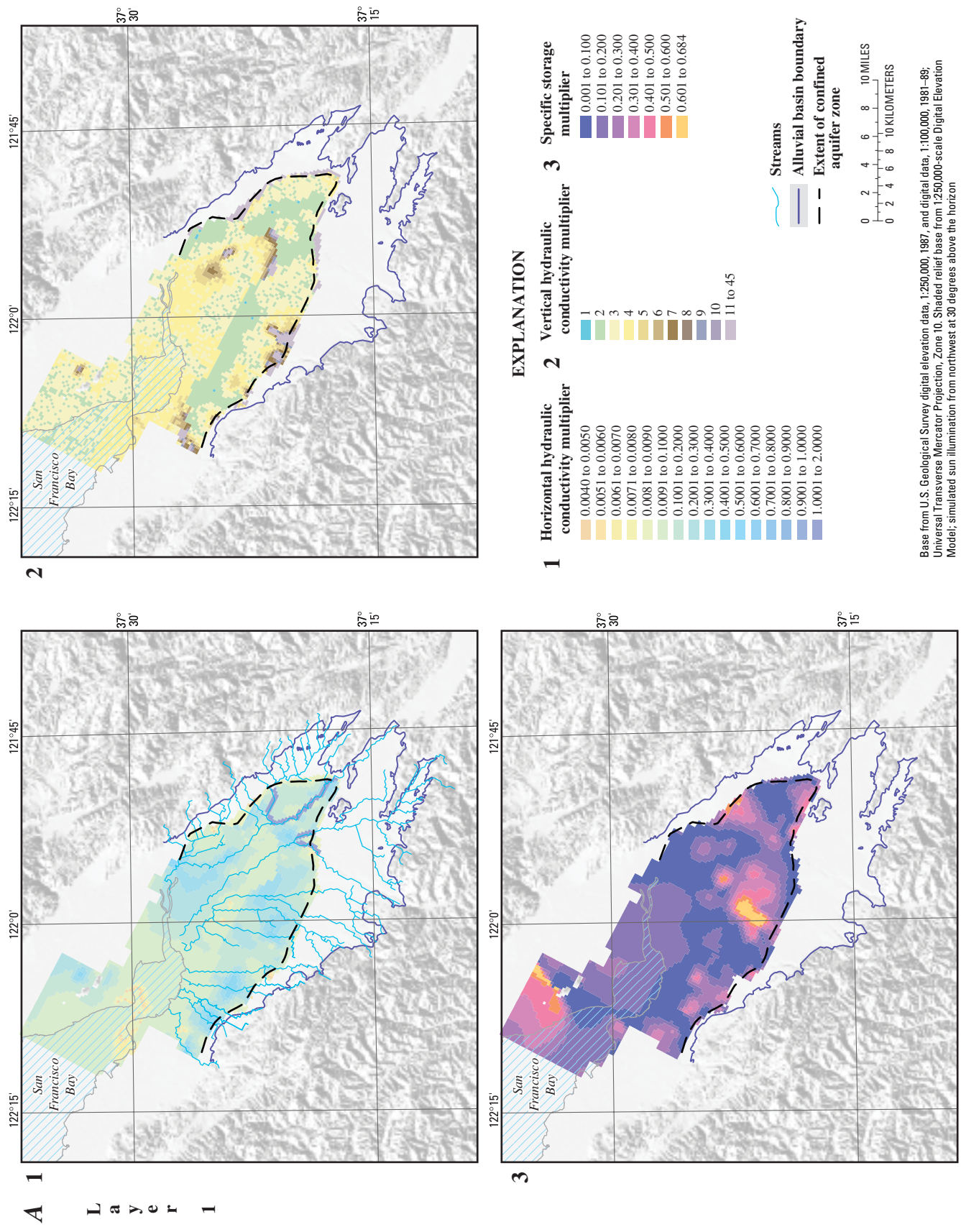

Figure 6. Ground-water flow model grid, and multiplier arrays for selected hydraulic properties for the Santa Clara Valley model, Santa Clara Valley, California.

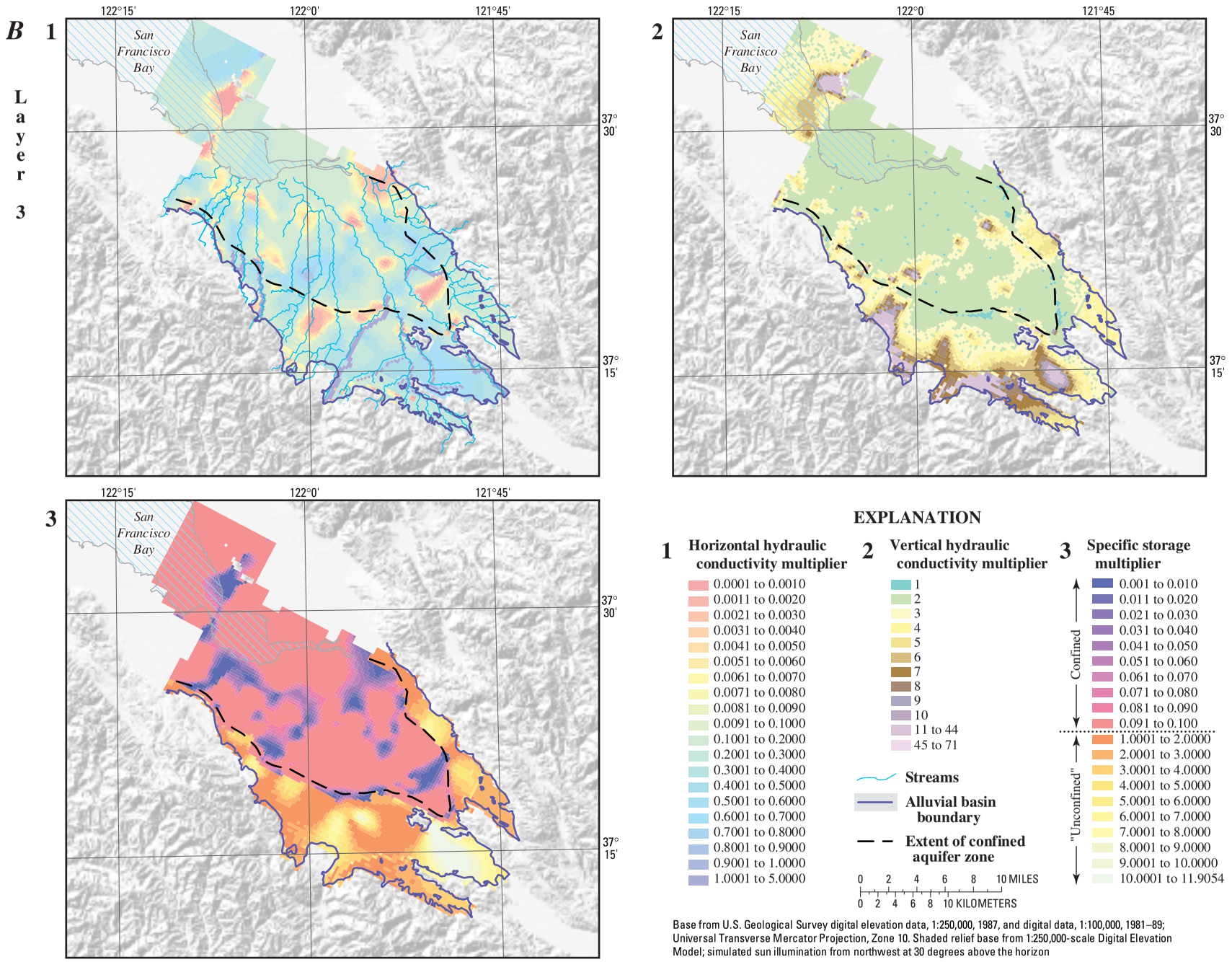

Base from U.S. Geological Survey digital elevation data, 1:250,000, 1987, and digital data, 1:100,000, 1981–89; Universal Transverse Mercator Projection, Zone 10. Shaded relief base from 1:250,000-scale Digital Elevation Model; simulated sun illumination from northwest at 30 degrees above the horizon

Figure 6.—Continued.

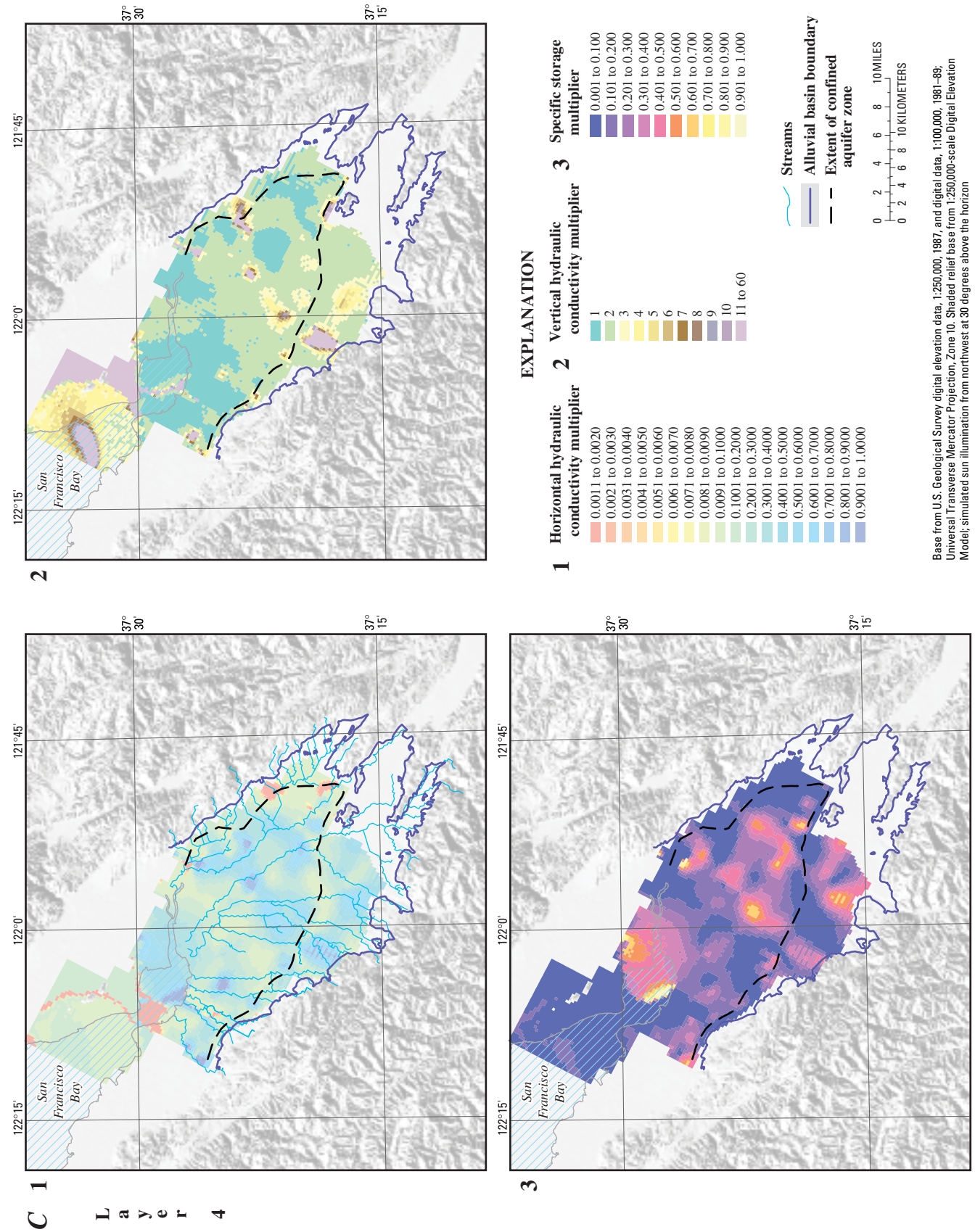

Figure 6. —Continued.

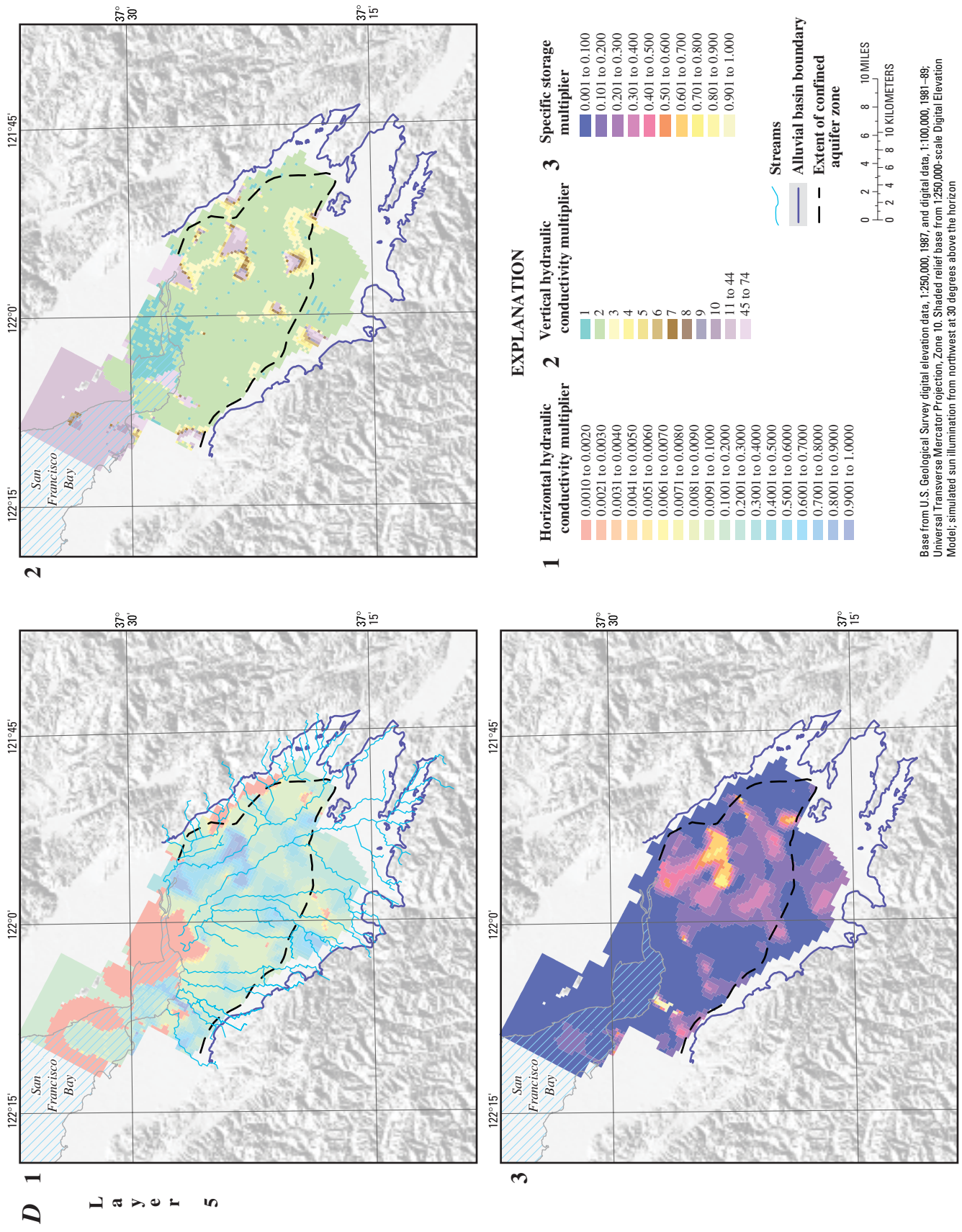

Figure 6. —Continued.

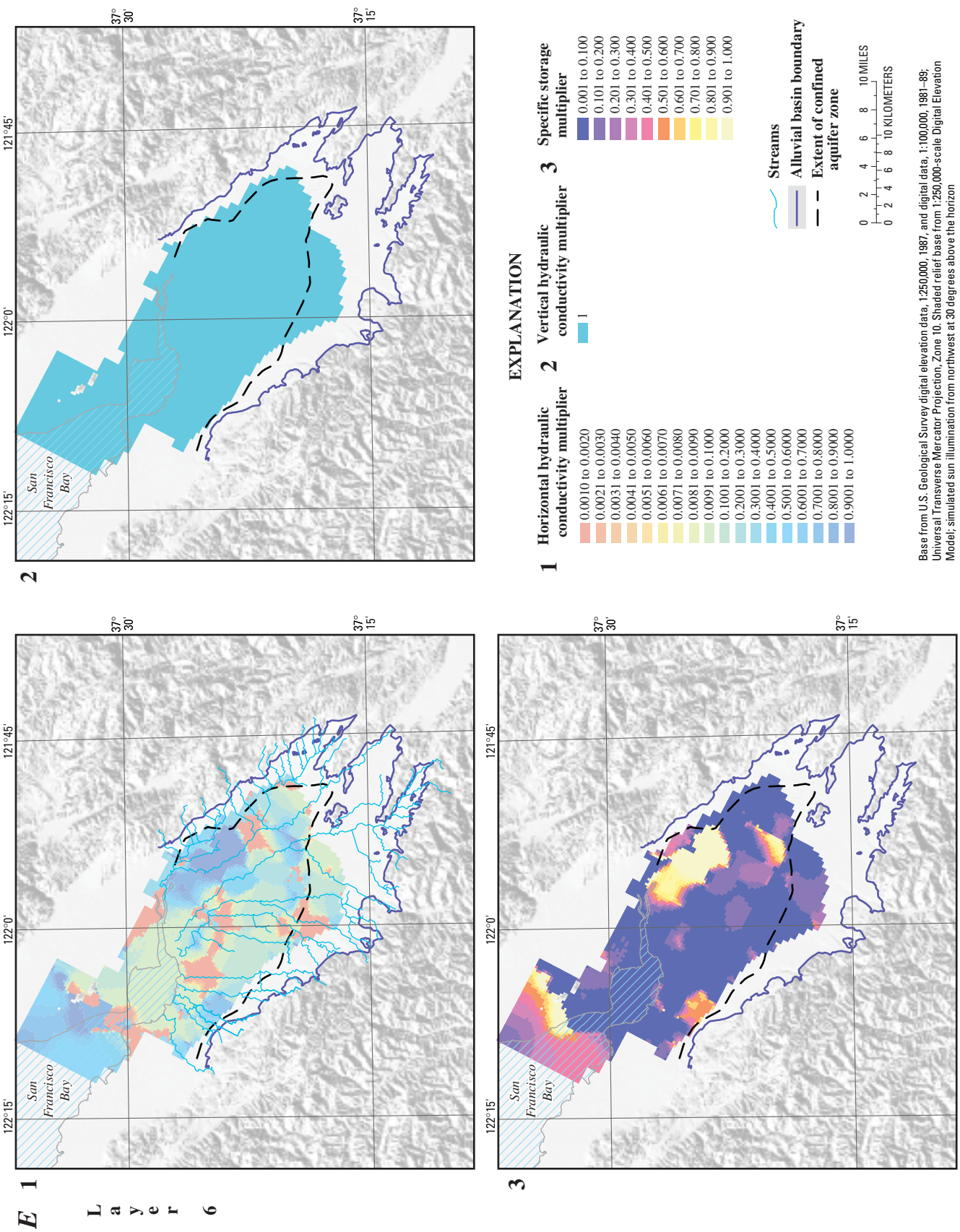

Figure 6. —Continued.

Table 1. Summary of calibrated base multiplier values for hydraulic properties of the Santa Clara Valley model, California

[ft, foot; ft/d, foot per day]

Model layer	Base multiplier values (LPF Package of MF2K)			Product of base multiplier values and initial specific storage values (IBS Package of MF2K)	
	Horizontal hydraulic conductivity, in ft/d (P_{HK})	Vertical hydraulic conductivity, in ft/d (P_{VK})	Aquifer specific storage, in ft^{-1} (P_{Ssk})	Interbed (aquitard) Skeletal Elastic Specific Storage, in ft^{-1} (S_{sfe})	Interbed (aquitard) Skeletal Inelastic Specific Storage[1], in ft^{-1} (S_{sfv})
1	900	3.0×10^{-6}	0.007	1.2×10^{-6}	2×10^{-4} 2×10^{-5}
2	5	1.0×10^{-7}	2.0×10^{-5}	1.2×10^{-6}	2×10^{-4} 2×10^{-5}
3	380	5.0×10^{-3}	2.0×10^{-5}	6.0×10^{-7}	1×10^{-4} 1×10^{-5}
4	120	8.5×10^{-3}	5.0×10^{-7}	6.0×10^{-7}	1×10^{-4} 1×10^{-5}
5	160	1.7×10^{-2}	5.0×10^{-7}	1.2×10^{-6}	2×10^{-4} 2×10^{-5}
6	.05	5.0×10^{-2}	5.0×10^{-7}	1.2×10^{-6}	2×10^{-4} 2×10^{-5}

[1]Top value represents S_{sfv} for compressible fine-grained deposits and bottom value represents S_{sfv} for incompressible fine-, mixed and coarse-grained deposits.

The representation of hydraulic properties using the Layer Property Flow package (LPF) of MF2K requires the separate specification of intrinsic hydraulic properties, such as hydraulic conductivity, specific storage or specific yield, and aquifer layer thickness for each model layer (Harbaugh and others, 2000b). MF2K estimates model-layer hydraulic properties as a product of intrinsic hydraulic property and model-layer thickness. The aggregate thickness of aquifers and aquitards collectively equals the model-layer thickness for any one cell. Therefore, the model hydraulic properties required the specification of the fraction of the model-layer thickness that represents the aquifer or aquitard thickness on a cell-by-cell basis. These fractions represent the multiplier arrays that are shown for all layers (model layers 1, 3–6) shown in figure 6 except for model layer 2 that was simulated with single hydraulic properties for all cells (table 1). The multiplier arrays were used to prorate the thickness of coarse-, mixed-, and fine-grained lithofacies at each model cell with the base multiplier values listed in table 1. In contrast to the zone-based approach, the cell-based definition of spatially distributed hydraulic properties represents the gradationally changing lithologic properties. This approach allows a more realistic representation of the coarse- and fine-grained lithofacies that control the hydraulic properties and related flow of ground water throughout the alluvial aquifer system. This approach also helps to minimize the number of hydraulic parameters needed to represent the variations in hydraulic properties. The hydraulic parameters are then used to scale the cell-based lithofacies multiplier arrays that represent the fractions of the model-layer thickness for each hydraulic property.

Transmission Properties

The revised model simulates confined-aquifer conditions for all model layers. MF2K calculates the transmissivity as the product of hydraulic conductivity and saturated thickness of the aquifers. Therefore, transmissivity values could be affected by changes in saturated thickness. Throughout much of the modeled area, most of the transmissivity is associated with the selected coarse-grained layers of the aquifers that remain saturated, and many parts of the aquifers are confined or show water-level changes that are a relatively small percentage of the saturated thickness, such as the area outside the confined region in the southwestern part of model layer 3. Because the effective saturated thickness is relatively constant over most of the model area, it was considered acceptable to use confined aquifers that have constant transmissivities for the entire period of simulation.

The transmission properties were based on the estimation of hydraulic conductivity, as required for simulation of ground-water flow with MF2K (Harbaugh and others, 2000b). Multiplier arrays were used to represent the spatial variation of horizontal and vertical hydraulic conductivity (fig. 6). Four categories were created for the alluvial deposits on the basis of the indexed numerical lithology database (Leighton and others, 1994): incompressible fine-grained (sc1), compressible fine-grained (sc2), mixed coarse- and fine-grained (sc3) and coarse-grained (sc4) sediments. The incompressible fine-grained material (sc1) is assumed to be relatively impermeable, is a relatively small fraction of the total thickness of alluvial deposits, and therefore was not included in any estimates of hydraulic properties. For each model layer the multiplier arrays were constructed as a combination of textural components as:

$$MLTc_{i,j,k} = Lsc4_{i,j,k} / L_{i,j,k}$$

$$MLTm_{i,j,k} = Lsc3_{i,j,k} / L_{i,j,k} \text{ and}$$

$$MLTf_{i,j,k} = Lsc2_{i,j,k} / L_{i,j,k}$$

where

i,j, and *k*	are row, column, and layer index for each model cell
$L_{i,j,k}$	is the layer thickness (in ft) of that cell;
$Lsc(2–4)_{i,j,k}$	refers to the thickness of an individual category fine–f (2), mixed–m (3), or coarse–c (4) at that cell; and
$MLTc_{i,j,k}$, $MLTm_{i,j,k}$, and $MLTf_{i,j,k}$	are multiplier arrays for category 4, 3, and 2, and represent the proportional layer thickness of coarse-grained, mixed, and compressible fine-grained sediments, respectively.

On the basis of these multiplier arrays (fig. 6), the hydraulic properties of each model cell are defined as a set of empirical relations as follows:

$$HK_{i,j,k} =$$

$$P_{HKk} \times (MLTc_{i,j,k} + 0.75 \times (MLTm_{i,j,k}))$$

and

$$VK_{i,j,k} = P_{VKk} \times MLTf_{i,j,k}$$

where

$HK_{i,j,k}$	is horizontal hydraulic conductivity,
$VK_{i,j,k}$	is vertical hydaulic conductivity, and
P_{HKk} and P_{VKk}	are regional base multiplier values for horizontal and vertical hydraulic conductivity for all of model cells of model layer *k*.

Values of P_{HK} and P_{VK} specified for each model layer (table1) were initially based on values from the previous model, and have been adjusted further during the calibration of the revised Santa Clara Valley model. The assumed fraction of 0.75 was empirically based upon the percentage of the mixed fraction that is typically coarse-grained material from the inspection of cores from recently drilled monitoring-well sites in the Santa Clara Valley. In addition, slug test values from recently completed multiple-well monitoring sites were used to confirm the possible range of hydraulic conductivities. These tests yielded values that ranged from 0.1 to 583 ft/d (Rhett Everett, U.S. Geological Survey, unpub. data, 2002), with the highest values for the shallower deposits.

Storage Properties

Aquifer storage properties that are simulated using the LPF package of MF2K were separated from the aquitard storage properties simulated using the IBS package in the revised model (fig. 6). The aquifer storage property includes the compressibility of water and the compressibility of the coarser grained aquifer material. The skeletal specific storage only includes the compressibility of the finer-grained matrix of the compressible interbeds. The finer-grained interbeds simulated with IBS in MF2K are collectively referred to as aquitards in this report. MF2K requires specification of aquifer specific storage for all active cells in every model layer. In a manner similar to that of the hydraulic conductivity estimates, the estimates of specific storage were based on the fractional aggregate thicknesses of the cell-by-cell textural facies (fig. 6):

$$S_{S,\,i,\,j,\,k} = P_{Ssk} \times MLTc_{i,j,k}$$

where

$S_{S,i,j,k}$ is aquifer specific storage,

P_{Ssk} is the common base multiplier value for specific storage for all model cells for model layer k, and

$MLTc_{i,j,k}$ is the fractional thickness of the coarse-grained deposits.

Ps_{sk} is the common base multiplier value for specific storage for all model cells for model layer k, and $MLTc_{i,j,k}$ is the fractional thickness of the coarse-grained deposits.
The remainder of the aquifer-system storage from the other textural categories is accounted for through the simulation of subsidence using the IBS package (described later in the Subsidence Section).

Values of Ps_s specified for each model layer (table 1) were initially based on values from the previous model, and were adjusted further during the calibration. Although the previous model simulated the uppermost layers as unconfined aquifers using specific-yield values for the cell-by-cell storage properties, the previous model contained numerous dry cells that impaired the simulation of ground-water flow and terminated some inflows and outflows. As noted above, the changes in saturated thickness are small, thus the use of confined aquifers does not impart any significant error and keeps all active cells active during the entire simulation. For the uppermost layers (model layers 1 and 3) values of specific yield were implemented by increasing the MLT array values in the region outside the confined zone defined for the previous model (fig. 1). This resulted in storage coefficients that are equivalent to specific-yield values ranging from about 0.01 to 0.125 as shown by the larger multiplier-array values outside of the confined region of model layer 3 (fig 6).

Flow Barriers

In the revised model, faults that represent potential barriers to ground-water flow were simulated using the Horizontal Flow Barrier package (HFB) (Hsieh and Freckleton, 1993). The initial distribution of mapped faults was based on the analysis provided by the California Department of Water Resources (California Department of Water Resources, 1967). This fault distribution was the basis for subsequent published maps of faults for the southern San Francisco Bay region (Pampeyan, 1970, 1993; Jennings, 1985, 1994; Oliver, 1990; Page, 1993). In particular, the faults were published again with assigned relative recencies of age for the State geologic map (Jennings, 1994), which was revised from the original distributions of fault recency (Pampeyan, 1979; Bartugno and others, 1991). However, the basis for the distribution of inferred faults and their distinction from potential facies boundaries remains uncertain and an element of ongoing research by the USGS (Wentworth and others, 2003a, b). The final distribution of faults used for the ground-water flow model is greatly simplified and has been modified on the basis of a revised set of mapped faults (Wentworth and others, 2003a). The hydraulic characteristic of these fault segments was uniformly set for specific faults and groups of layers as determined during model calibration. Information regarding fault names, value of hydraulic characteristic, and the distribution among model layers is summarized in table 2.

Table 2. Summary of horizontal flow barriers used in the Santa Clara Valley ground-water flow model, California

[ft/d, foot per day]

Fault name	Fault identification number[1]	Calibrated hydraulic characteristic, in ft/d	Model layers
North Silver Creek	3480	0.01	1^{-6}
North-Central Silver Creek	3636	.01.001	1^{-2} 3^{-6}
South-Central Silver Creek	3751	.01.001	1^{-2} 3^{-6}
North Evergreen	3574	.01	1^{-6}
New Cascade	[2]3819	.0001	3^{-6}
Monte Vista	[3]3836	.0001	3^{-6}
Fault gaps	3819 and 3636	.1	3^{-6}

[1]Fault identification number from Geologic Digital Data Base (Jennings, 1994)
[2]Fault replaces original Cascade Fault location (Jennings, 1994)
[3]Fault location partly revised from original fault location.

The Silver Creek Fault is represented by three segments: North Silver Creek, North-Central Silver Creek, and South-Central Silver Creek (fig. 5A). The fault location was based either on the mapped trace (Jennings, 1994) at the ground surface or on the inferred location that is aligned with interferometric synthetic aperture radar (InSAR) images (Galloway and others, 2000). Additional seismic imaging across the fault (Catchings and others, 2000; Williams and others, 2002) and geophysical investigations (Williams and others, 2002; Jachens and others, 2002) confirms the location of the fault and the potential displacement of layering within the sedimentary deposits in the uppermost model layer. These fault segments were used in all model layers for all active model cells coincident with the fault trace. The North Evergreen Fault is a single north-northwest-trending segment that traverses the Evergreen Basin between the Silver Creek and Hayward Faults (Wentworth and others, 2003a) (fig. 5A).

The Cascade Fault was relocated from the original trace (California Department of Water Resources, 1967; Jennings, 1994) (figs. 1, 5A). The relocation of the fault (herein referred to as the "New Cascade" fault) was based on the trace of surface damage from the Loma Prieta earthquake in 1989 (Bob Jachens, U.S. Geological Survey, unpub. data, 2002) and on the envelope delineating the northeastern side of photo-lineaments (Carl Wentworth, U.S. Geological Survey, unpub. data, 2002) in conjunction with other estimates of deformation and folding along the western edge of the valley (Hitchcock and Kelson, 1999; Hitchcock and others, 1994). In addition, different hydrologic response across the proposed fault trace was inferred from the water-level hydrographs of two wells located east (7S/1W-30C2) and west (7S/1W-30E3) of the revised fault-trace location (figs. 1, 5A). The revised location also was moved to the southwest of two wells and the Los Gatos recharge ponds that were used to improve model calibration of water-level changes (7S/1W-30C2, -34F2) along the western side of the basin. The revised fault trace is an extension of mapped faults that occur in the bedrock outcrops along the western side of the basin (Wentworth and others, 2003a). The Monte Vista Fault also was relocated on the basis of recent geologic mapping (Wentworth and others, 2003a). The revised "New Cascade" Fault also contains gaps represented by larger fault conductances coincident with Los Gatos Creek, Stevens Creek, and Ross Creek on the west side of the valley (fig. 5A). Similarly, a gap in the Silver Creek Fault along the lower Silver Creek was required on the east side of the valley to simulate larger fault conductances (fig. 5A).

Simulated Inflows and Outflows

The previous model had simplified and fixed some of the head-dependent inflows and outflows for each stress period that were estimated a priori outside of the model. Therefore some of the inflows such as streamflow infiltration and outflows such as evapotranspiration were not dependent on the simulated heads in the ground-water flow model. In addition, the model had fixed regional hydraulic gradients and related basin inflows and outflows, and constant-head boundaries at the Coyote Narrows and San Francisco Bay coastal boundary (fig. 1). The previous model also combined inflows and outflows and set the spatial distribution. For example, a composite net-recharge was used that was composed of the combined inflows from artificial recharge, natural areal and streamflow infiltration, and transmission-pipe losses minus the estimated outflow from potential evapotranspiration. Similarly, pumpage that spans up to four model layers for multi-aquifer wells had a fixed vertical distribution between model layers for each well for all stress periods.

The revised model simulates inflows and outflows separately and more dynamically. Therefore, natural valley-floor recharge, artificial recharge plus leakage from water-supply transmission-line, streamflow routing, and evapotranspiration are explicitly simulated as separate flow components. In addition, the constant-head boundaries that provided a potentially infinite source of simulated inflow and outflow in the previous model (CH2M Hill, 1991) were replaced with general-head boundaries at the San Francisco Bay boundary. The constant-head boundary at Coyote Narrows was replaced with streamflow routing inflow along Coyote Creek. Subsidence is a new simulated source of water from recoverable and non-recoverable storage. Faults as horizontal-flow boundaries affect the flow of ground water both parallel and perpendicular to the regional hydraulic gradients. Pumpage from wells that are screened across multiple aquifers is now simulated using multi-node wells that dynamically distribute the vertical distribution of ground-water pumpage or intrawellbore flow from unpumped wells.

The revised model simulates inflows and outflow components needed to assess water-resource management issues. Recharge to the ground-water system is simulated as natural areal recharge from the deep percolation of rainfall in excess of evapotranspiration and runoff, deep percolation of artificial recharge and losses from transmission lines, and streamflow infiltration that occurs during the routing of streamflow through the numerous creeks that drain the surrounding mountains. Outflows are simulated as ground-water pumpage, as ground water discharged to creeks as base flow, evapotranspiration, and underflow at and leakage to the San Francisco Bay boundary.

Valley-Floor Recharge

For the Santa Clara Valley model, natural areal recharge was simulated as infiltration from a percentage of rainfall using the recharge package in MODFLOW. To capture the spatial and temporal variation of natural precipitation in the basin, 12 monthly average precipitation estimates were transferred to the SCVM model grid from mean monthly precipitation maps (fig. 7) for the period 1950–99 (Joseph A. Hevesi and Alan L. Flint, U.S. Geological Survey, unpub. data, 2000). These maps were estimated from historical precipitation records (1950–99) in this region, and spatially interpolated for each 90- by 90-meter pixel using a precipitation-elevation correlation model (Hevesi and others, 2002). This approach to estimating precipitation and recharge has been applied to other regional models (Hanson and others, 2002a; D'Agnese and others, 2002; Reichard and others, 2003). To impose temporally varying rainfall characteristics on these precipitation-recharge matrices, a scaling ratio was calculated and applied to the matrices for each month simulated. The ratio is defined as the measured total monthly precipitation at the San Jose station divided by the average total precipitation for that month for the period 1950–99.

The precipitation-recharge relation has been applied uniformly throughout the basin. However, the infiltration of excess rainfall as valley-floor recharge to the ground-water flow system could be quite complex and influenced by a number of factors, such as land use, vegetation, soil type, and thickness of the unsaturated zone. Although this approach may overestimate infiltration from excess rainfall at highly developed municipal and industrial areas, such as the urban corridor in the central part of Santa Clara Valley, on the basis of model calibration of simulated and measured water-level hydrographs, the resulting recharge estimate generally captures the spatial variation of natural recharge. Conversely, on the basis of model calibration of simulated and measured water-level hydrographs, the temporal variation of natural recharge based on a single percentage of precipitation as applied in the previous model seems inadequate owing to the lack of multi-year variation in the simulated water-level hydrographs, which must reflect wet and dry climatic periods observed in the measured water-level hydrographs. Therefore, the single linear relation was subdivided into wet- and dry-month relations, separately, in order to manifest the effect of climate cycle on the hydraulic system. The distinction between wet and dry months was based on the ratio of monthly precipitation at San Jose to the period-of-record average precipitation for the respective month at San Jose. The monthly recharge is assumed to be occurring in a wet month if this precipitation-scaling ratio is larger than 1; and the recharge is assumed to occur in a dry month if the ratio is less than or equal to 1. For the Santa Clara Valley model, a simple linear precipitation-recharge relation was adopted initially, with recharge estimated to be 7.5 and 15 percent of the mean monthly scaled precipitation for wet months for the dryer Pacific Decadal Oscillation (PDO) period of 1970–77 and the wetter PDO period of 1978–99, respectively. The valley-floor recharge during dry months of wet and dry PDO periods was held constant at 4.5 percent of the scaled mean monthly precipitation. These percentages are collectively comparable to the 10 percent used in the previous model. In addition the resulting distributions of monthly precipitation are aligned with increasing precipitation and increasing elevation along the valley margins (fig. 7).

The final equations used for the calibrated model used to calculate recharge for the SCVM are specified as follows.

For the wet months for dry PDO periods:

$$RCH_{i,j,T} = 0.075 \times (P_{SJ,T(M)} / Avg_{-PSJ,1950-99}) \times Pmap_{I,J,M}$$

For the wet months for wet PDO periods:

$$RCH_{i,j,T} = 0.15 \times (P_{SJ,T(M)} / Avg_{-PSJ,1950-99}) \times Pmap_{I,J,M}$$

For all the dry months in wet and dry PDO periods:

$$RCH_{i,j,T} = 0.045 \times (P_{SJ,T(M)} / Avg_{-PSJ,1950-99}) \times Pmap_{I,J,M}$$

where

$RCH_{i,j,T}$ is the recharge matrix of the M monthly stress period T for all cells in the I rows and J columns of the SCVM model grid;

$P_{SJ,T(M)}$ is the measured precipitation at the San Jose (SJ) precipitation gage for each M month of the year for all T stress periods over the simulation period 1970–99;

$Avg\_P_{SJ,1950–99}$ is the average measured precipitation at the San Jose (SJ) precipitation gage for the M month over the PDO periods 1950–99; and

$Pmap_{I,J,M}$ is the averaged monthly precipitation matrix for one of the 12 months (M) (fig. 7), depending on the month of stress period T.

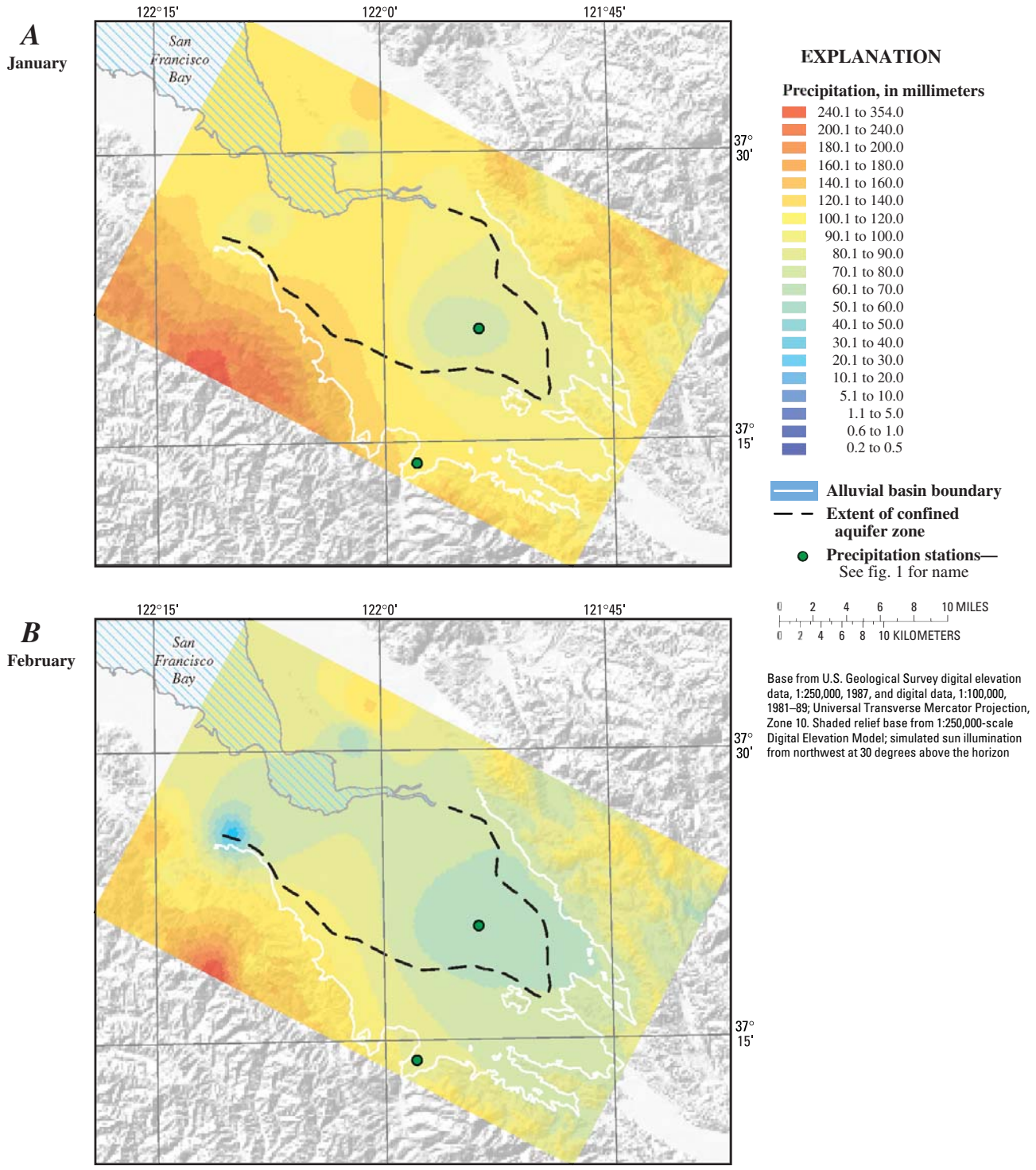

Figure 7. Ground-water flow model grid and estimated mean monthly precipitation for the period 1952–99 for the Santa Clara Valley model, Santa Clara Valley, California.

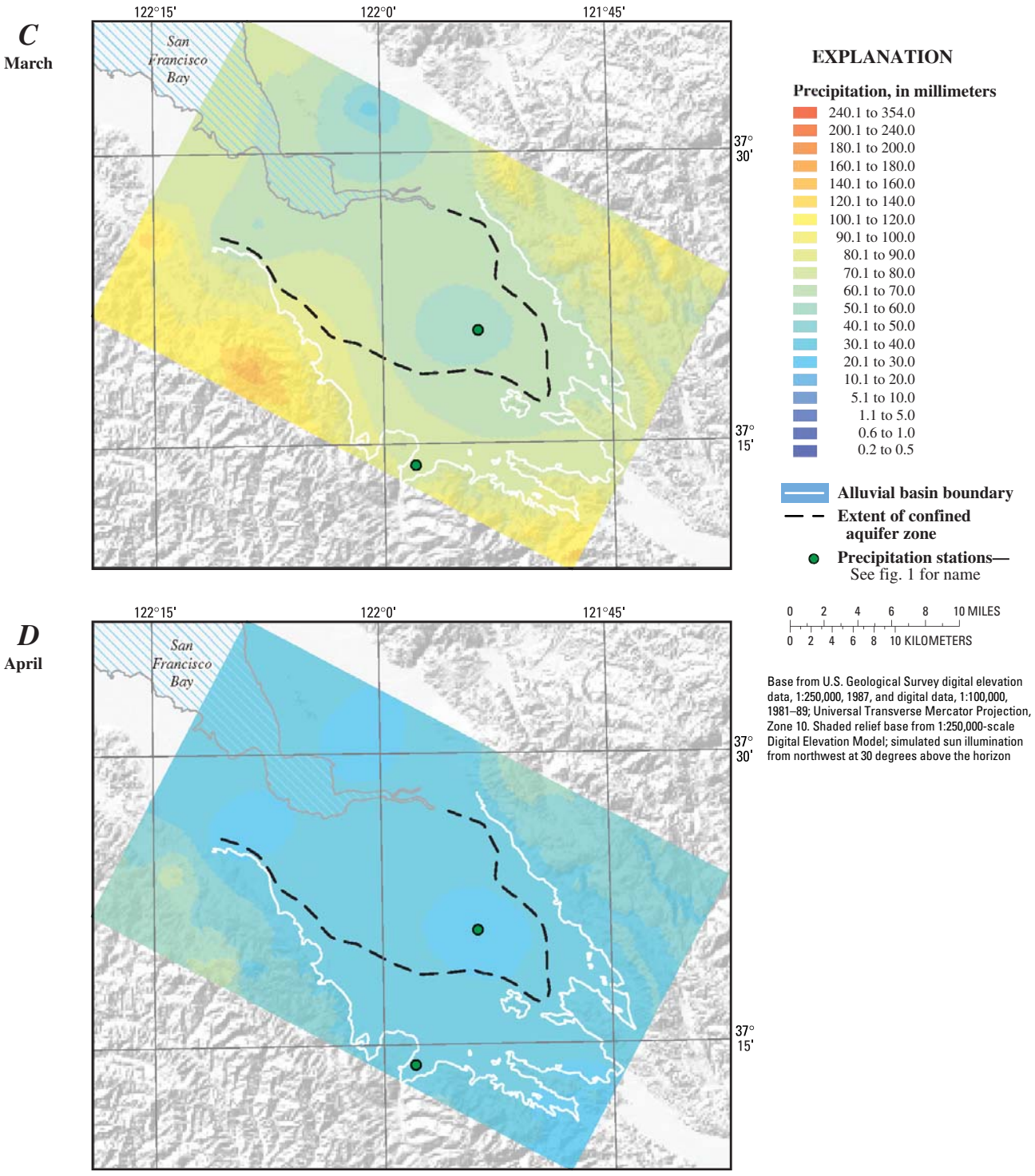

Figure 7. —Continued.

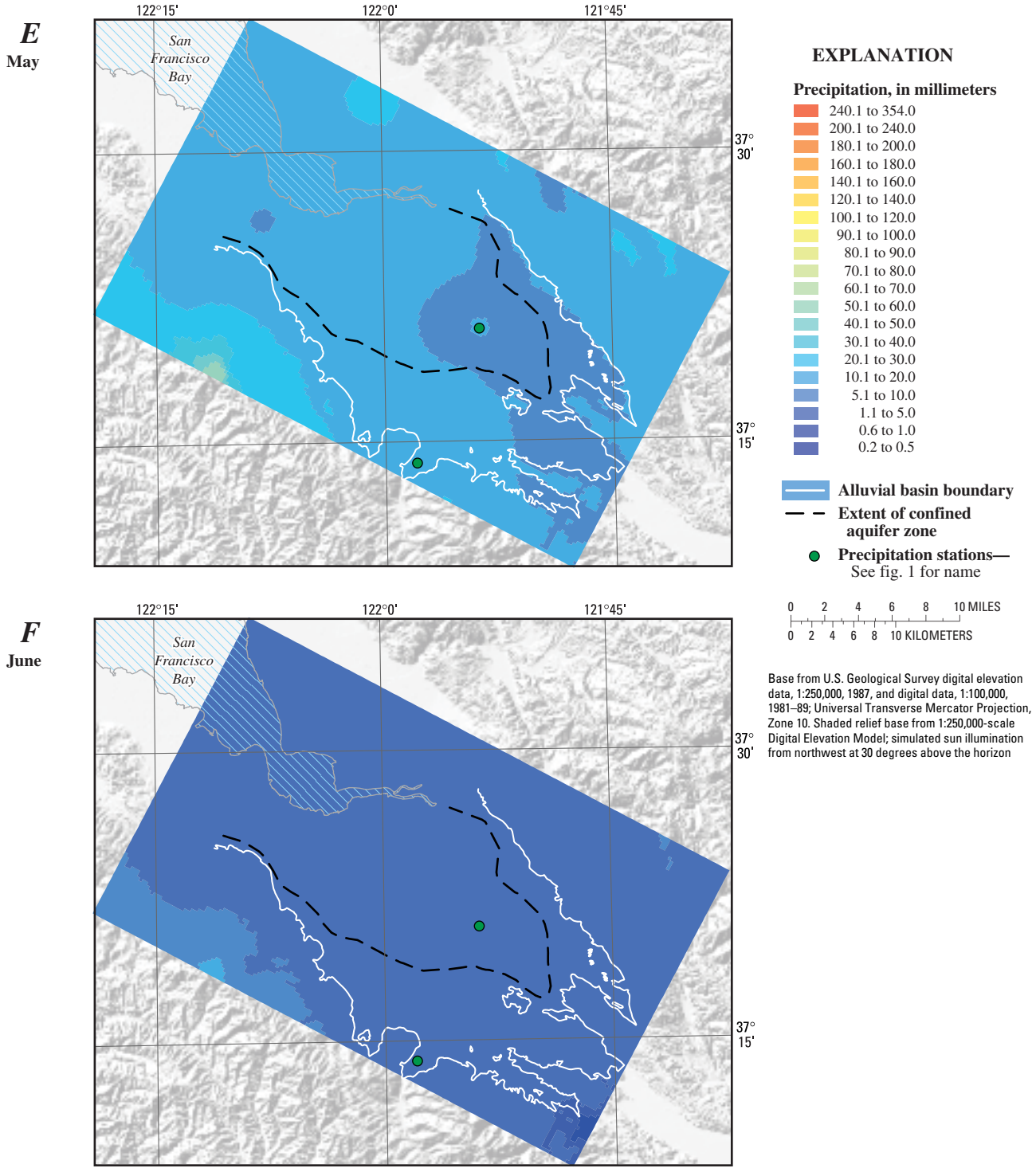

Figure 7. —Continued.

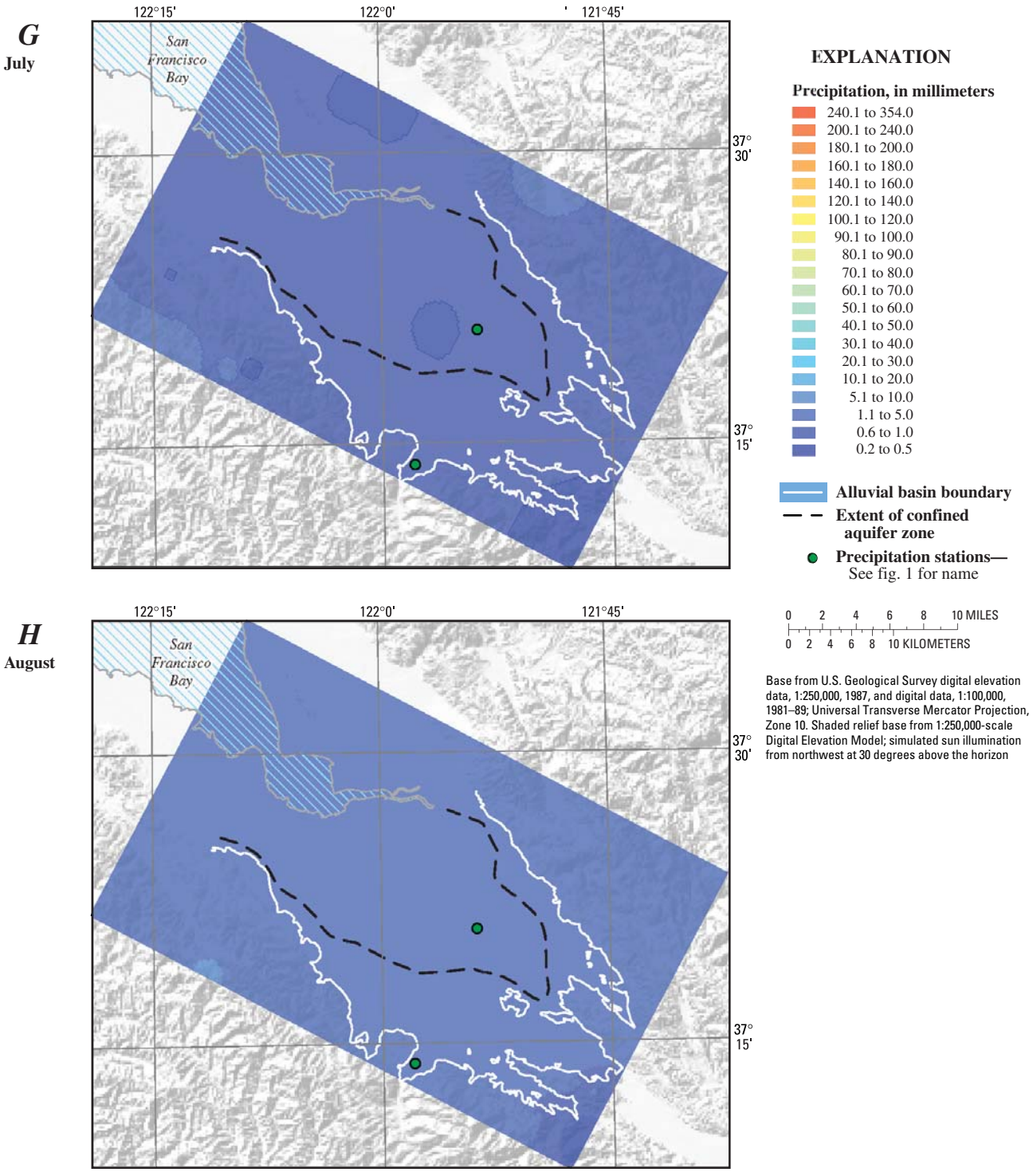

Figure 7. —Continued.

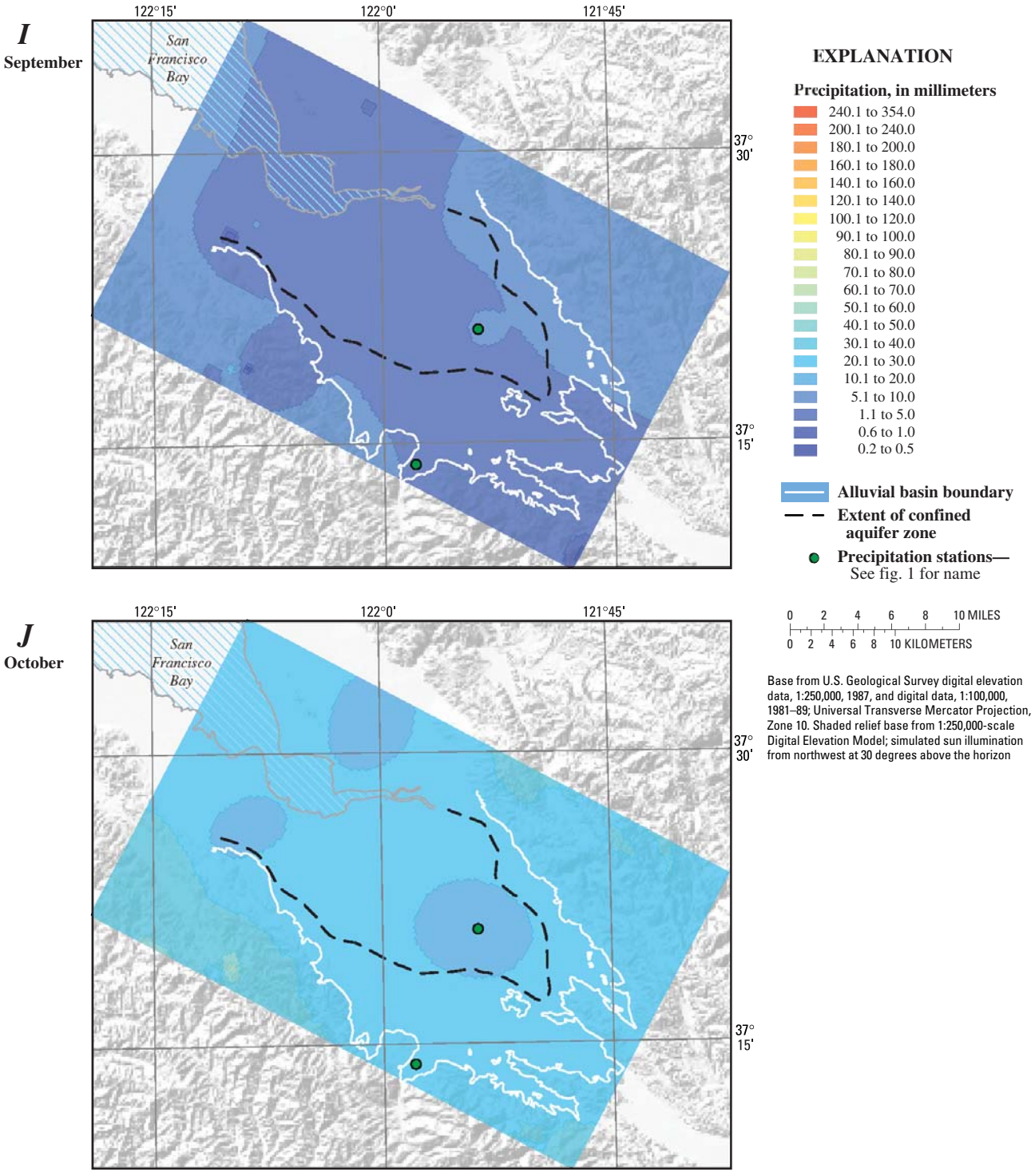

Figure 7. —Continued.

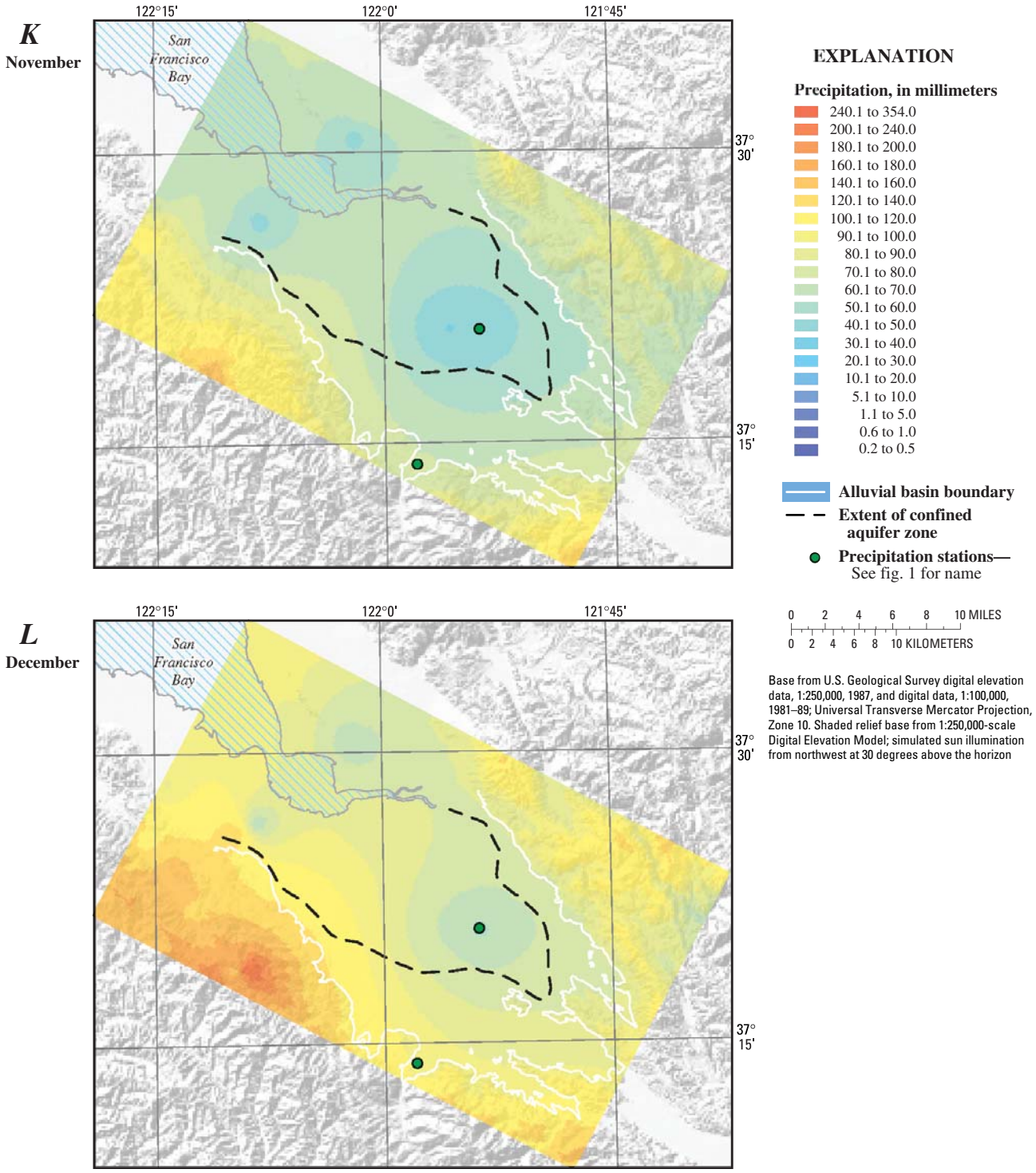

Figure 7. —Continued.

Artificial Recharge

Artificial recharge occurs from the deep percolation of imported water, specifically from leakage from transmission pipelines that carry the imported water to water-treatment plants and SCVWD recharge ponds. The deep percolation of imported water was simulated using wells as constant inflows in the uppermost model layers (layers 1 and 3) at 11 groups of percolation ponds that are operated by SCVWD (fig. 5*A*). Inflows were located at the percolation ponds and were subdivided between multiple model cells and multiple ponds on the basis of the area of individual ponds for each group of ponds. The inflows used in the model were the reported monthly infiltration volumes (Mark Merritt, Santa Clara Valley Water District, unpub. data, 2002). Additional artificial recharge that is applied to selected stream channels was applied as an additional inflow to the streamflow-routing system. Artificial recharge was applied to Stevens, Regnart, Calabasas, Rodeo, Saratoga, San Tomas, Los Gatos, Ross, and Thompson Creeks (fig. 8). Additional artificial recharge that is applied along stream channels was applied to adjacent ponds for Penetencia, Guadalupe, and Coyote Creeks.

Additional artificial recharge was assumed to occur as leakage from the transmission pipelines that convey treated water and include the Penetencia delivery main, Evergreen, Parallel east, Snell, Santa Clara distributary, Campbell distributary, Sunnyvale distributary, West, Mountain View distributary pipelines, and the Santa Teresa tunnel (fig. 5*A*). An assumed leakage rate of about 10 percent was used for these cells, with the overall delivery of Hetch Hetchy imported water uniformly distributed over all the pipeline cells. The seasonal imported water ranged from 22,075 acre-ft in the winter of 1970 to as much as 85,900 acre-ft in the spring of 1994 (Bezhad Ahmadi, Santa Clara Valley Water District, unpub. data, 2001). This component of recharge was adopted from the previous model (CH2M Hill, 1991), which had a similar distribution of model cells, pipeline segments, leakage rates of 9.5 percent, and reported volumes of imported water (Bezhad Ahmadi, Santa Clara Valley Water District, unpub. data, 2001).

The previous model also contained additional artificial recharge as sewer leakage and irrigation return flow. The previous model applied the sewer leakage uniformly over the entire active model region. This small inflow of water of about 5,600 acre-ft/yr was not retained in the revised model. Similarly, the small amount of agricultural irrigation return flow was not included in the revised model.

Evapotranspiration

Evapotranspiration (ET) that was embedded as part of the net recharge simulated by the previous model (CH2M Hill, 1992a) is now simulated separately using the ET package (McDonald and Harbaugh, 1988) in the revised model. The areal distribution of ET was limited to the cells that represent the streams and creeks owing to the considerable urbanization of the valley. Therefore, the ET cells were coincident with the streamflow network (fig. 5*B*). An assumed width of 100 ft was used as a fraction of the area of the cells representing the typical channel and flood-plain width covered by phreatophytes. As in the previous model, the ET rate was set to 0.011 ft/day to represent ET from willow trees that are the common broad-leaf vegetation along many of the stream channels. An assumed ET extinction depth of 5 ft below the top of the uppermost model layers (layers 1 and 3) was used at all model cells where ET was potentially active.

Streamflow Routing

The streamflow-routing network used for the SCVM consists of 69 rivers, creeks, canals, and diversions. The previous model used estimated streamflow infiltration that was calculated independently and a priori and then added to the net-recharge array. Therefore, this head-dependent approach to routing and infiltration of streamflow is a major improvement in the representation of one of the major sources of recharge in the Santa Clara Valley. The model network is composed of 1,724 cells within 137 stream segments that are subdivided into segments at the points of confluence or diversion (fig. 8). There are four streamflow diversions that divert streamflow to the artificial-recharge ponds in the network (fig. 8). The network includes both natural and manmade channels that collectively drain the Santa Clara Valley toward South San Francisco Bay. These are monitored near the points of inflow into the alluvial basin and at selected downstream gages. The simulation of streamflow routing uses the streamflow routing (STR) package (Prudic, 1989). The routing of streamflow is based upon the specification of streamflow at user-specified cells within the most upstream inflow segments. Geometric and hydraulic properties specified for every cell are streambed elevation, stream-channel width, Manning coefficient, and streambed conductance. The stream cells were assigned on the basis of the intersection of the model grid with the stream network for all cells that have a stream length of more than 150 ft within a cell.

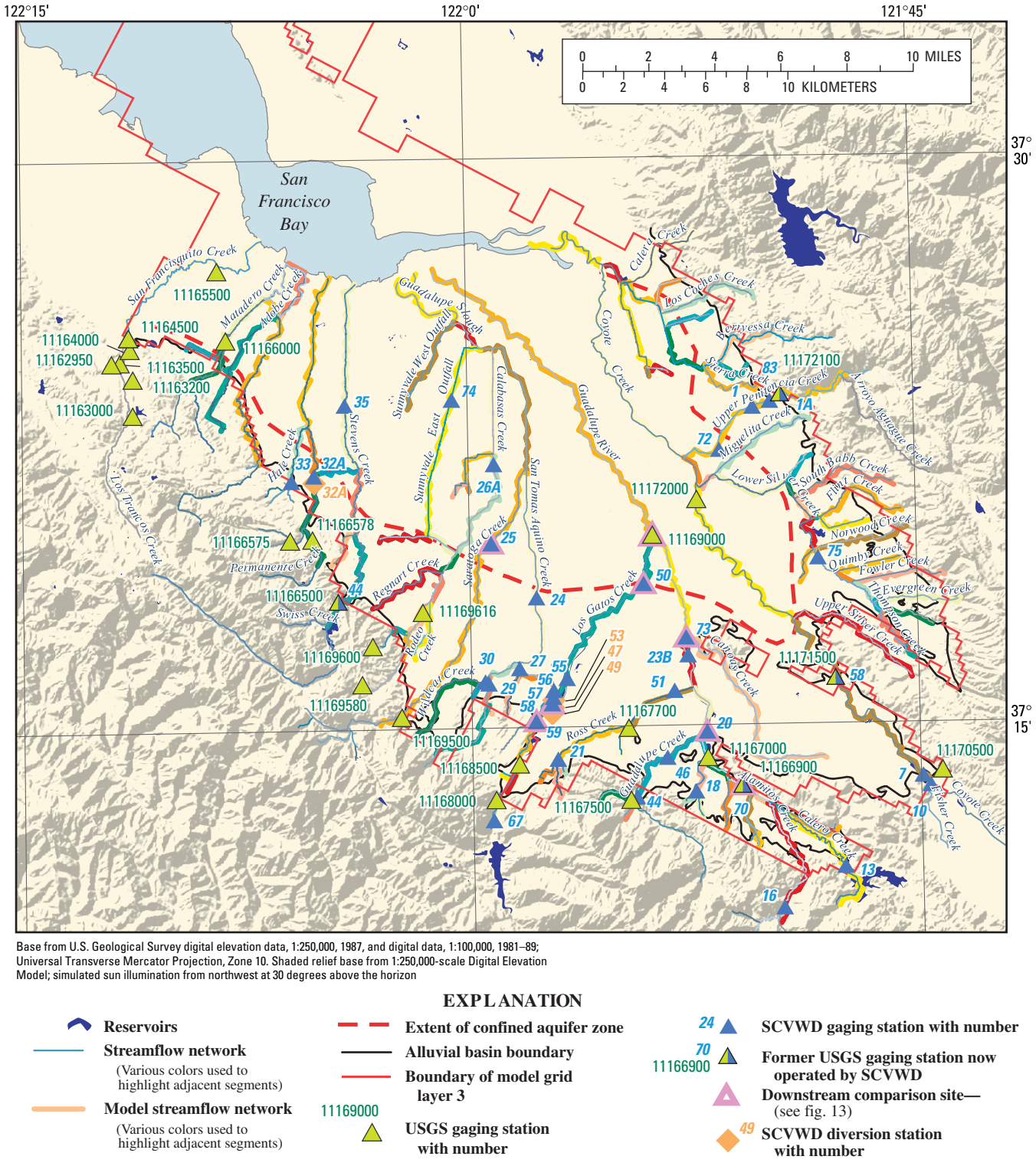

Base from U.S. Geological Survey digital elevation data, 1:250,000, 1987, and digital data, 1:100,000, 1981–89; Universal Transverse Mercator Projection, Zone 10. Shaded relief base from 1:250,000-scale Digital Elevation Model; simulated sun illumination from northwest at 30 degrees above the horizon

Figure 8. Streamflow-routing network for the Santa Clara Valley model and selected inflow and comparison gaging stations, Santa Clara Valley, California.

The vertical flow along stream cells can be downward or upward. Downward flow represents streamflow infiltration as recharge into the shallow aquifers of the ground-water flow system. Upward flow represents stream base flow as discharge from the shallow aquifer. The flow is calculated for each weekly time step of each monthly stress period. The flow is based on the streambed conductance and the hydraulic gradient between the stream and the uppermost active model cell. The hydraulic gradient is based on the difference between the simulated water levels (that is, head) in the stream that represents the stream stage and the ground-water level in the corresponding model cell divided by the distance between the model-cell center and the bottom of the streambed. The stage is internally calculated by the STR package.

The inflows are a combination of natural runoff, controlled releases from reservoirs and artificial-recharge facilities, gaged streamflow, and ungaged streamflow. The inflows are specified monthly and represent the combination of inflows that occur on each stream channel at the point of entry onto the ground-water flow model grid (fig. 8). Each inflow rate is the average of the total inflow for each month of the simulation period. The gaged inflows for eight creeks are based on streamflow-gaging station data from the USGS (Friebel and others, 2002) and from the SCVWD (Behzad Ahmadi, Santa Clara Valley Water District, unpub. data, 2000). Additional artificial recharge released to selected streams was specified from SCVWD data (Mark Merritt, Santa Clara Valley Water District, unpub. data, 2001). Ungaged streamflow for 47 selected tributaries were estimated from runoff estimates by the USGS (Alan L. Flint, U.S. Geological Survey, unpub. data, 2000) that were based on the methods described by Hevesi and others (2002). Outflows from the streamflow network occur as discharge to the southern San Francisco Bay and as streamflow infiltration to the upper-aquifer system. The streamflow diversions occur at Kirk Ditch and Page Ditch on Los Gatos Creek and Junipero Serra Channel and Permanente Diversion channel on Stevens Creek (fig. 8).

The geometric and hydraulic properties were assigned to each stream cell. The streambed elevations were specified on the basis of the lowest Digital Elevation Model elevation coincident with the trace of the stream channel. The elevation of the bottom of the streambed was assumed to be a constant 10 ft below the top of the streambed for all stream cells.

The stage is computed by the STR package using the stream channel width, slope, and Manning roughness coefficient for various bed materials (eqn. 2, Prudic, 1989). The channel widths for each stream cell were derived from data obtained from SCVWD for the entire streamflow network (Mark Merritt, Santa Clara Valley Water District, unpub. data, 2001). The slopes were calculated from the difference in stream-cell elevations and cell dimensions. The channel bottom materials and related Manning coefficients are specified as part of the STR package input for each stream cell and were based on SCVWD data (Mark Merritt, Santa Clara Valley Water District, unpub. data, 2001). The Manning coefficients ranged from 0.01 to 0.50 (Mark Merritt, Santa Clara Valley Water District, unpub. data, 2001) for rivers, creeks, and channels in the Santa Clara Valley.

The initial nonzero values of streambed conductances were based on previous modeling studies that have streamflow-routing networks with streambed conductances determined through model calibration (Hanson and others, 2002a; Stamos and others, 2001). Streambed conductances were categorized into five groups based on the specified stream-channel bottom material. Lined channels were specified with a conductance of zero. Channel bottoms described as rock, natural, or "no data" for channel segments with earth levees, gabion, trapezoidal, U-frame, or sack concrete channels initially were assigned a value of 8,640 ft^2/d. Channel bottoms described as "rock" or "no data" for channel segments with "rock lined," "natural unmodified," or "modified flood plain" channels initially were assigned a value of 43,200 ft^2/d. Channel bottoms described as "earth excavated" or "natural" initially were assigned a value of 86,400 ft^2/d. Additional streamflow segments had streambed conductances set to zero on the basis of the detailed description of reaches available for recharge delineated by SCVWD (J. Aguilera, Santa Clara Valley Water District, unpub. data, 2002). In addition, the streambed conductances for all of the flood control channels and lined stream channels were set to zero. The natural bed material throughout the lower parts of the streamflow network below an elevation of 21 ft above sea level were assigned a zero streambed conductance. This assumed elevation was based on the distribution of losing and gaining reaches determined for San Francisquito Creek (Metzger, 2002) and the distribution of gaining and losing reaches provided by SCVWD (J. Aguilera, Santa Clara Valley Water District, unpub. data, 2002).

Subsidence

The simulation of land subsidence for the revised ground-water flow model (SCVM) included all six model layers. The simulation of subsidence uses the interbed storage (IBS) package (Leake and Prudic, 1991). The simulation of subsidence is based on the simulation of compression and compaction in all model layers. The IBS package requires specification for each model layer of elastic (S_{fe}) and inelastic (S_{fv}) storage coefficients, previous compaction, and critical head (HC) (fig. 9). Although the Santa Clara Valley is the site of well documented historical subsidence of as much as 12.7 ft near San Jose (Poland and Ireland, 1988), for the purposes of this study no historical subsidence prior to 1970 was added to the simulated compaction.

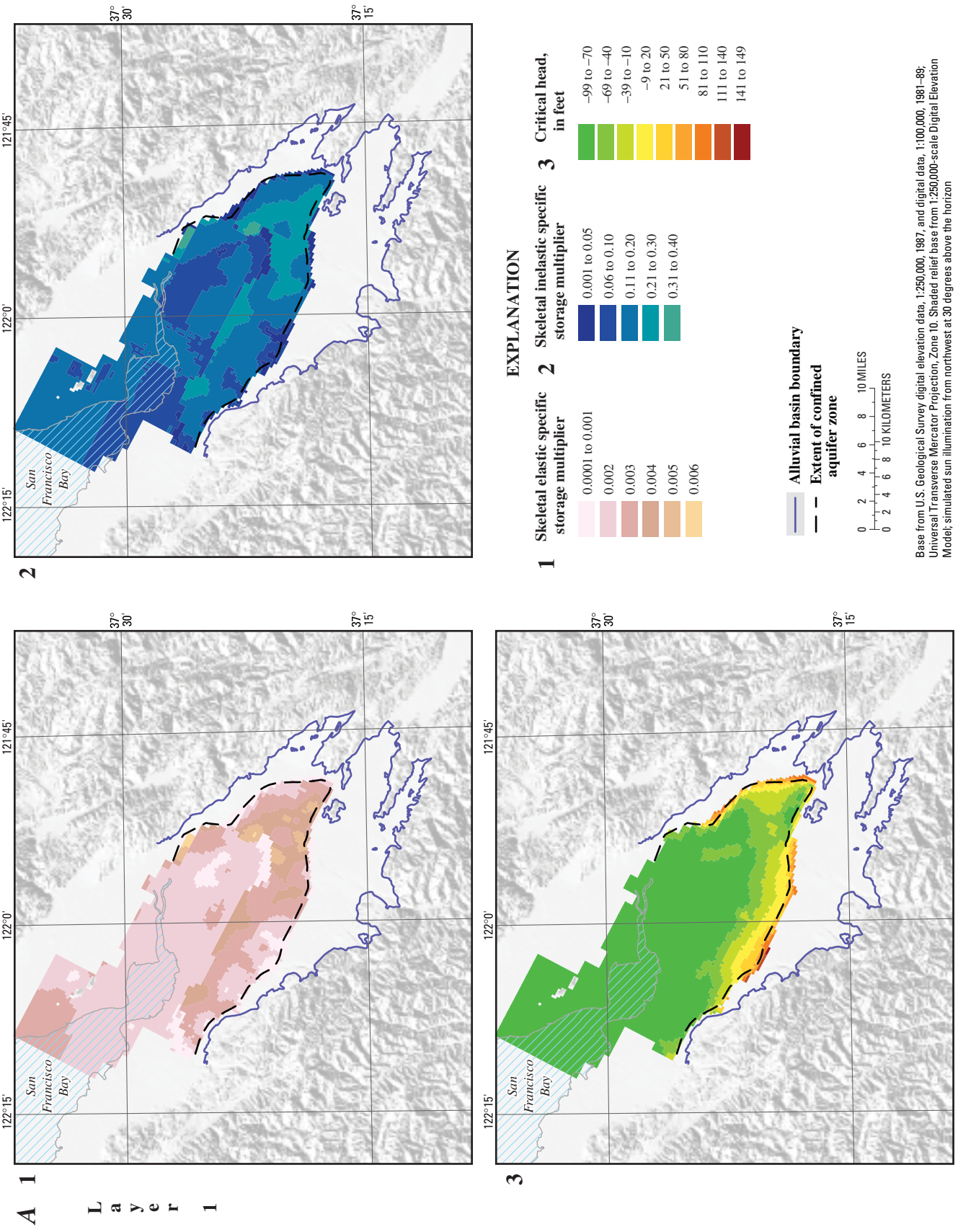

Figure 9. Ground-water flow model grid, skeletal elastic and inelastic storage multipliers, and critical heads for all model layers of the Santa Clara Valley model, Santa Clara Valley, California.

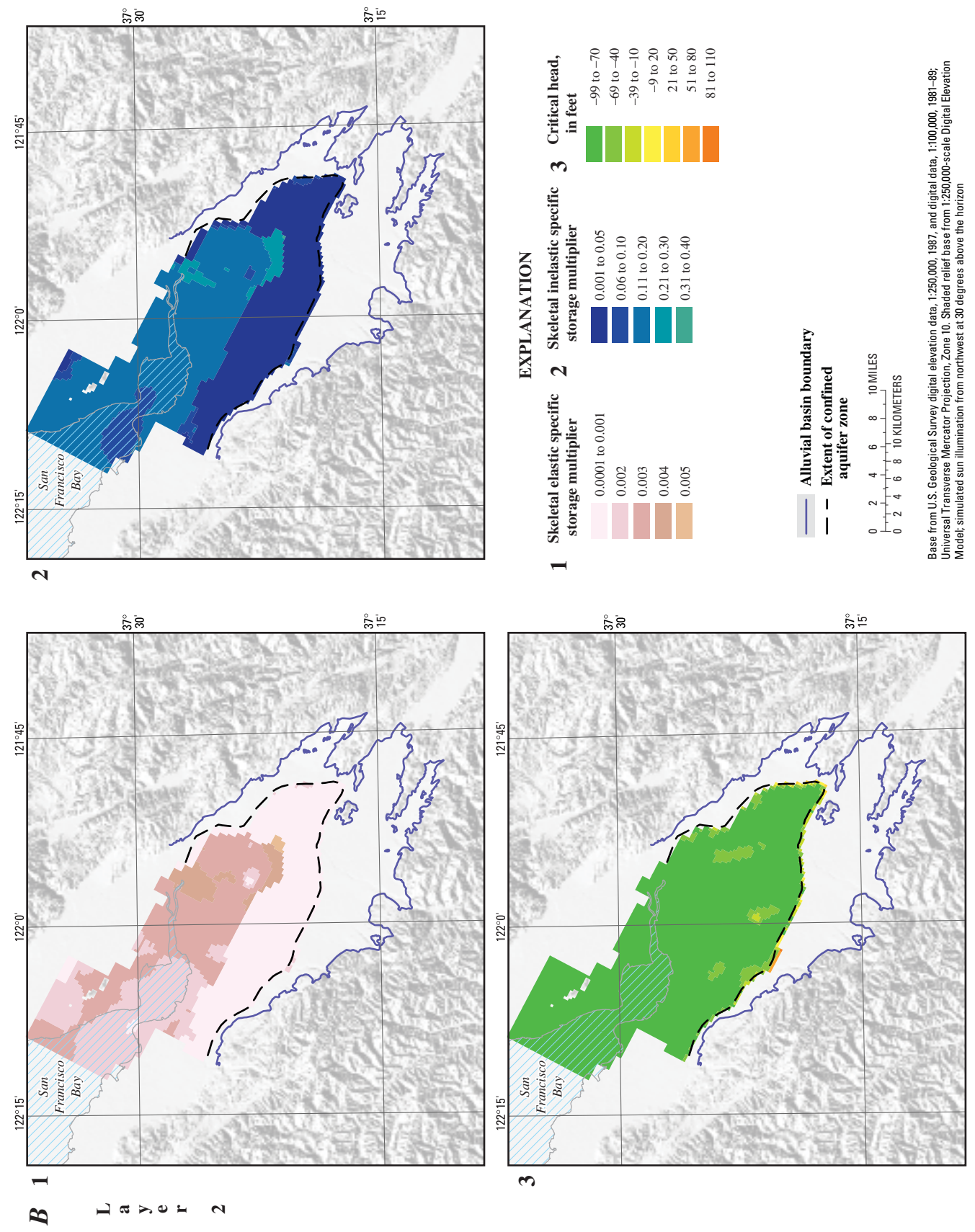

Figure 9. —Continued.

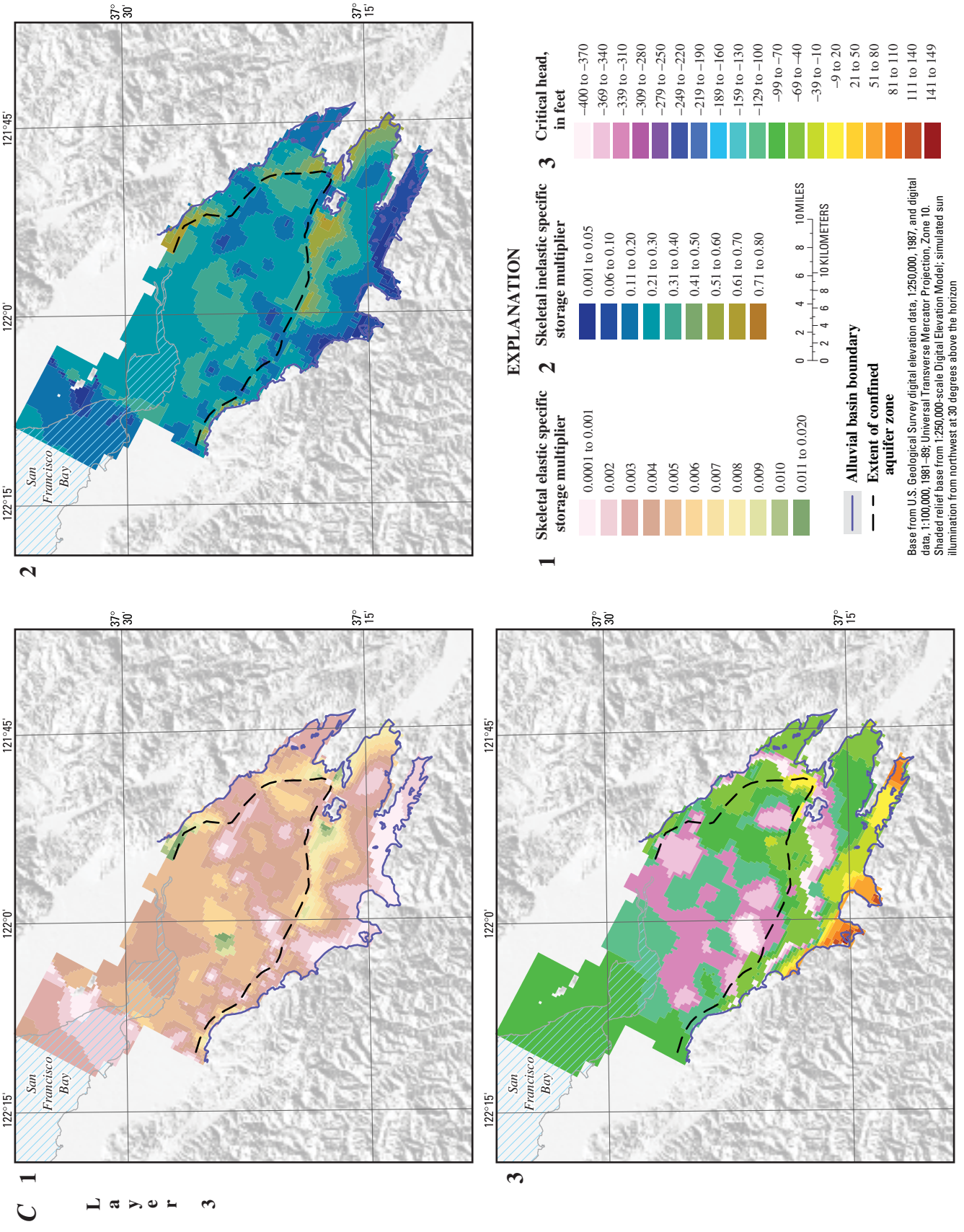

Figure 9. —Continued.

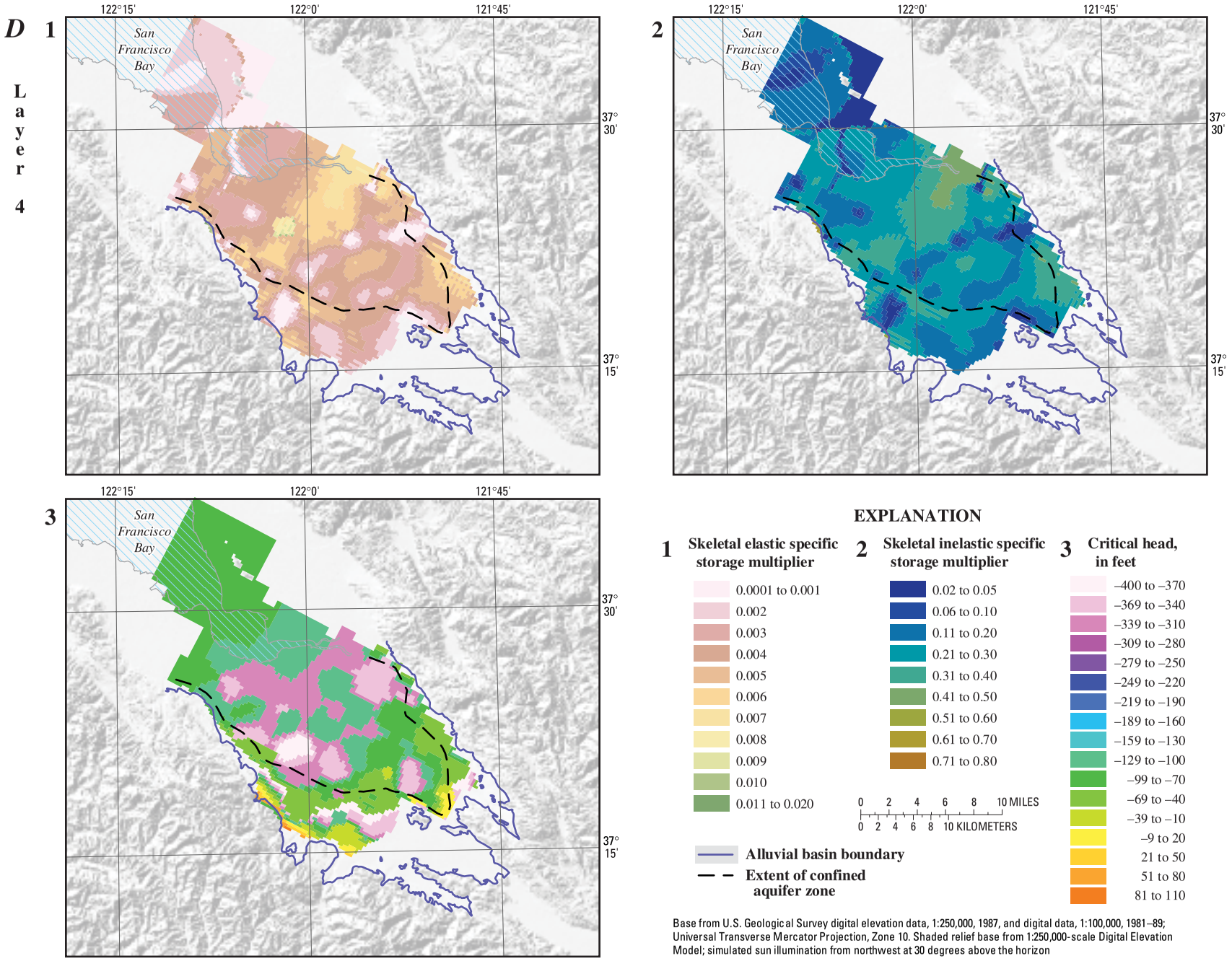

Figure 9.—Continued.

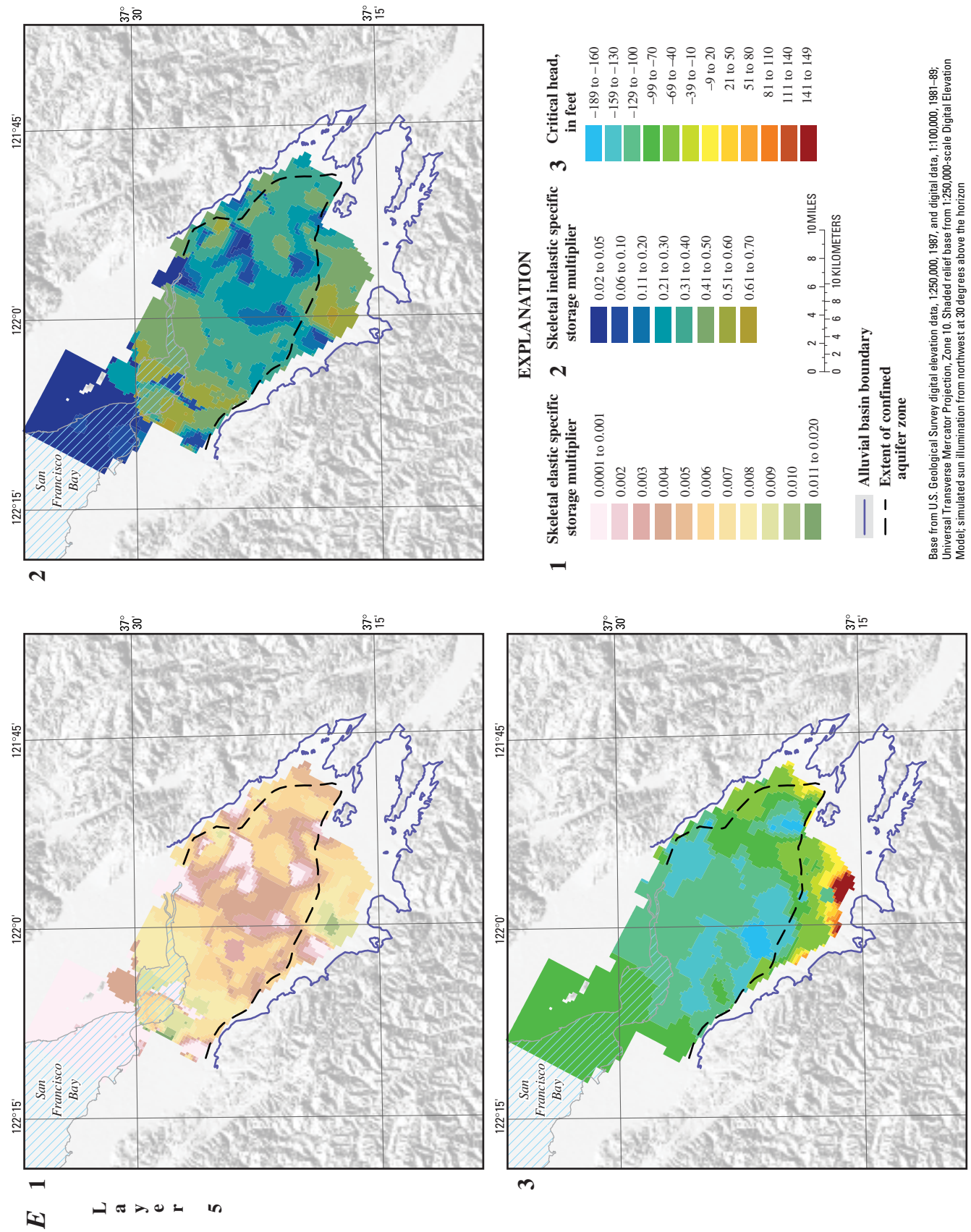

Figure 9. —Continued.

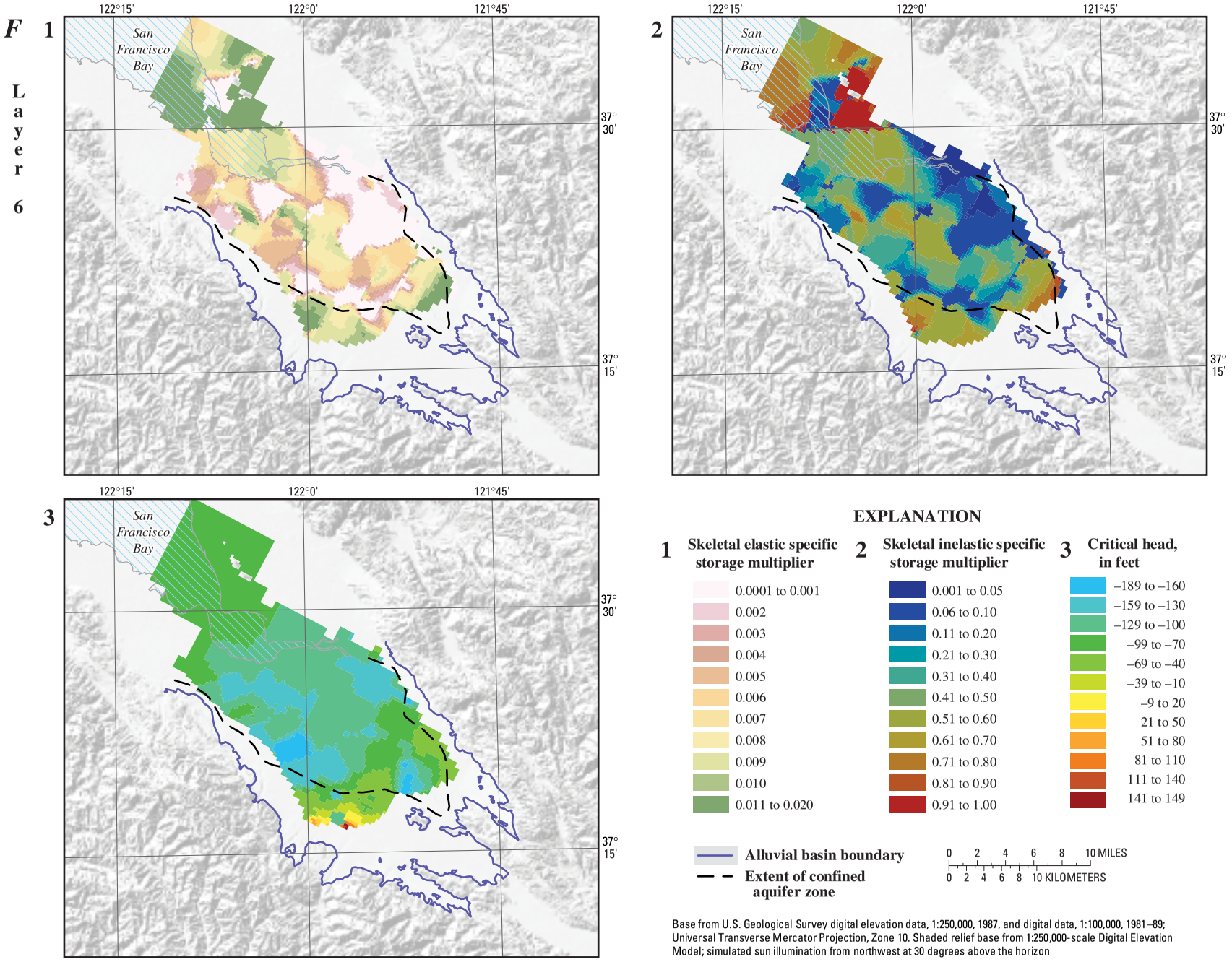

Figure 9.—Continued.

The simulated deformation is based on the change in head over each time step. The amount of deformation is based on the product of the compressibility of the aquitard and confining units within the regional system and their aggregate thickness in each cell of each model layer. The computed deformation represents the ultimate compression or compaction for a change in head that is instantaneous. Thus, the heads in adjacent aquifers and aquitards are assumed to be in equilibrium for each time step which, therefore, does not simulate delayed compaction. Because many of the individual aquitards are relatively thin (less than 20 ft thick), this was considered an acceptable approximation. In addition, the compressibilities are assumed to be constant for the entire simulation and are not dependent on changes in effective stress. Elastic compression or expansion is computed if the ground-water level (that is, head) in any cell is above the respective critical head. Inelastic compaction is computed if the ground-water level (that is, head) in any cell is below the critical head. If the simulated water level falls below the critical head in any time step, the critical head is updated to equal the new lower simulated ground-water level.

The estimates of skeletal elastic storage coefficients (S'_{fe}) were based on a combination of estimated values from consolidation tests, extensometers, and reported values (Ireland and others, 1984; Poland and Ireland, 1988; Hanson, 1989). An initial value of S'_{sfe} for fine-grained deposits of 3×10^{-6} ft^{-1} was assumed from other reported values for alluvial deposits (Ireland and others, 1984; Hanson, 1989). New specific storage values were estimated from consolidation-test data from samples of cores acquired during the recently completed monitoring-well sites (fig. 1). The skeletal elastic specific storage (S'_{sfe}) data from consolidation tests range from 2.7×10^{-6} ft^{-1} to 1.4 x 10^{-4} ft^{-1} and represent a geometric mean S'_{sfe} of 1.2×10^{-5} ft^{-1}. The graphical estimates of S'_{fe} for data collected for the period 1983–2001 are about 1.2×10^{-3} and 6.2×10^{-3} from the San Jose and Sunnyvale extensometers, respectively (location shown in fig. 1). These graphical estimates from extensometer data result in S'_{sfe} values on the order of 1.5×10^{-6} ft^{-1} and 1.5×10^{-5} ft^{-1} for San Jose and Sunnyvale, respectively, based on the aggregate thickness of fine-grained deposits. The S'_{fe} and S'_{sfe} estimates for the San Jose extensometer are comparable to the previous estimates of S'_{sfe} reported for the San Jose extensometer of 1.5×10^{-3} for S'_{fe} and 1.9×10^{-6} ft^{-1} for S'_{sfe} (Poland and Ireland, 1988). Even though the geometric mean from consolidation tests is about four times greater than the value commonly estimated from reported values, they fall within the range of values derived from graphical estimates of local extensometer data.

The estimates of inelastic storage (S'_{fv}) also were based on a combination of estimated values from consolidation tests, extensometers, and reported values. New specific storage values were estimated from consolidation-test data from samples of cores acquired during the recently completed monitoring-well sites. The inelastic specific storage (S'_{sfv}) values, which are consistent with the previously reported values, range from 6.0×10^{-5} ft^{-1} to 6.6×10^{-4} ft^{-1} and represent a geometric mean S'_{sfv} of 1.5×10^{-4} ft^{-1}. A graphical estimate of S'_{fv} for data collected for the period 1985–89 from the San Jose and Sunnyvale extensometers was 0.01, and results in an S'_{sfv} value of 2.1×10^{-5} ft^{-1}. A reported value of S'_{sfv} for fine-grained deposits of 2×10^{-4} ft^{-1} was assumed from reported values for other alluvial deposits (Ireland and others, 1984; Hanson, 1989) and reported values range from 1.5×10^{-4} ft^{-1} to 1.3×10^{-3} ft^{-1} for the Santa Clara Valley (Poland and Ireland, 1988).

The fine-grained interbed elastic skeletal storage coefficient (S'_{fe}) is denoted with the prime and was estimated on a cell-by-cell basis as the product of a single value of the aquifer skeletal specific storage (S'_{sfe}), 3×10^{-6} ft^{-1}, and the aggregate cell-by-cell thickness of the compressible fine-grained deposits (Leighton and others, 1994) for each active cell in every model layer (fig. 9) as:

$$S'_{fe,i,j,k} = S'_{sfe} \times Lsc2_{i,j,k}$$

where

$S'_{fe,i,j,k}$ is interbed elastic skeletal storage,

S'_{sfe} is the common, base multiplier value of interbed elastic skeletal specific storage for all model cells for model layer k; and

$Lsc2_{i,j,k}$ refers to the thickness of fine-grained sediments (2) for each cell in each model layer k.

The composite inelastic skeletal storage coefficient (S'_{fv}) was estimated as the sum of the products of the non-interbed inelastic skeletal specific storage coefficient (S'_{sfv1}) of 2.0×10^{-5} ft^{-1} with the thickness of coarse-grained sediments (sc4), the incompressible fine-grained sediments (sc1), and the mixed sediments (sc3), and the product of the inelastic specific storage coefficient (S'_{sfv2}) of 2.0×10^{-4} ft^{-1} and the thickness of the compressible fine-grained sediments (sc2) (fig. 9) as:

$$S'_{fv,i,j,k} = (S'_{sfv1} \times [Lsc1_{i,,j,k} + Lsc3_{i,j,k} + Lsc4_{i,j,k}]) + (S'_{sfv2} \times Lsc2_{i,j,k})$$

where

$S'_{fv,i,j,k}$ is inelastic skeletal storage,

S'_{sfv1} is the base multiplier value of non-interbed inelastic skeletal specific storage for all model cells for model layer *k*;

S'_{sfv2} is the base multiplier value of interbed inelastic skeletal specific storage for all model cells for model layer *k*; and

$Lsc(1–4)_{i,j,k}$ refers to the thickness of sediments for category 4, 3, 2, and 1 and represents the proportional layer thickness of coarse-grained (4), mixed (3), and compressible fine-grained sediments (2) and incompressible fine-grained sediments (1), for each cell in each model layer *k*.

The application of aggregate thickness for estimation of interbed and confining-layer storage properties has been applied in similar alluvial aquifer systems (Hanson and others, 2002a; Hanson and Benedict, 1994; Hanson and others, 1990) and has been shown to be related to depositional environments in alluvial aquifers (Anderson and Hanson, 1987; Johnson and Dreiss, 1989; Johnson, 1995a, b).

The critical head is defined as the past maximum water-level altitude that resulted in inelastic compaction and was determined during model calibration. The critical head was initially set equal to the initial head, with the assumptions that the initial heads were representative of January, 1970, conditions and that the fine-grained deposits were normally consolidated. This approach resulted in anomalous changes in storage and increased water levels during the first few years of the simulation. Critical heads were previously estimated as being 80 ft lower in 1967 than in 1978 on the basis of the artesian head recovery at the San Jose index well (7S/1E-7R1/6M1; Poland and Ireland, 1988); this estimate is consistent with other estimates of critical (preconsolidation) heads (Holzer, 1981). Thus the critical heads were then uniformly reset to 80 ft below the initial conditions. A large decrease in head in the peripheral parts of model layer 3 outside a region defined by more than 0.1 ft of historical subsidence continued creating large contributions to storage. To eliminate this artifact, the critical heads were decreased another 160 ft in the peripheral areas of model layer 3. In addition, for cells located within the historical cones of depression, the critical heads were reduced another 10 ft to allow for a small amount of inelastic compaction in the late 1980s near the San Jose index well after the dry period in the late 1970s. The resulting critical-head values were based on model calibration and may represent a lower bound of critical heads within the basin and within specific model layers (fig. 9). Critical heads may nevertheless be uncertain in some parts of the basin because water-level declines during the droughts of the simulation period may not have exceeded historical low water levels.

Pumpage

The pumpage for the USGS–SCVWD Santa Clara Valley Model (SCVM) simulates pumpage from water-supply, industrial, and irrigation wells throughout the valley. Many of these wells are screened across multiple aquifers. In addition to these multi-aquifer wells, there are hundreds of wells that are not used or are used intermittently and may transmit flow between aquifers screened in these wells (fig. 10). For this reason, the multi-node well (MNW) package was developed as part of this project to more accurately simulate the effects of thousands of multi-aquifer wells (Halford and Hanson, 2002; McDonald, 1986). The multi-aquifer well package (McDonald, 1986) was initially developed for the original MODFLOW-88 (McDonald and Harbaugh, 1988); the new multi-node well package is used with MF2K (Harbaugh and others, 2000b) for the SCVM. The ability to dynamically apportion wellbore flow and allow for wellbore flow in unpumped wells has a significant effect on the calibration of regional ground-water flow systems (Halford and Hanson, 2003a,b) and on the distribution of other head-dependent inflows and outflows such as subsidence and streamflow infiltration (Hanson and others, 2003).

The pumpage for the initial calibration and verification period (1970–89) was modified from the seasonal distribution of pumpage used in the original ground-water flow model of the Santa Clara Valley (CH2M Hill, 1991, 1992a,b). The revised pumpage reuses the original seasonal pumpage but it is specified on a monthly basis. This initial distribution of pumpage only specified wells that were actively pumped. This resulted in a monotonic decrease in the number of wells from 1,466 to 647 (fig. 11). This distribution of wells through time does not account for the possibility of wells providing intrawellbore flow between aquifers under nonpumped conditions. The revised pumpage includes all unpumped wells that span more than one model layer to simulate the potential for intrawellbore flow. Few new wells have been constructed in the 1990s, and hundreds have been destroyed since the 1970s (Behzad Ahmadi, Santa Clara Valley Water District, unpub. data, 2000). The number of unpumped wells is additionally reduced by the wells that have been destroyed for each month of the simulation.

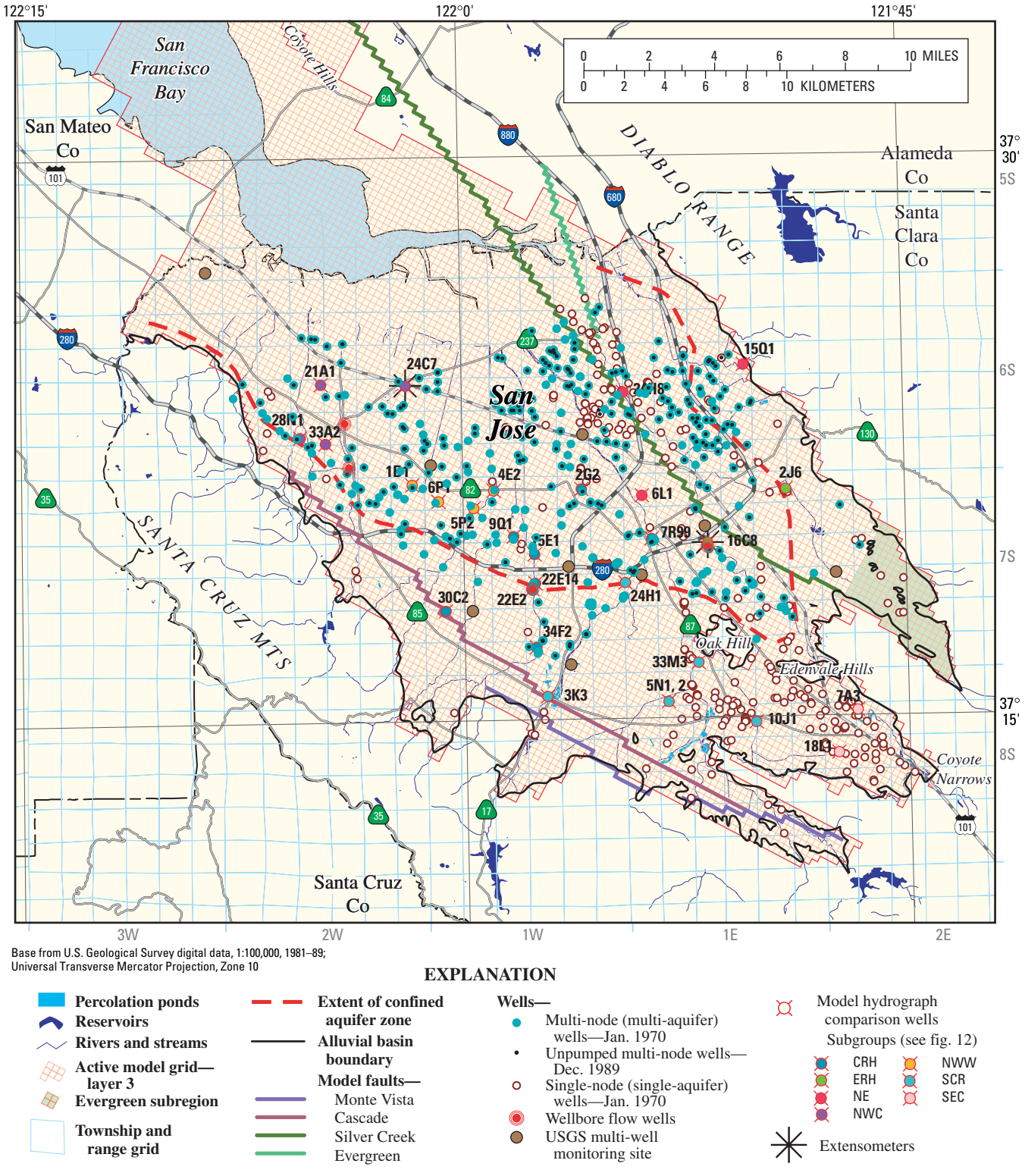

Figure 10. Distributions of simulated pumped and nonpumped multi-aquifer wells, and single-aquifer wells for the Santa Clara Valley, California.

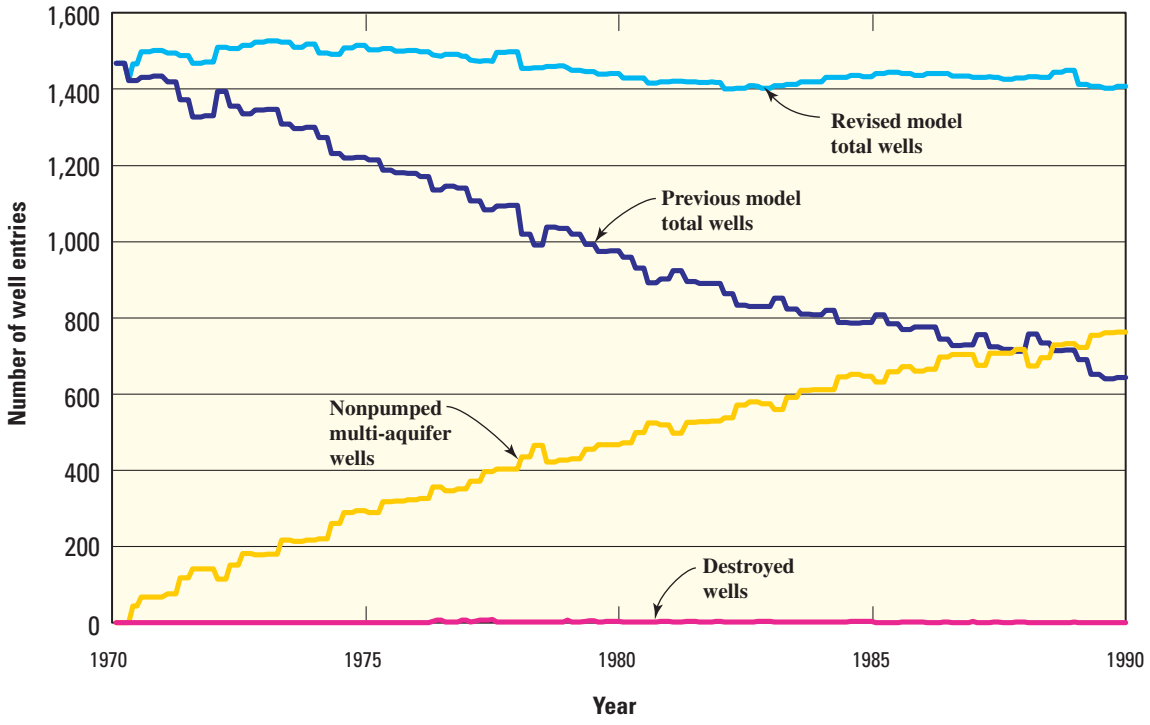

Figure 11. Distributions of simulated pumped, nonpumped, and destroyed wells for selected monitoring wells, Santa Clara Valley, California.

The revised pumpage is composed of three types of wells: single-aquifer wells, multiple-aquifer pumped wells, and multiple-aquifer unpumped wells. The single-aquifer wells predominantly occur in the southern and central parts of the valley (fig. 10). The multiple-aquifer wells occur throughout the valley and can span two to four model layers (fig. 10). Similarly unpumped multiple-aquifer wells occur throughout the valley as shown for December1989 (fig. 10).

The application of the MNW package to simulate multiple-aquifer well pumpage required the specification of the location of the wells (model row and column), the layers spanned by the well screens, the well radius, and the skin factor (Halford and Hanson, 2002). For single-aquifer wells, the well is specified as a single entry for any stress period that has nonzero pumpage. For multiple-aquifer wells, the well is specified using multiple records that are grouped together and represent the set of model layers that the well screens span. The initial distribution of pumpage from the previous model for the period 1970–89 was specified for layer specific pumpage. However, the MNW package reestimates the distribution of pumpage from the set of model layers for each well and for each time step because this vertical distribution of pumpage is head dependent. The reported well radius was specified if known or was assumed to be 0.87 ft (i.e. 8 in.) if unknown. The skin factor represents the potential linear, wellbore frictional-entrance flow losses (Halford and Hanson, 2002, eqn. 3) and was initially estimated to be 5 for all wells in all layers in all stress periods. The discharge for unpumped multiple-aquifer wells was specified as zero for any stress periods that had no reported pumpage. Similar to pumped wells, the vertical distribution of wellbore flow in unpumped wells is head dependent and is reestimated by the MNW package for every unpumped well for all time steps.

The updated pumpage for the period 1990–99 was estimated on a monthly basis for each well by SCVWD (Roger Pierno, Santa Clara Valley Water District, unpub. data, 2002) and added to the previous pumpage used for the previous model simulation period, 1970–89. Over 90 percent of the pumpage represents pumpage by the major water purveyors. This pumpage was reported on a monthly basis. The remaining 10 percent of predominantly domestic pumpage is reported on a biannual or annual basis. This pumpage was prorated on a monthly basis from the annual distribution of the monthly reported pumpage (Roger Pierno, Santa Clara Valley Water District, unpub. data, 2002). These pumpage data also include wells that are not pumped and have not been destroyed and therefore provide a conduit for flow.

Coastal Flow

Flow along the coastal boundary and beneath southern San Francisco Bay is represented by general-head boundaries. In the revised model, water exchange between the aquifer and San Francisco Bay is simulated using the general-head boundary (GHB). Two types of GHBs were specified. The first type of GHB simulates potential submarine and estuary areal leakage, which represents the vertical flow coming across the bay mud from or to the aquifer just below it in the coastal and offshore regions of model layer 1 (fig. 5). The second GHB type simulates offshore ground-water underflow along the northwestern edge of the model grid. These underflow GHB boundaries were represented by a line of GHB cells along the offshore northwestern margin of model layers 2 through 6. The GHB line simulates the potential lateral inflows and outflows of the lower aquifers (model layers 2 to 6) from external sources such as adjacent Bay Area aquifers. For model layer 1, GHB is specified for cells northwest of the shoreline; for the rest of the model layers, GHB is specified only at the edge cells below the Bay.

The boundary heads of the external source in GHBs are assumed to be approximately equal to the average hydrostatic head of the Bay and were set equal to sea level. They are uniform everywhere regardless of depth and surface location. The conductance of GHB is defined as the product of the hydraulic conductivity of the aquifer along the submarine boundary of the aquifer within the model GHB cells and the cross-sectional area perpendicular to the ground-water flow divided by the distance from the center of the GHB cells to the external point of reference.

For the first type of GHB boundary that represents areal vertical leakage in model layer 1, the area of the model cells is a constant value equal to the area of the model cells, and a value of 0.0027 ft/d was assigned to the vertical hydraulic conductivity, K_V. This K_V is the same as the vertical hydraulic conductivity of bay mud estimated by the CDWR (California Department of Water Resources, 1967). The thickness of the bay mud may vary areally and was assumed to be equivalent to half of the aggregate thickness of compressible fine-grained deposits of each areal-GHB cell in model layer 1.

For the second GHB type where the line of GHB cells simulates underflow beneath the San Francisco Bay, the K of the conductance is equal to the horizontal hydraulic conductivity of the model cell where the line GHB is located. The distance to the boundary is a uniform half width of the boundary model cell of 500 ft. The area perpendicular to flow is the product of the cell-by-cell thickness of the layer and the constant model-cell width. The conductance of each boundary line-GHB cell was set to twice the transmissivity of that model cell.

Initial Conditions

Initial conditions are the distribution of water levels at every active cell within each of the six model layers. The initial water levels were those of the previous model (CH2M Hill, 1991) and were derived from historical water levels; they represent average winter 1970 conditions. These water levels did not contain water-level differences between model layers that are inherently present in a regional ground-water flow system. However, minor adjustments to the initial water levels were required to compensate for numerous dry cells that were simulated in the previous model. Therefore, the initial heads may not represent steady-state conditions in some parts of the model and for parts of some layers.

Model Revisions

Calibration and model development began with the previous model (CH2M Hill, 1991). The transition from the previous model to the revised model was a sequence of revisions and related calibration steps. The first revisions from the previous model were the modifications to the temporal and spatial discretization, which helps to better separate the supply (inflow) and demand (outflow) components of the ground-water flow system. On the basis of the finer discretization, the new estimates of artificial and natural recharge, evapotranspiration, and coastal flow boundaries were then implemented. The model was then transformed from the MODFLOW-88 structure to the MODFLOW-96 structure. After the revised boundary conditions were implemented, the multi-node well package, the interbed storage package, and the horizontal flow barrier package were added to the revised model.

The revised model was then transformed from MODFLOW-96 to MF2K. After intermediate calibration, the estimation of the hydraulic properties was transitioned from the zone-based estimates of the previous model to the lithological cell-based estimates of the revised model using the LPF package of MF2K. The Evergreen subregion, which was deactivated in the previous model, was then added back into the active flow region. Finally, the model was updated to include the additional inflows and outflows for the period January 1990 through September 1999.

Model Calibration

Model calibration was an integral part of upgrading and updating the previous model. Calibration was achieved through trial-and-error adjustments to natural recharge and hydraulic properties in order to achieve a good fit within each subarea over the historical period of simulation. These adjustments were made as systematically as possible, starting with the boundary inflows, recharge, and streamflow and then hydraulic properties. The initial calibration was completed for the model upgraded with new inflows, outflows, and hydraulic properties during the original historical period of simulation, 1970–89. Then the model was updated to simulate an additional 9.75 years (1990–99) of inflows and outflows. Additional calibration adjustments were made on the basis of model performance during this additional historical period of simulation. The addition of the remaining historical period, 2000–03, was not made because selected measured inflows and outflows were not available at the time of completion of this study.

Transient-State Calibration

Transient-state calibration was based primarily on spatially distributed temporal comparisons. Calibration adjustments were related to the combined fitting of the ground-water levels (fig. 12), streamflow (fig. 13), and subsidence (fig. 14) time series. In addition, comparisons of all ground-water levels were made relative to the previous model and for selected portions of the period of calibration (fig. 15). Maps of ground-water levels were used for limited comparisons for the updated period but were considered less reliable than time-series data because the composite water-level measurements and hand contours represent averaged conditions in many areas where there are large vertical-head differences within some parts of the aquifer systems. An overall estimate of model fit was made using all of the temporal comparison ground-water level data and extensometer data for the transient simulation. The final distribution of ground-water levels through time shows the effects of the time-varying recharge and pumpage as well as the effects of the faults on ground-water flow (Animation 1. Map showing simulated water levels, 1970–99, for the Santa Clara Valley model, Santa Clara Valley, California.).

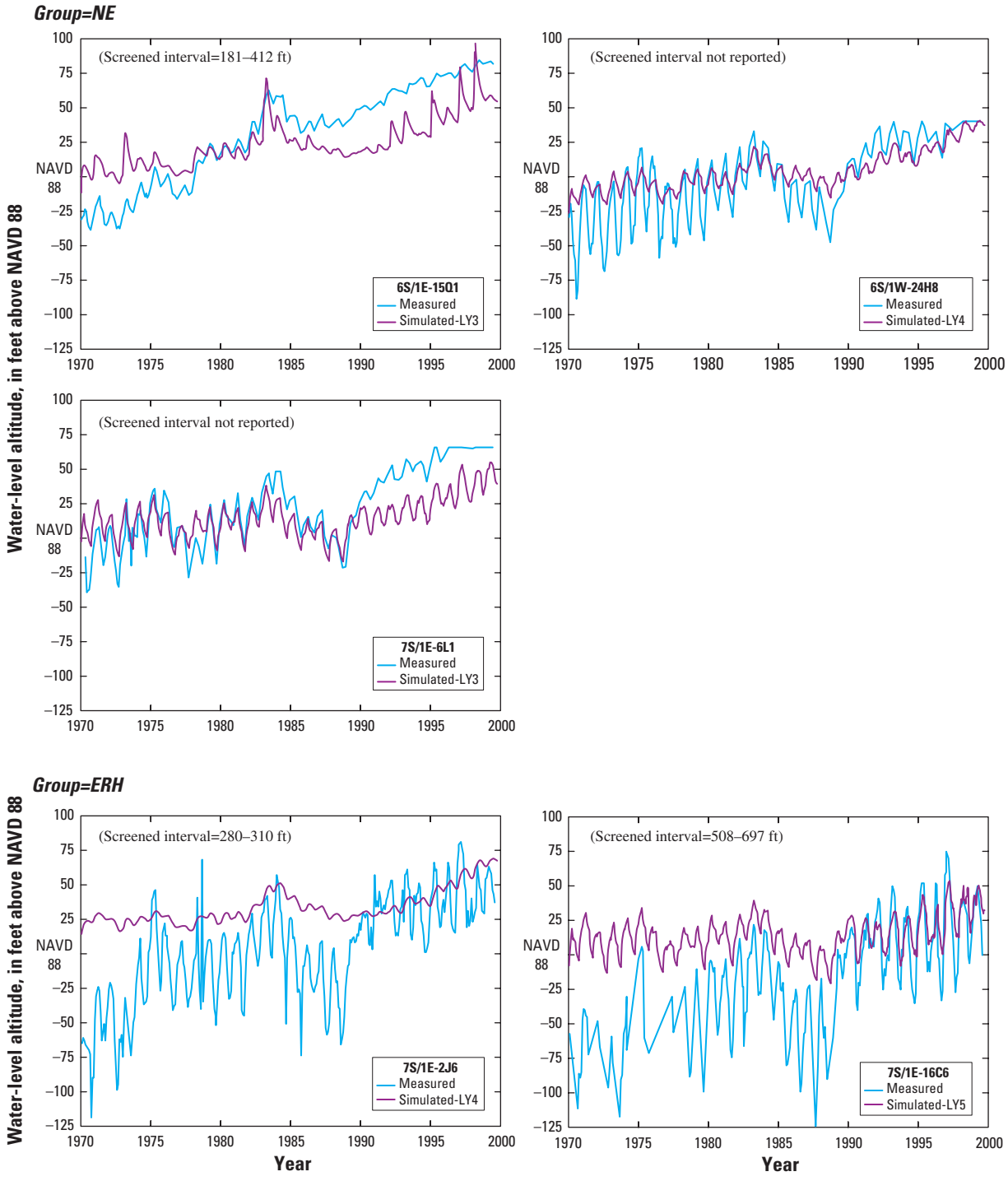

Figure 12. Measured and simulated water-level for selected long-term monitoring wells, Santa Clara Valley, California.

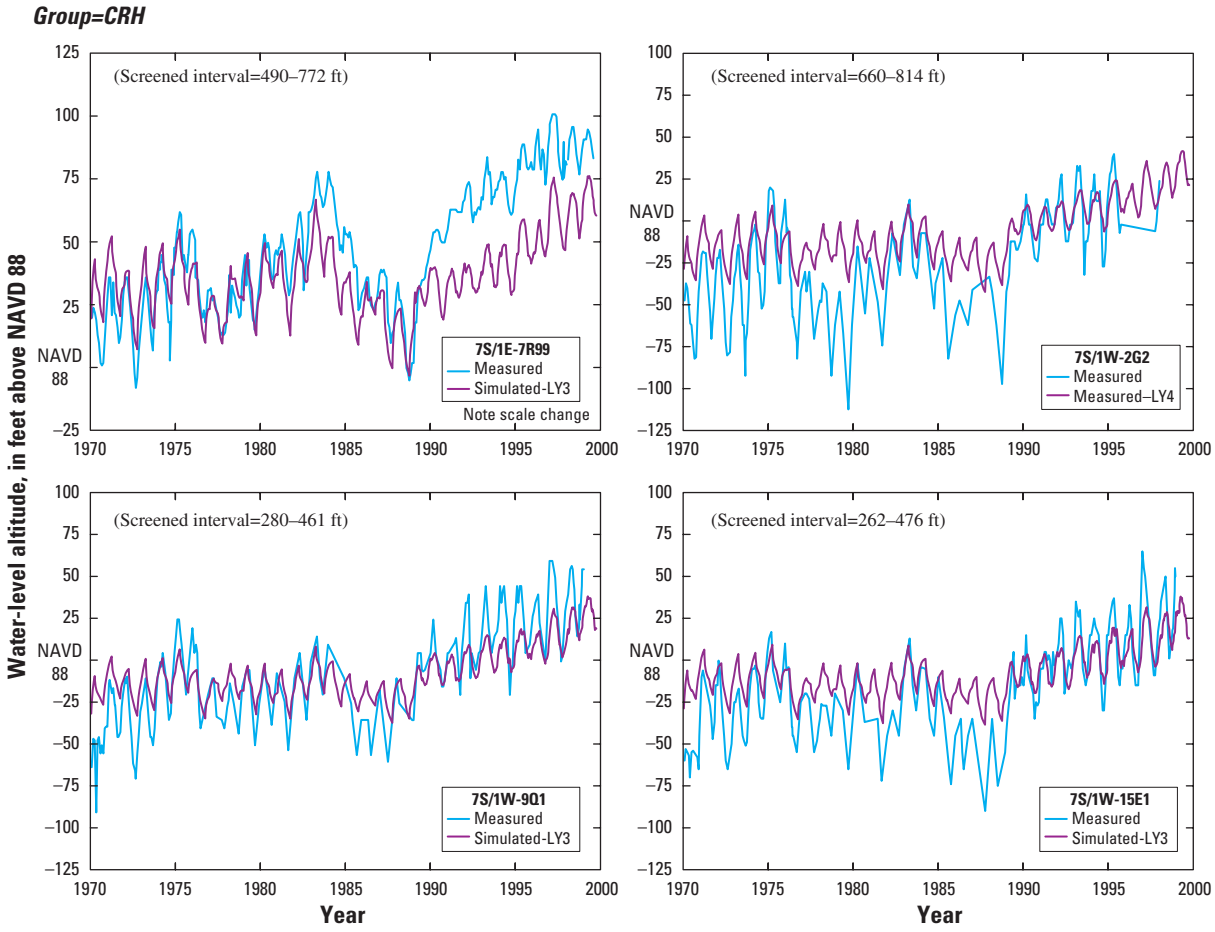

Figure 12. —Continued.

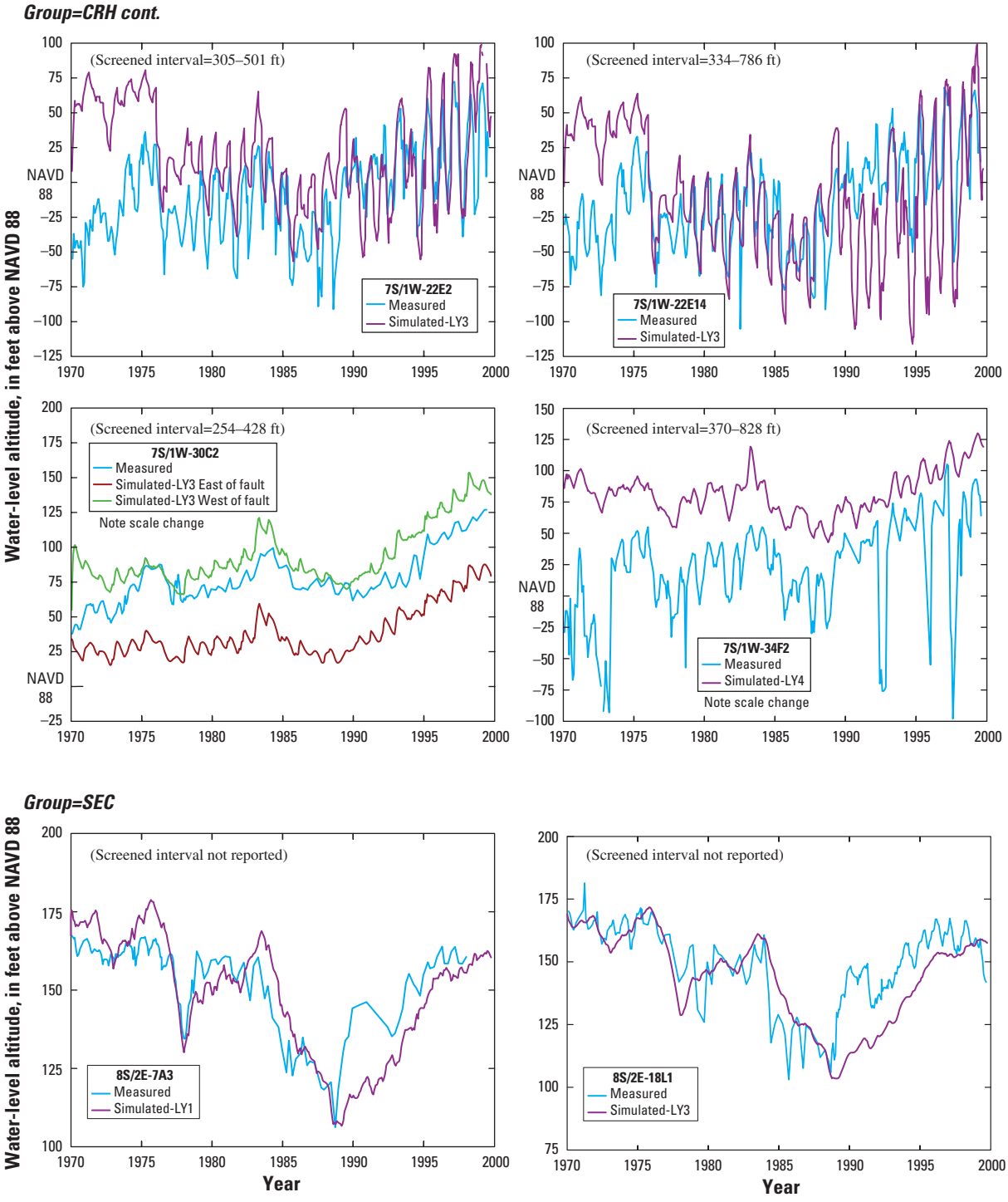

Figure 12. —Continued.

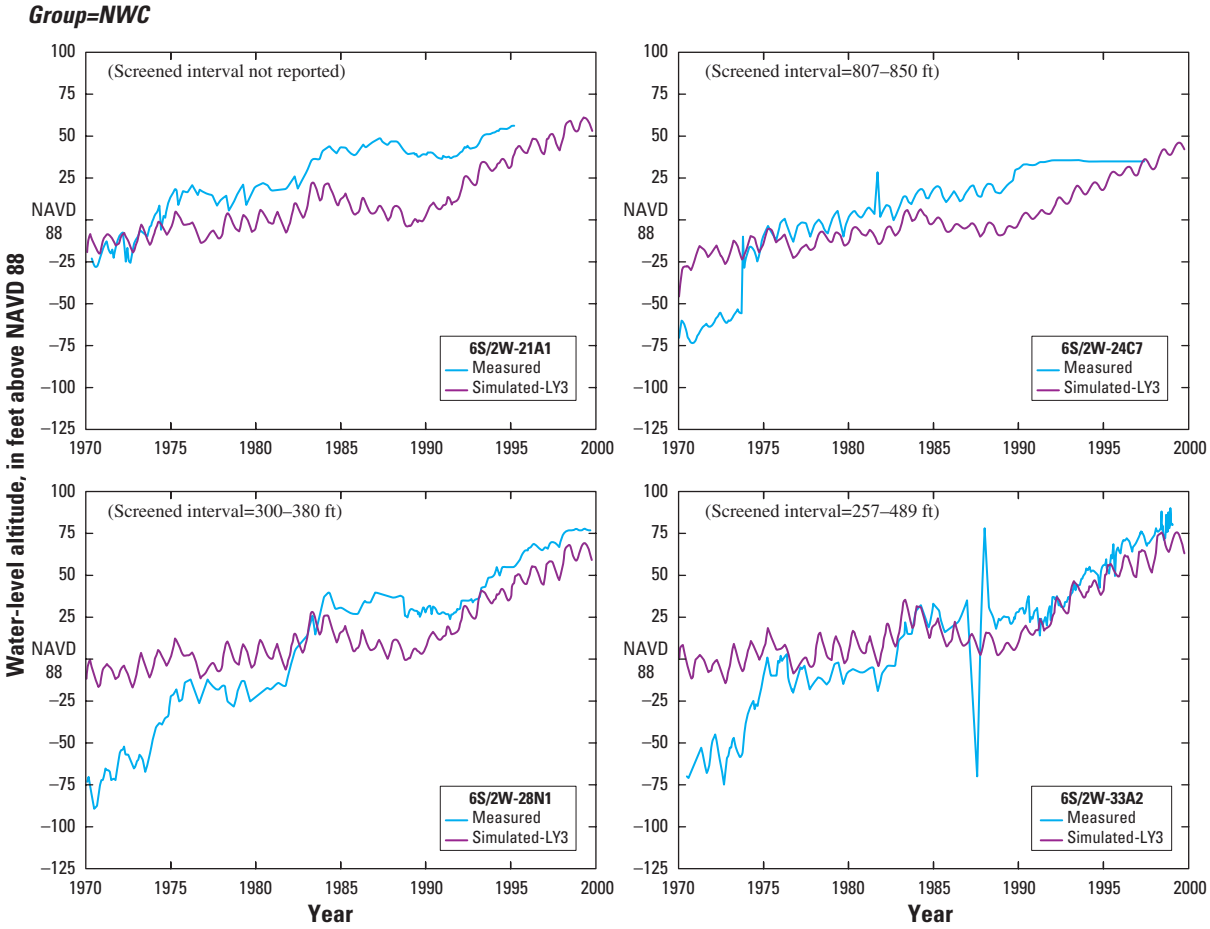

Figure 12. —Continued.

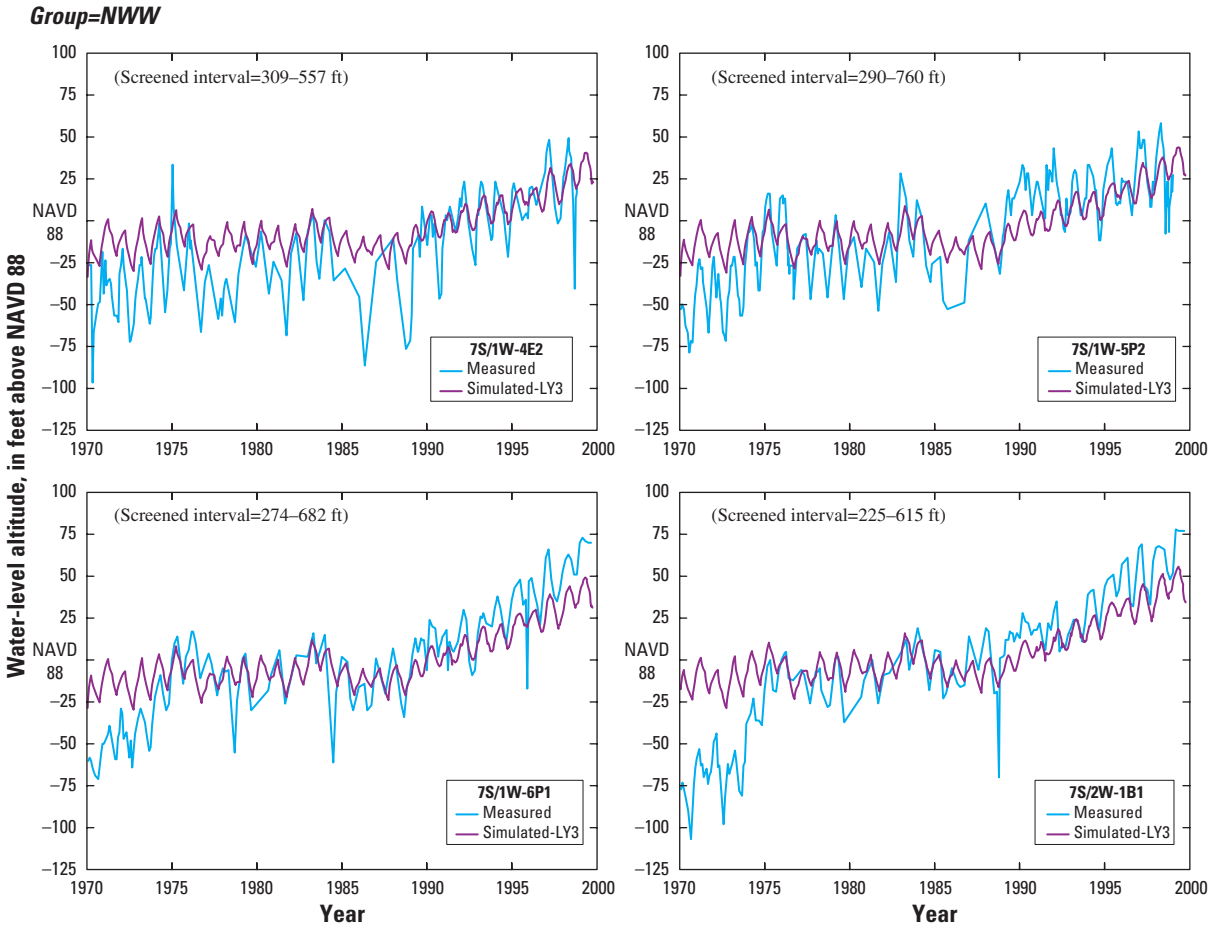

Figure 12. —Continued.

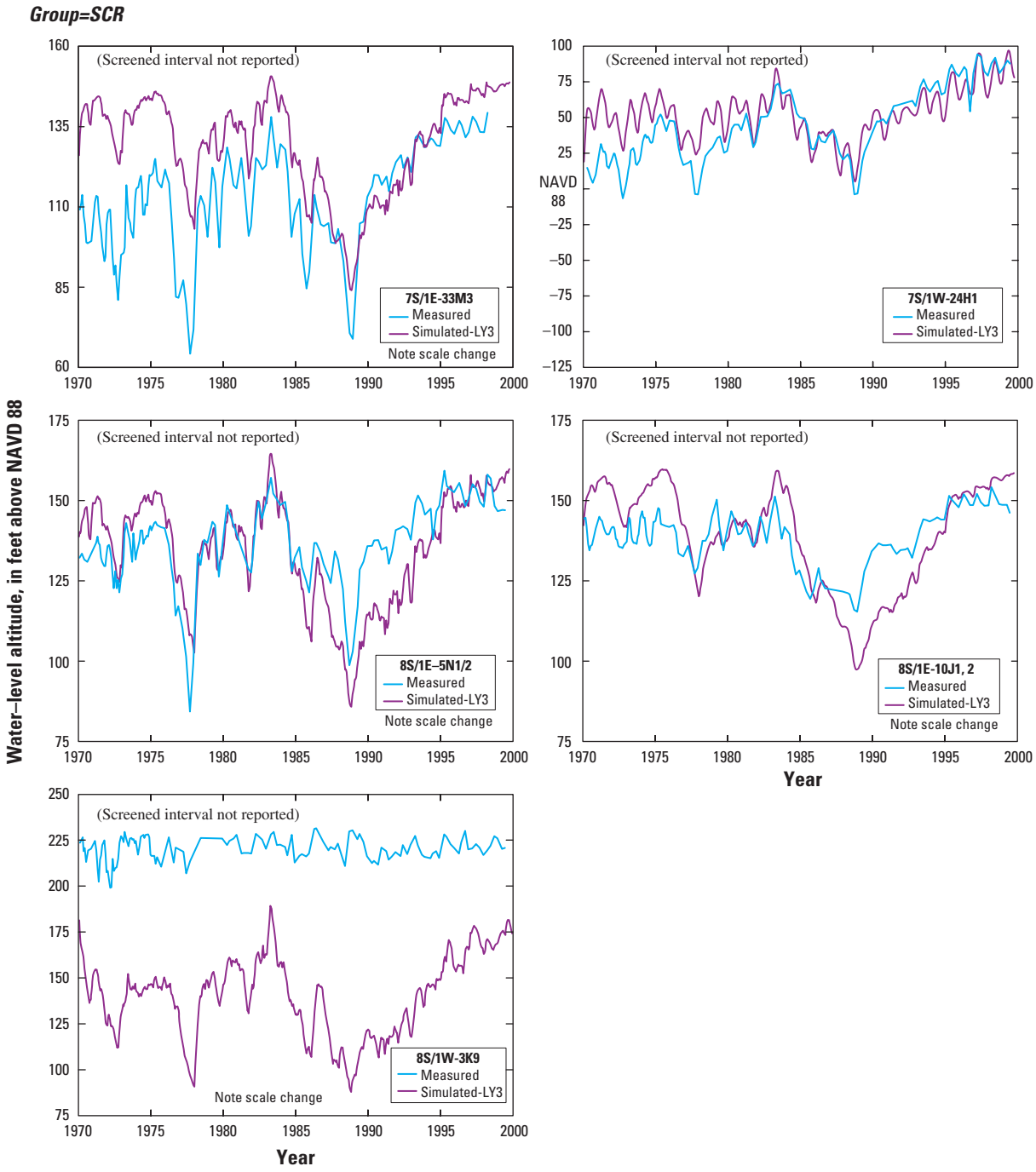

Figure 12. —Continued.

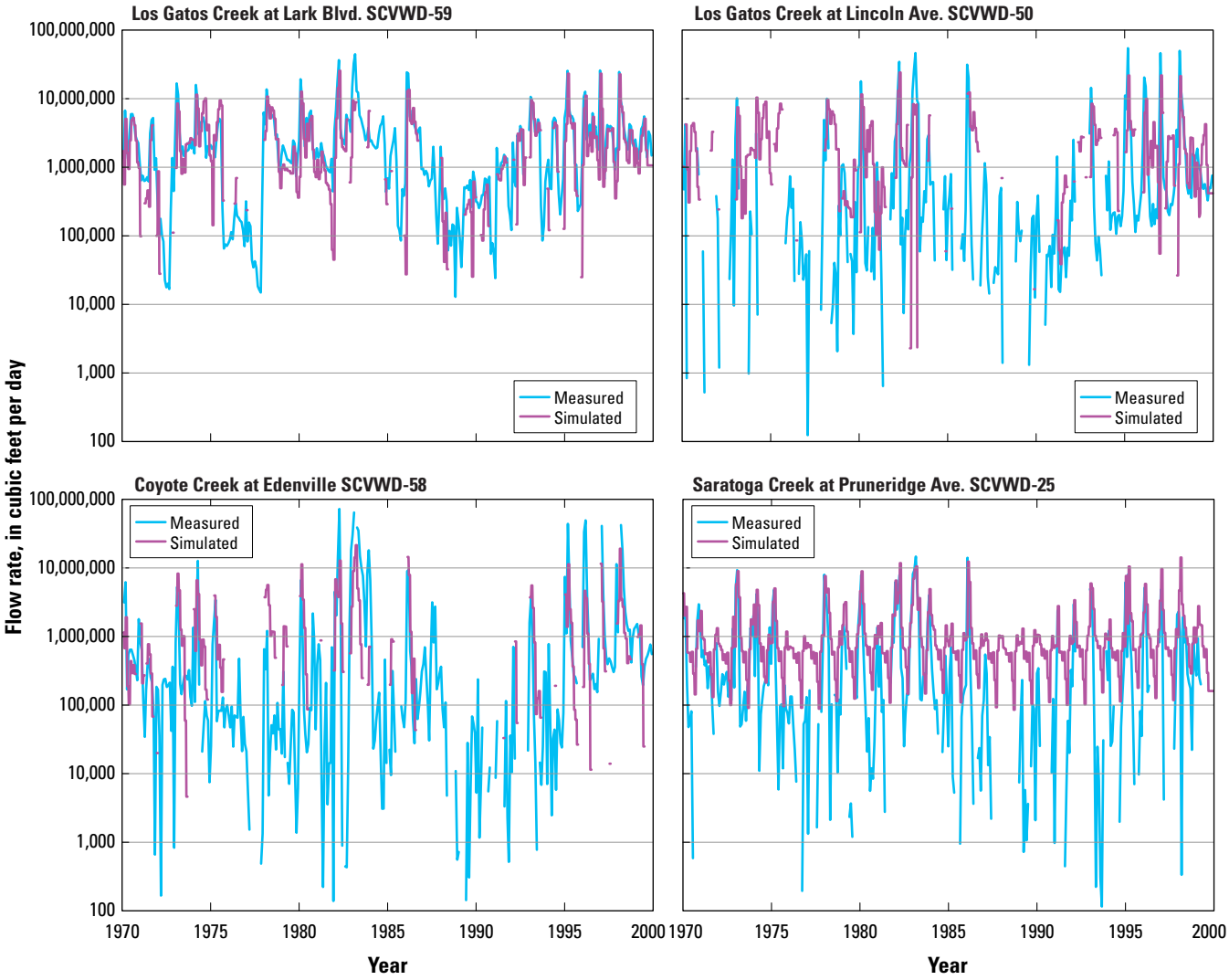

Figure 13. Measured and simulated streamflow for selected downstream gaging stations, Santa Clara Valley, California (Well locations shown on figure 1).

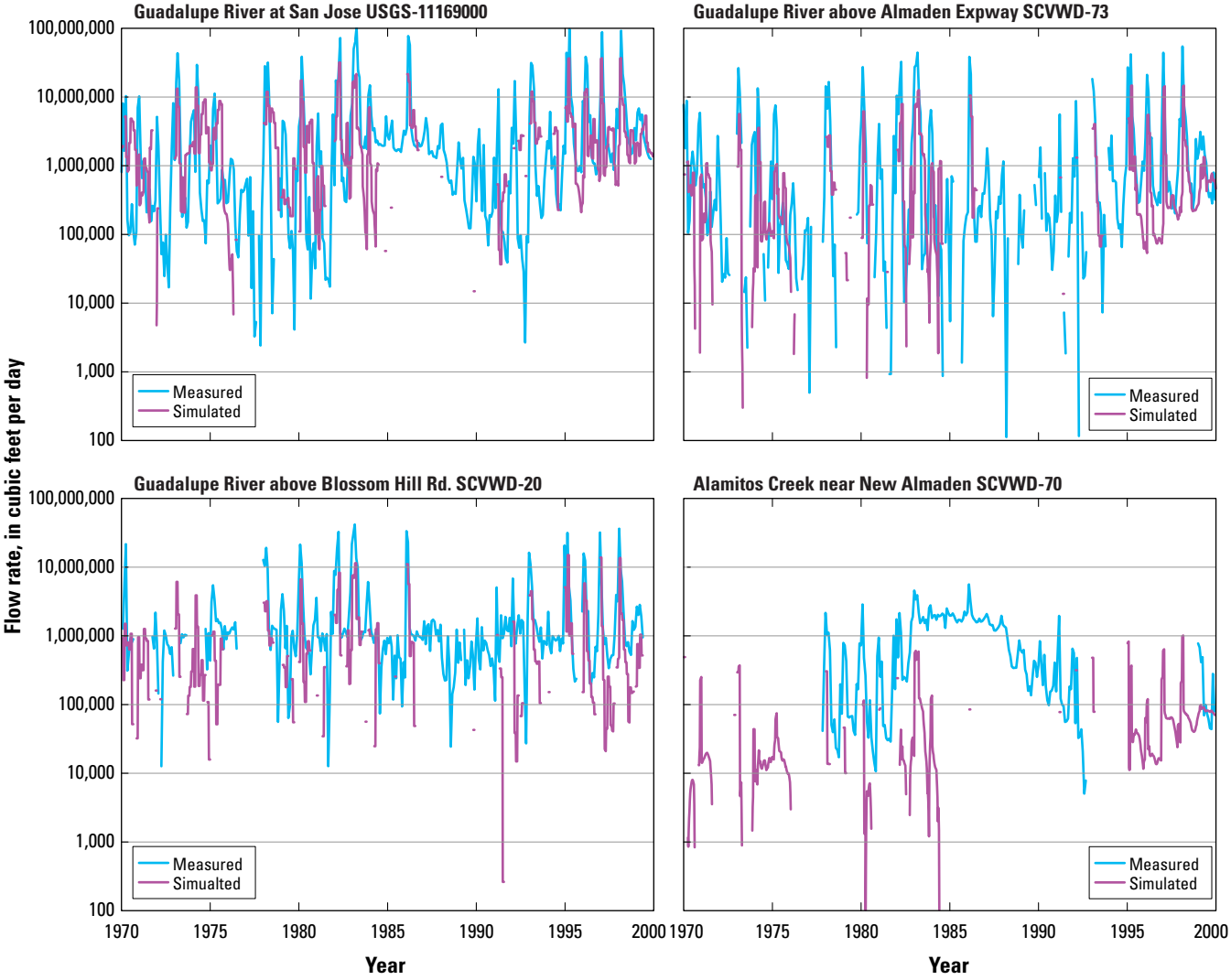

Figure 13. —Continued.

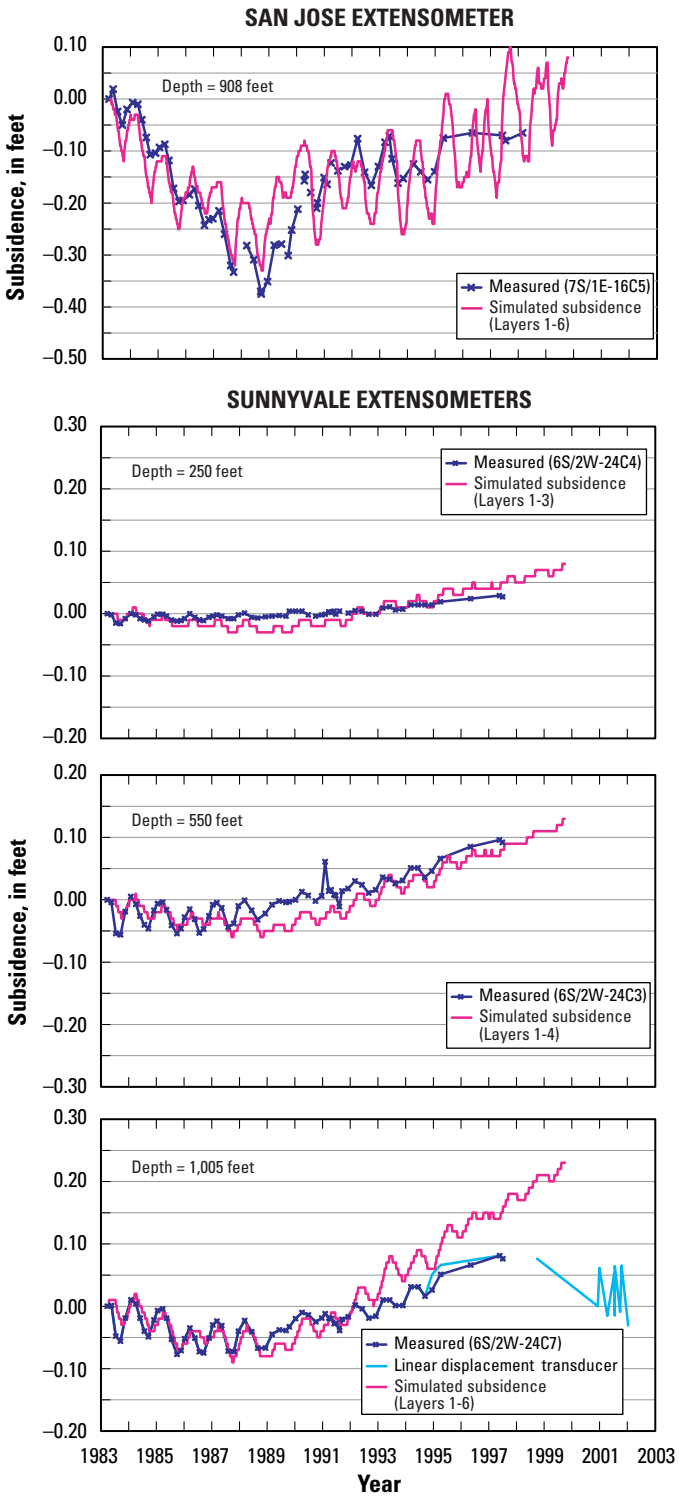

Figure 14. Measured and simulated aquifer-system subsidence for selected extensometer wells, Santa Clara Valley, California.

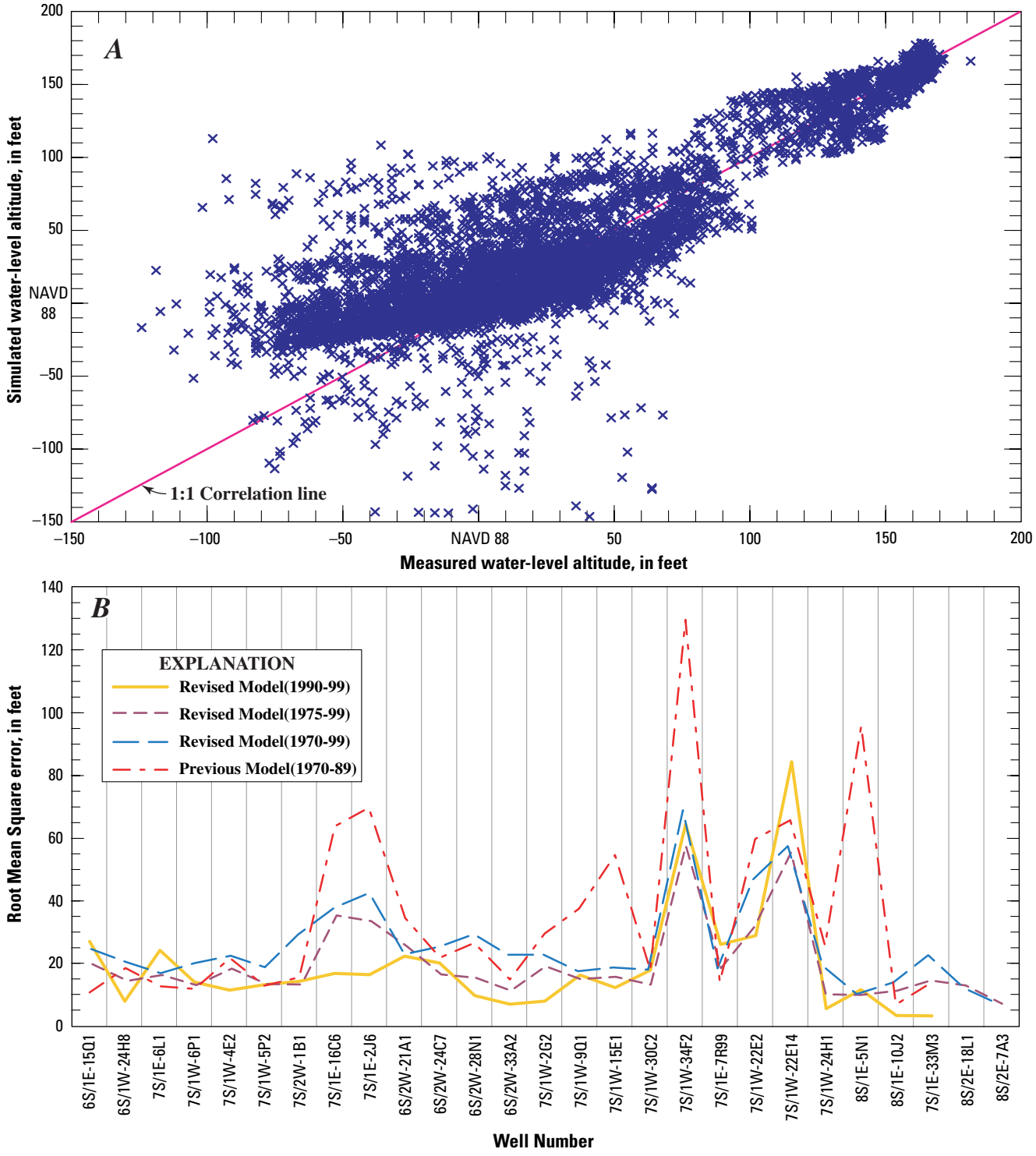

Figure 15. Measured and simulated water-level error for selected monitoring wells (A) for all measurements and (B) for each comparison well, Santa Clara Valley, California.

Calibration of transient-state conditions was dependent on recharge (streamflow, valley-floor recharge, and artificial recharge) to and discharge (pumpage, streamflow, and ET) from the aquifer system and on hydraulic conductivity, storage, vertical hydraulic conductivity between layers, fault hydraulic characteristic, and general-head boundary conductance. During calibration, inflows such as reported pumpage and reported artificial recharge were implemented at the reported values and were not adjusted. The implementation of the multi-node well package maintained the net pumpage but redistributed ground-water flow vertically between layers through intrawellbore flow (Animation 2. Map showing simulated wellbore flow for model layers 3 and 5, 1970–99, for the Santa Clara Valley model, Santa Clara Valley, California.). Model parameters related to smaller inflows and outflows such as ET and GHB also were not adjusted during model calibration. The transformation in layer 1 from constant heads in the previous model to general-head cells also resulted in a smaller region of cells that are now restricted to the offshore region beyond the present coastline.

After replacement of the recharge, evapotranspiration, and coastal flow boundaries, the model was calibrated for goodness of fit for the 28 water-level hydrographs (fig. 12). These hydrographs were combined into seven groups on the basis of location, hydrologic setting, and related characteristics of the water-level fluctuations (figs. 1, 12). Model calibration began with a quantification of the model error and flow analysis from the previous model as a partial basis of comparison for the revised model.

After the new recharge boundary conditions were implemented, the recharge was adjusted. The mountain-front recharge in the previous model was replaced by estimates of runoff simulated using the STR package in the numerous small ungaged creeks that drain the surrounding mountains. The runoff derived from the precipitation-runoff model underestimated streamflow from smaller creeks such as Hale and Ross Creeks. To better match the streamflow from smaller creeks, the runoff estimated from the precipitation-runoff model was increased by a factor of 10 from the initial estimates. This resulted in inflows closer to measured inflows for smaller drainage areas. In addition, selected streambed conductances were reduced from initial estimates to improve the match of measured and simulated streamflow for the downstream gages on the major streams and tributaries. In particular, conductances were reduced from 86, 400 ft^2/d to 50,000 ft^2/d and from 43,200 ft^2/d to 25,000 ft^2/d to improve conveyance to downstream streamflow gages used for comparisons of streamflow. In addition, selected downstream segments on Los Gatos, Stevens, Permanente, Saratoga, Coyote, Lower Silver, and Penetencia Creeks and on the Guadalupe River were reduced to 200 ft^2/d to reduce the stream base flow that was draining the upper model layer and preventing the full recovery of ground-water levels. These downstream segments with reduced conductances were based on reaches with little increased or decreased flow delineated by SCVWD (J. Aguilera, Santa Clara Valley Water District, unpub. data, 2002). The final distribution of streamflow also is aligned with the distribution of inflow and outflow reaches and shows a complex distribution of gains and losses through time and space (Animation 3. Map showing simulated streamflow gains and losses and ground-water recharge from precipitation for model layers 1 and 3, 1970–99, for the Santa Clara Valley model, Santa Clara Valley, California.).

The revised model represented climatic variation in valley-floor recharge through the use of wet- and dry-month indices applied to monthly precipitation maps (Animation 3, Animation 4. Map showing simulated water levels, stream inflow, and artificial recharge for model layers 1 and 3, 1970–99, for the Santa Clara Valley model, Santa Clara Valley, California.), and climatic variation in artificial recharge (Animation 4). This method is simpler than the approach used in the previous model where valley-floor recharge was estimated using a linear relation that applied about 10 percent of the square of precipitation from San Jose and Los Gatos as recharge within seven zones.

The revised model uses percentages of valley-floor recharge that include wet- and dry-month recharge percentages of precipitation, which are aligned with the major climatic cycles of the Pacific Decadal Oscillation (PDO) (Mantua and Steven, 2002) which, in turn, control the frequency and magnitude of major winter frontal storms. The temporal categories were based, in part, on the cumulative departure curve of precipitation for San Jose. This required segregation of the recharge percentages into the period 1970–77, which represents a period with drier wet months, and the subsequent period 1978–99, which represented wetter wet months. Wet years were about 23 percent wetter in the positive-index PDO period (1978–99) than they were during the dryer negative-index PDO period (1947–77). The percentage of recharge for the dry months in positive and negative PDO periods was about the same and was kept the same for both PDO periods. Although these percentages result in more recharge during the wetter periods, they are consistent with the surface recharge and runoff estimates made for the Santa Clara Valley (Joe Hevesi, U.S. Geological Survey, unpub. data, 2001) for the historical period segregated by climate periods. The use of these indices helped improve the temporal match of multi-year cycles present in all the types of hydrologic time series used for model calibration. The final percentages of recharge were 7.5 percent for wet months and 4.5 percent for dry months for the period 1970–77 (drier PDO period), and 15 percent for wet months and 4.5 percent for dry months for the period 1978–99 (wetter PDO period).

Hydraulic properties were changed in the revised model as part of the calibration process. The distribution of aquifer and aquitard storage properties was replaced, followed by the replacement of vertical hydraulic conductivity and finally by the replacement of horizontal hydraulic conductivity. The replacement and separation of aquifer and aquitard properties facilitated the seasonal and multi-year variations that control changes in ground-water storage and related changes in water levels. The multipliers for specific storage for layer 3 also were increased outside the confined region to represent unconfined storage properties within layer 3.

After replacement of the aquifer and aquitard storage properties, large errors in water levels persisted during the initial period of the transient simulation. These water-level errors were largely eliminated by changing the critical-head estimates. Initially critical heads were set equal to initial heads, which assumed a normally consolidated distribution of compacted sediments. These critical heads were required to represent an overconsolidated estimate where critical heads vary spatially and are tens to hundreds of feet below the 1970 initial heads. The assumption of critical heads equal to initial heads resulted in initial rises in water levels related to water entering the ground-water flow system from inelastic compaction; this resulted in erroneous simulation of subsidence, contributions of water to ground-water flow, and initial water-level rises that dissipated after about 5 to 7 years of simulation. Some error still persists along the edge of the historical subsidence bowl where more recent ground-water pumpage is relatively larger than in decades prior to the simulation period (see fig. 18, later in report). This may indicate that critical heads remain uncertain in this region.

The base value for the skeletal elastic specific storage also was reduced by 80 percent for model layers 3 and 4 and decreased by 60 percent for model layers 1, 2, 5, and 6 in order to improve the match between measured and simulated compression and compaction at the extensometer sites for the period 1983–99. Even though smaller values were needed to fit the measured seasonal compression from extensometers, the consolidation tests from selected cores at depth suggest that the elastic compressibility was 2 to 3 times greater than the initial estimate used for all depths. However, the smaller estimates are for cores from the depth regions that have the greatest pumpage. Reduction of the base value for the inelastic storage of 80 percent for model layers 3 and 4 is consistent with the core-consolidation tests. The final distribution of subsidence parameters resulted in a simulation of subsidence for the period 1983–99 that shows predominantly elastic deformation and recovery with some inelastic deformation along the southwestern edge of the confined region during the 1984–91 drought (Animation 5. Map showing simulated subsidence for all model layers and water-level change for layer 3, 1983–99, for the Santa Clara Valley model, Santa Clara Valley, California.).

Another major adjustment that affected the fit to water levels in the central part of the valley (CRH region) was the westward relocation of the "new Cascade" Fault as a horizontal ground-water flow barrier (figs. 1, 5). This barrier is needed to reduce the overestimation of water levels in the central part of the valley. Final adjustments to the barrier included gaps in the fault along the major creeks to allow recharge into the south-central part of the valley. A similar gap also was required along the Silver Creek Fault at its intersection with lower Silver Creek to facilitate the flow of streamflow infiltration into the south-central part of the valley. In addition to the gaps, channels with higher hydraulic conductivities were emplaced in layers 1 and 3 beneath the major stream channels that extended through the gaps in the fault along selected tributaries and also northward from Coyote Narrows beneath Coyote Creek. The range of the horizontal hydraulic conductivity (HK) array values also were expanded for layers 1 and 3 from one to four orders of magnitude. The revised range for layer 1 is now from 0.004 to 0.684 with the additional selected stream cells set to a value of 2 in the multiplier array for HK (fig. 6*A*). Similarly, the revised range for layer 3 is now 0.0001 to 0.875 with the additional selected stream cells set to a value of 5 in the multiplier array for HK (fig. 6*B*).

Several additional adjustments were made after extending the simulation through the update period of 1990–99. The skin factor (that is, resistance to inflow) for wellbore flow entrance losses (Halford and Hanson, 2002, eqn. 3) was increased from 5 to 15 during calibration in order to better fit the potential head differences indicated at nearby multiple-well monitoring sites such as the Coyote Creek Outdoor Classroom (CCOC) site (Hanson and others, 2002b) (fig. 1). The increased skin factor also resulted in a better match with the measured and simulated percentages of wellbore flow per model layer at selected wellbores (fig. 16). The base value for horizontal hydraulic conductivity in model layer 5 also was increased with the change in skin factor. This increased the amount of water that was pumped from layer 5, improved the match between measured and simulated head differences, and improved the distribution of estimated wellbore flow from model layers. The wellbore flow generally matches peak wellbore flows in selected water-supply wells measured under actual operating conditions using dye-tracing methods (Izbicki and others, 1999) in the Santa Clara Valley (Hanson and others, 2003). The distribution of wellbore flow also is consistent with the relative depth distribution of artificial-recharge estimates from depth-specific monitoring-well samples and from depth-dependent water-supply well samples (fig. 16) (Hanson and others, 2003). The alignment of increased recharge in the upper model layers also is consistent with the relatively larger hydraulic conductivity and related wellbore outflow from pumpage. However, the distribution of wellbore flow is subject to considerable changes through time as wells are turned on and off. The transient nature of the wellbore flow distribution is indicated by the temporal distribution of wellbore flow for model layers 3 and 5 (Animation 2).

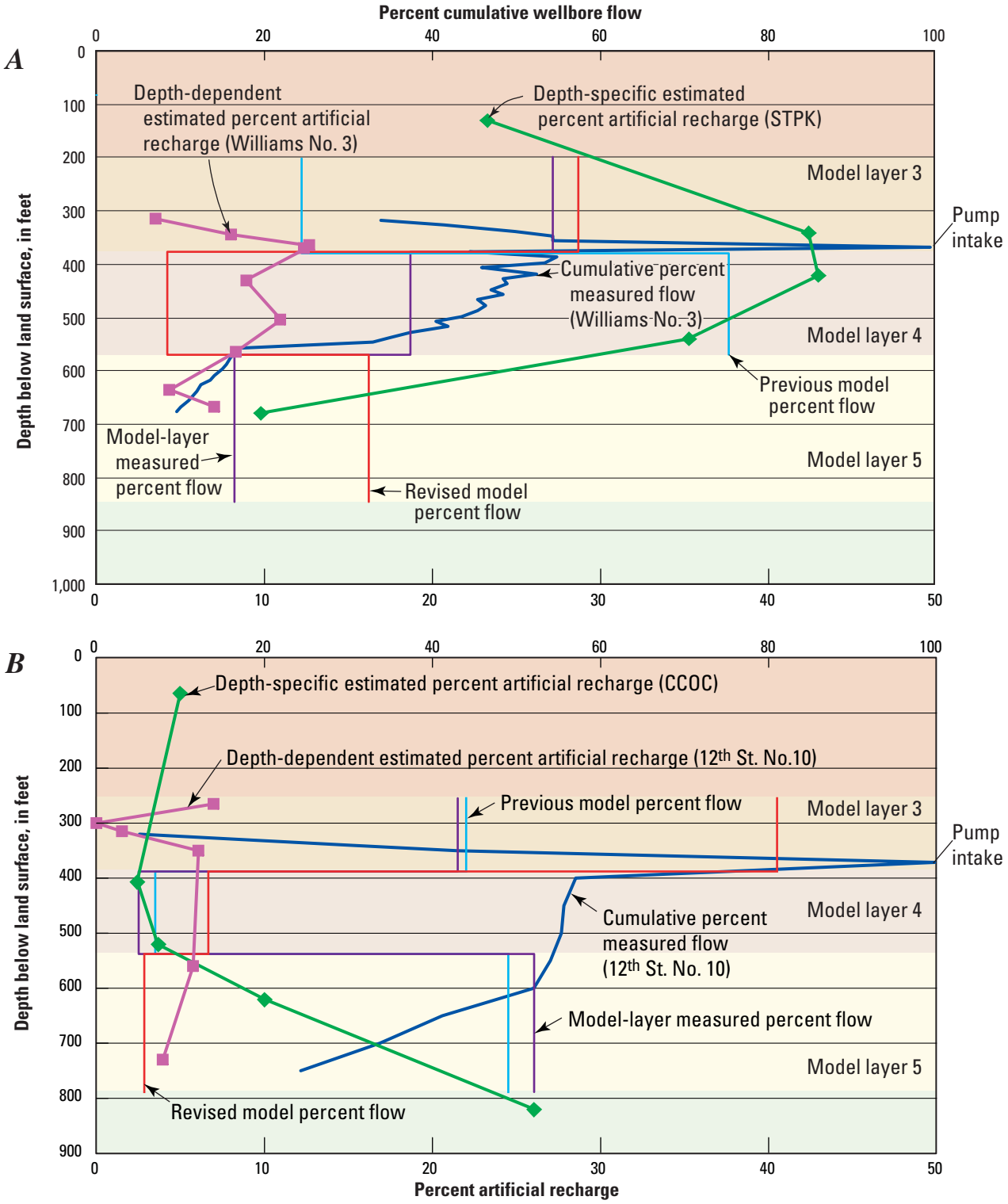

Figure 16. Distribution of measured and simulated wellbore flow and estimated percentage of artificial recharge for (A) Williams No. 3 and (B) 12th St. No. 10 water-supply wells, Santa Clara Valley, California.

The final model has an average root-mean-square (RMS) error for water levels from the 27 comparison wells of 27 ft for the 29.75-year simulation period 1970–99 for 5,703 water-level measurements and shows a generally good correlation between measured and simulated water levels (fig. 12). When the first 5 years of the simulation are excluded for the dissipation of initial-condition errors, the average RMS error is reduced to 22 ft for the period 1975–99. The average RMS error for the updated period is 23 ft. The previous model had an average RMS error of 36 ft for the period 1970–89. When subdivided into the seven groups of wells, the revised model has improved the fit to water levels in the ERH, CRH, and SCR groups relative to the previous model (figs. 1, 15) and is generally comparable in the other groups. When the observations also are interpolated in time (Harbaugh and others, 2000a), the average error for the calibrated revised model is −7.34 ft. The negative error for the revised model generally represents an underestimation of extreme water-level declines for some regions (fig. 15*A*). These water-level declines may reflect instantaneous pumping conditions that are not simulated exactly when using average monthly pumping rates. Overall, the revised model substantially reduces the model error for almost all comparison wells relative to the previous model (fig. 15*B*).

The simulated streamflow generally matches measured streamflow for flows above 100,000 ft^3/d (greater than 1.2 ft^3/s) for the simulated streamflow along Guadalupe River at San Jose (USGS Gage 11169000), and above Blossom Hill Road (SCVWD Gage 20), above Almaden Expressway (SCVWD Gage 73), and its tributary Alamitos Creek near New Almaden (SCVWB Gage 70); and along Los Gatos Creek at Lark Boulevard (SCVWD Gage 59), and at Lincoln Avenue (SCVWD Gage 50), Coyote Creek at Edenville (SCVWD Gage 58), and Saratoga Creek at Pruneridge Avenue (SCVWD Gage 25) (fig. 13). In addition, the losing and gaining reaches are generally consistent with the observed reaches within the streamflow network (Joseph Aguilera, Santa Clara Valley Water District, unpub. data, 2002) (Animation 3).

The revised model also fits the range of measured compression and compaction at the two extensometer sites located near San Jose within 15 to 27 percent and near Sunnyvale within less than 3 percent of the range of measured seasonal deformation for the deepest extensometers, respectively (fig. 14). The RMS errors for simulated subsidence at the San Jose extensometers are 0.06 (16C5) and 0.12 ft (16C11) for the period 1983–93. The RMS errors for the simulated subsidence at the Sunnyvale extensometers are 0.03 ft (24C3), 0.02 ft (24C4), and 0.04 ft (24C7) for the period 1983–97. The simulated deformation is within 48 and 53 percent of the range of deformation for the two shallower extensometers near Sunnyvale. Monthly stress-period data improved the temporal detail of simulated changes in aquifer storage, and was in phase with resulting observed seasonal compression. This suggests that the simulation of ultimate compression was adequate for the predominantly elastic compression observed in the historical period of simulation. Elastic rebound is overestimated at depth, which may suggest that there is some delayed response in elastic rebound from the water-level recovery in the deeper parts of the aquifer system (see 1,005-ft depth extensometer 24C7, fig. 14).

The spatial comparison of the revised model includes water-level maps and estimated subsidence from multiple-year and seasonal water-level changes derived from InSAR images (Galloway and others, 2000). The simulated ground-water levels are in general agreement with the hand-contoured water-level maps (Behzad Ahmadi, Santa Clara Valley Water District, unpub. data, 2000) for the spring and fall of 1995 and 1997 (fig. 17). The hand-contoured maps were completed without the faults as potential ground-water flow barriers and include specific cones of depression around selected well fields. The simulated subsidence also shows a similar pattern of deformation with respect to the spatial distribution derived from the historical subsidence (fig. 18), from the seasonal and multi-year InSAR images (fig. 19), and the overall recovery of the basin (Animation 5). The general trend of recovery of the land surface since 1992 also is in agreement with the analysis of the complete set (115) of InSAR images that indicate both long-term uplift along with the recovery of ground-water levels and continuation of seasonal deformation and recovery (Schmidt, 2002). The simulated data from the model also show the multi-year elastic deformation related to the drought (1984–91) superimposed onto the seasonal deformation that is not present in the limited (post-1991) InSAR data.

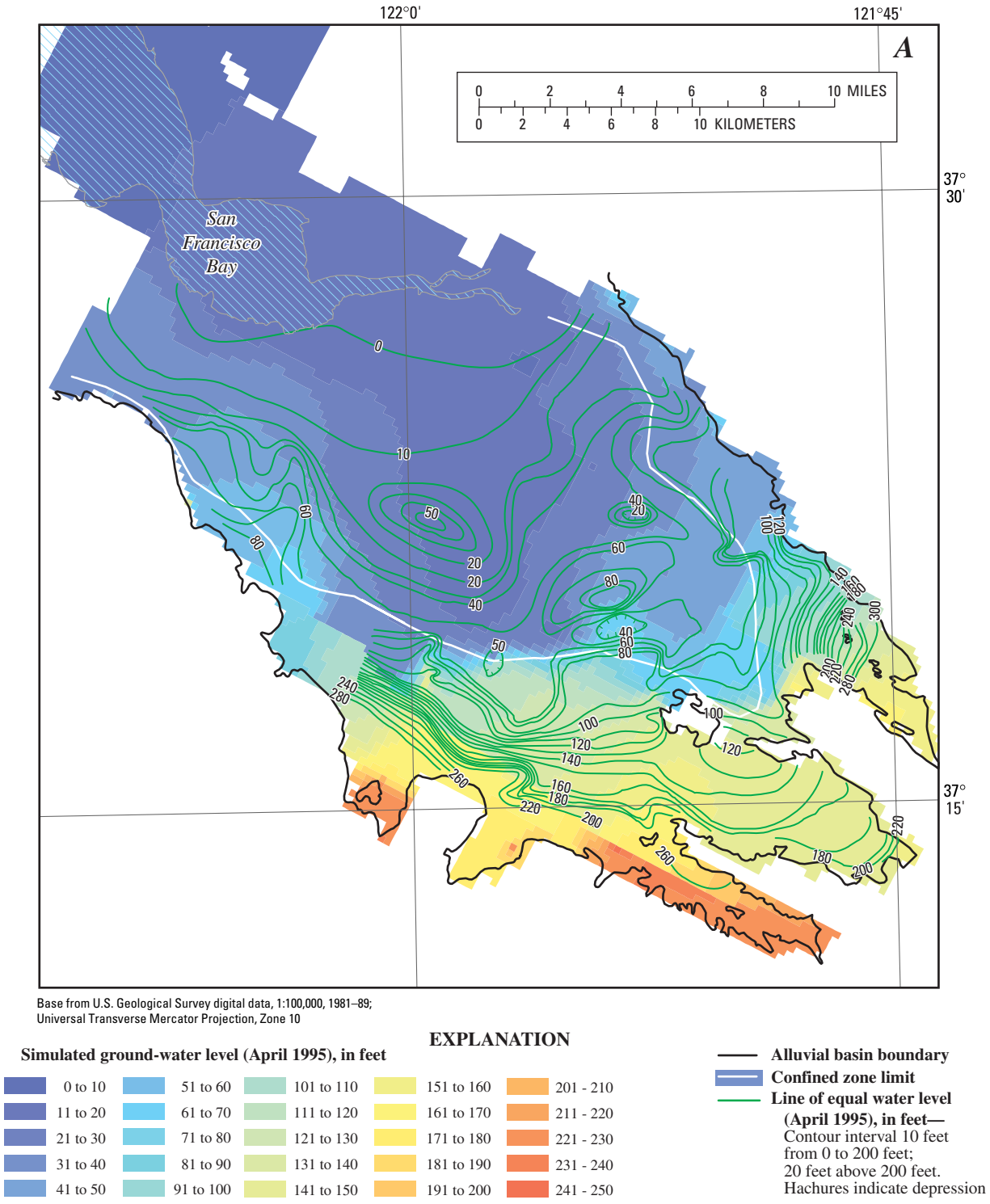

Figure 17. Hand-contoured measured and simulated ground-water levels, April and September, 1995, and March and September, 1997, for the Santa Clara Valley model, Santa Clara Valley, California.

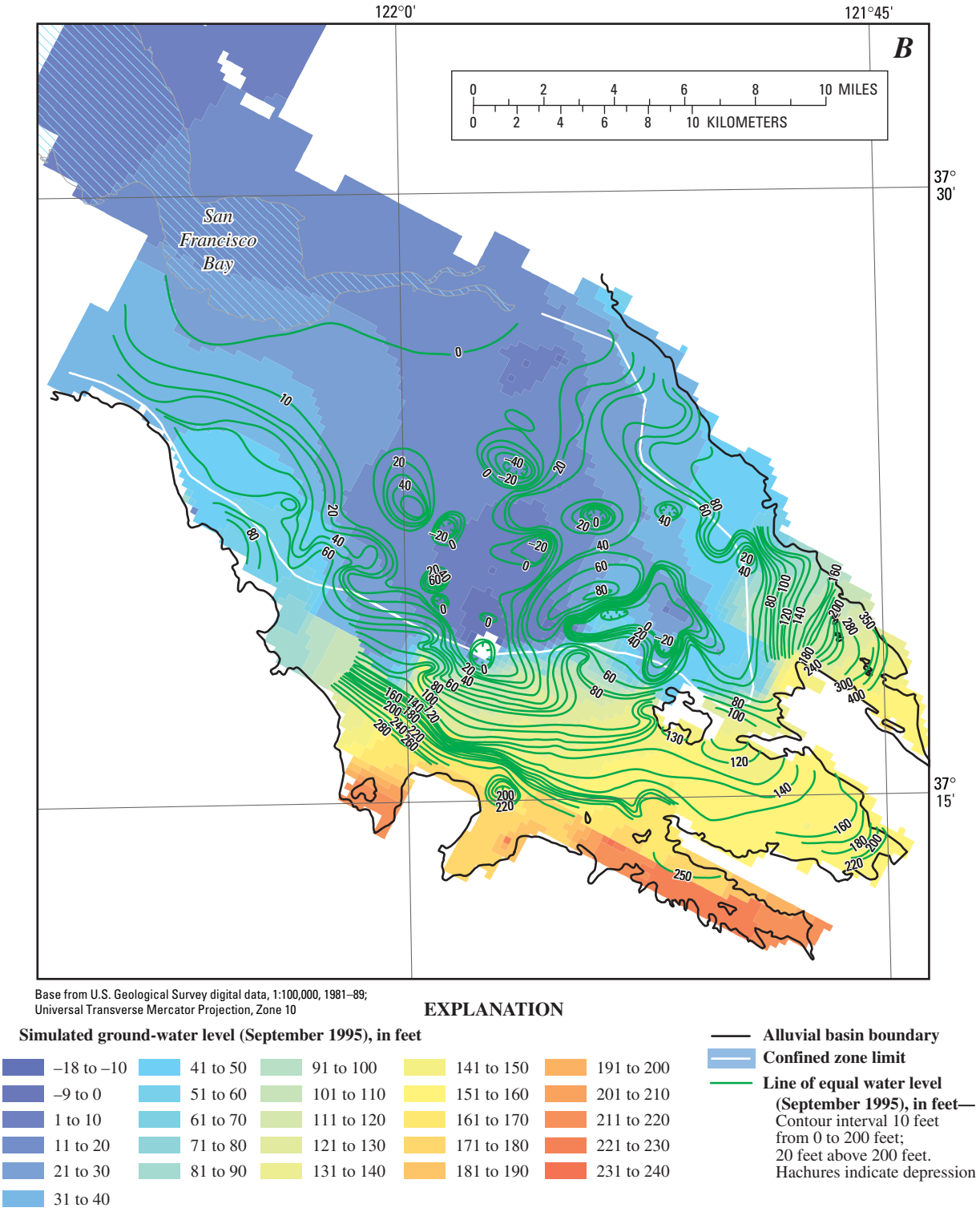

Figure 17. —Continued.

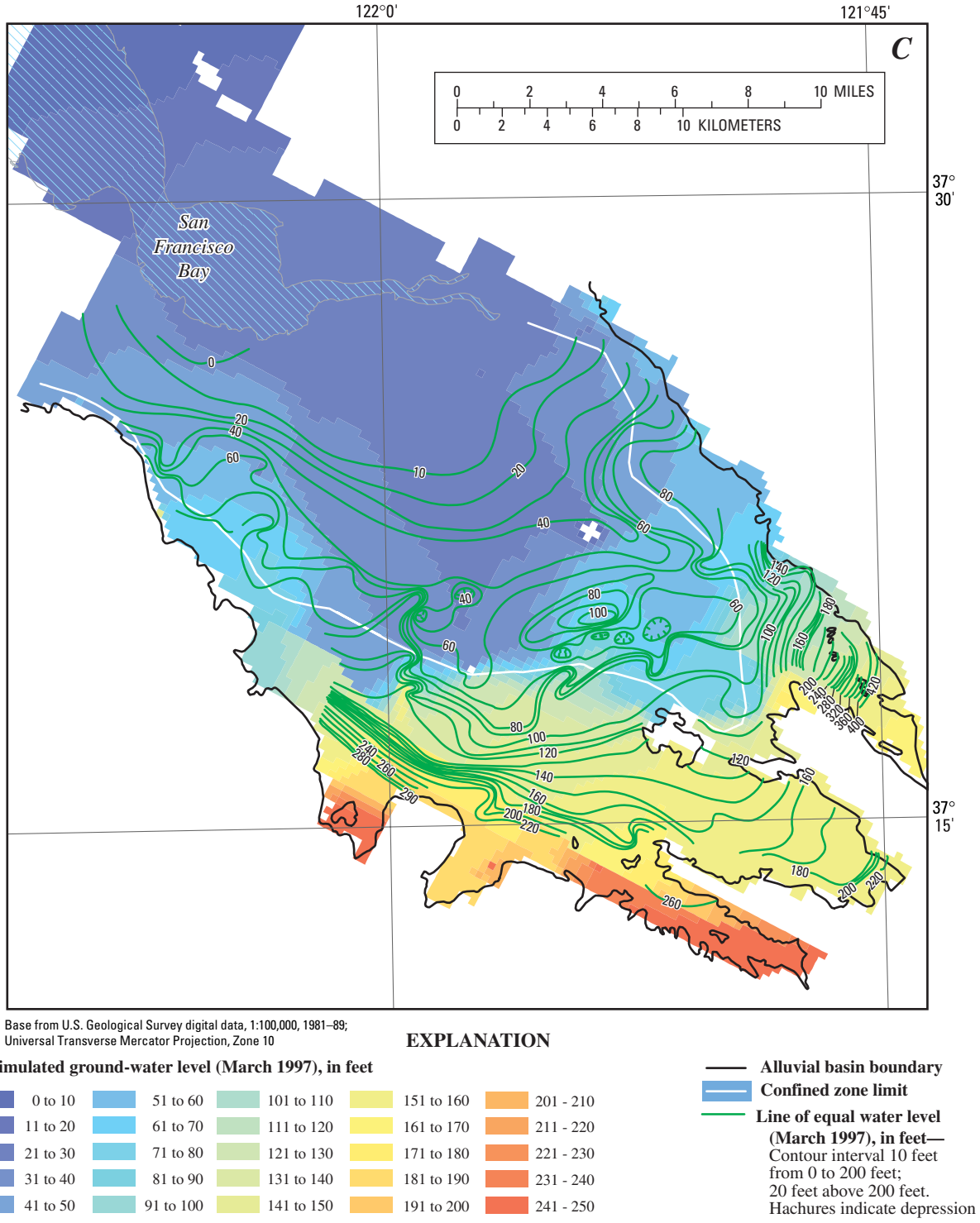

Figure 17. —Continued.

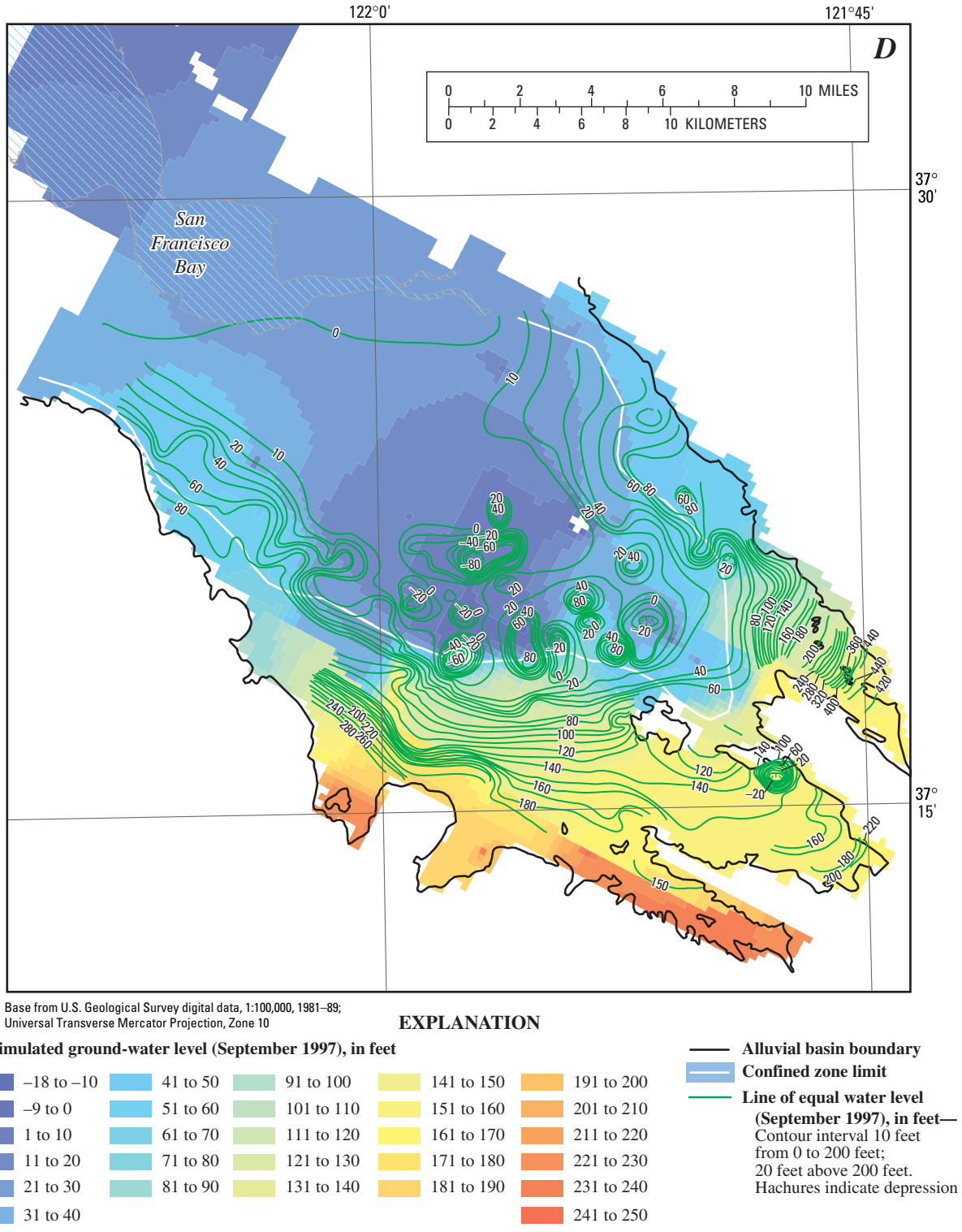

Figure 17. —Continued.

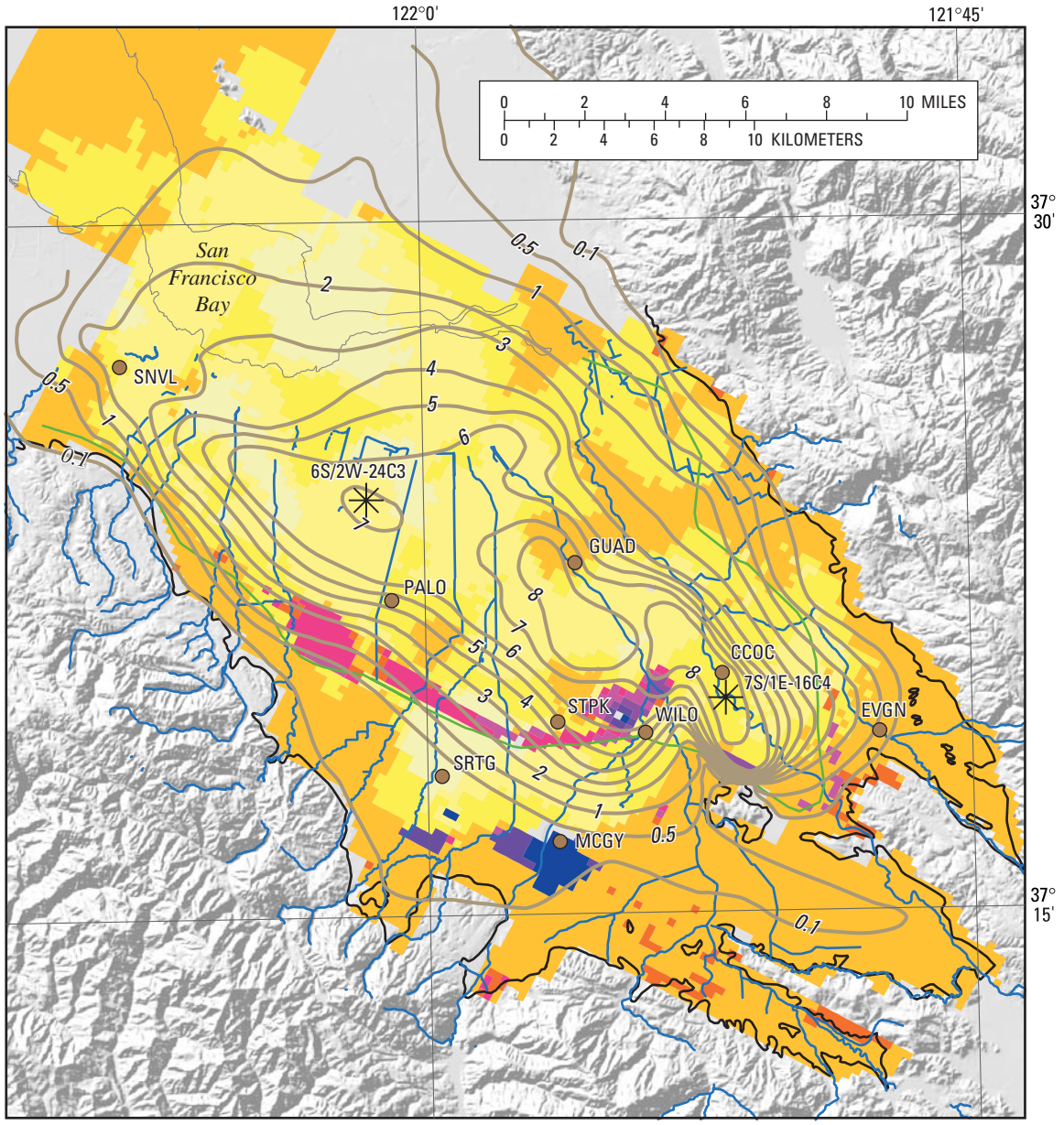

Base from U.S. Geological Survey digital elevation data, 1:250,000, 1987, and digital data, 1:100,000, 1981–89; Universal Transverse Mercator Projection, Zone 10. Shaded relief base from 1:250,000-scale Digital Elevation Model; simulated sun illumination from northwest at 30 degrees above the horizon

EXPLANATION

Simulated land subsidence, in feet (Jan 83–Sep 99)—
Negative number indicates uplift

–0.62 to –0.30	0.01 to 0.10	1.51 to 3.00
–0.29 to –0.20	0.11 to 0.50	3.01 to 6.00
–0.19 to –0.10	0.51 to 1.50	6.01 to 9.00
–0.09 to 0.00		

Line of measured subsidence (1939–80), in feet—
(Poland and Ireland, 1988)

Creeks

Basin boundary

Extent of confined aquifer zone

Monitoring wells

Extensometers

Figure 18. Hand-contoured measured subsidence, 1939–80, and simulated ground compaction, 1983–99, for the Santa Clara Valley model, Santa Clara Valley, California.

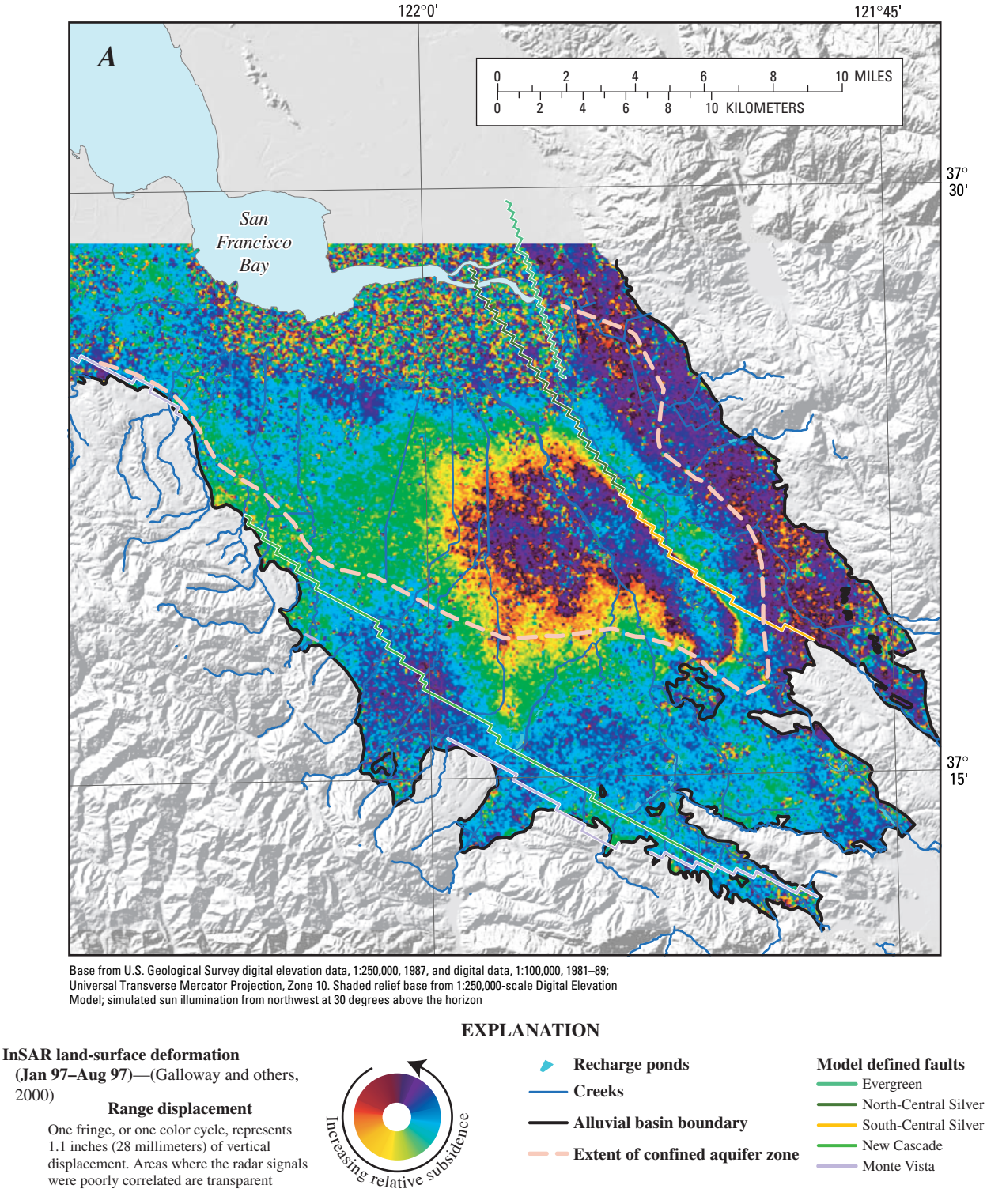

Figure 19. (A) InSAR-estimated seasonal compression and (B) simulated deformation, January to September 1997, for the Santa Clara Valley model, Santa Clara Valley, California.

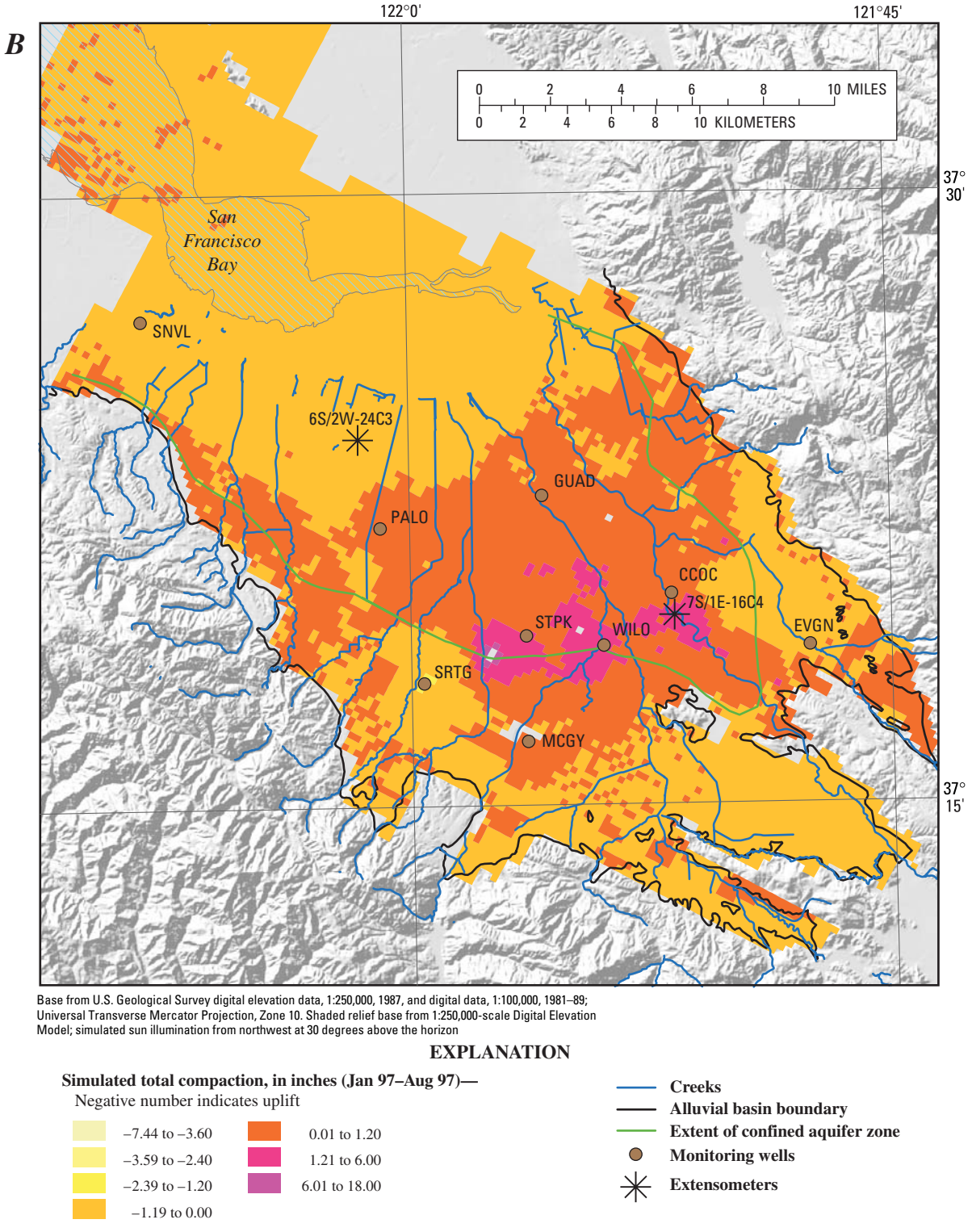

Figure 19. —Continued.

The ground-water inflow and outflow also was compared with that of the previous model (fig. 20*A*). The total average simulated flow from the previous model was about 207,200 acre-ft/yr for the period 1970–99. The revised model now has a slightly increased flow of about 225,500 acre-ft/yr for the same period. The total inflow and outflow is about 205,300 acre-ft/yr for the period 1970–99. The net change in ground-water storage for the entire historical simulation period is variable and aligned with the climate cycles (fig. 20*B*). Overall the simulated net change in storage increased by about 189,500 acre-ft/yr for the entire period of simulation, which represents about one and a half years of the 1970–99 average pumping. The multi-node well package now replaces most of the interlayer flow of the previous model. This flow represents about 19 percent of the total ground-water inflow as interlayer flow between model layers and represents wellbore flow through multi-aquifer wells. The rates of recharge of about 155,300 acre-ft/yr for the previous model and 147,800 acre-ft/yr for the revised model are similar for the period 1970–89. The average total recharge rate from natural and artificial recharge and from streamflow infiltration for the revised model for the entire simulation period of 1970–99 was about 157,100 acre-ft/yr, which represents about 72 percent of the inflow to the ground-water flow system with respect to net pumpage (fig. 20*A*). The average rate of artificial recharge of about 77,600 acre-ft/yr represents about 36 percent of the inflow to the ground-water flow system and about half of the outflow as pumpage (fig. 20*A*). Similarly, rates of pumpage of about 146,900 acre-ft/yr for the previous model and 147,000 acre-ft/yr for the revised model are comparable for the period 1970–89. The average pumpage rate is somewhat less for the entire 29.75-year simulation period, averaging about 133,400 acre-ft/yr. The average pumpage represents about 61 percent of the outflow from the ground-water flow system (fig. 20*A*).

The changes in ground-water flow generally reflect the major climate cycles and the additional importation of water by SCVWD (fig. 20*B*). The basin has been in recovery since the drought of the late 1980s and early 1990s as demonstrated by the trend towards negative change in storage (that is, water going out of ground-water flow and back into ground-water storage) (fig. 20*B*). While the imported water has slightly declined with some year-to-year variation on the order of 25,000 to 50,000 acre-ft/yr, the water-level recovery and related increase in ground-water storage generally is driven by a substantial decrease in ground-water pumpage since 1989 (fig. 20*B*). The water derived from interbed storage has alternated around zero (fig. 20*B*) and represents a small percentage of the total change in storage over the period of simulation (fig. 20*A*). The ET has been a small and relatively constant component of the budget (fig. 20*A*). The streamflow infiltration shows some climatic variability and has remained between 20,000 and 50,000 acre-ft/yr through the 29.75-year period (fig. 20*B*). The outflow at the San Francisco Bay (Net GHB) has shown a small but steady increase during the basin recovery (fig. 20*B*). This is consistent with most of the recharge infiltrating and flowing through the uppermost layers (i.e. model layers 1 and 3) of the aquifer system. Most of the water that flows to the deeper model layers is occurring through wellbores, with wellbore flow representing 19 percent of the total ground-water inflow between model layers.

Model Sensitivity and Uncertainty

The SCVM model was extremely sensitive to changes in inflows, outflows, and selected hydraulic properties. In particular, the model failed convergence when some of the model parameters were perturbed out of the range of the final set of specified values. This, in part, prevented the use of systematic parameter-estimation techniques to estimate selected model parameters and related sensitivities that are based on perturbation approaches. During trial-and-error calibration, the model was noted to be most sensitive to increases in vertical hydraulic conductivity, decreases in horizontal hydraulic conductivity, decreases in streambed conductance, increases in conductances of horizontal flow barriers, decreases in specific storage, and increases in hydraulic characteristics for horizontal flow barriers. The application of the MNW package affected streamflow infiltration and the vertical distribution of water derived from compression and compaction (Hanson and others, 2003). The skin factor in the MNW package affected the interlayer flow and related water-level difference between model layers. The refined monthly specification of inflows and outflows has created more separation of the supply and demand components of the ground-water and surface-water resources. Therefore, the revised model is more capable of addressing water-management issues at the annual and seasonal time scales as reflected in the simulated ground-water levels, streamflow, and deformation time seires. The improved temporal and spatial separation, as well as individual simulation of inflows and outflows, also will facilitate the application of optimization modeling analysis to help SCVWD address the feasible solutions to water-resource goals subject to subsidence, streamflow, water-quality, and related economic constraints.

A

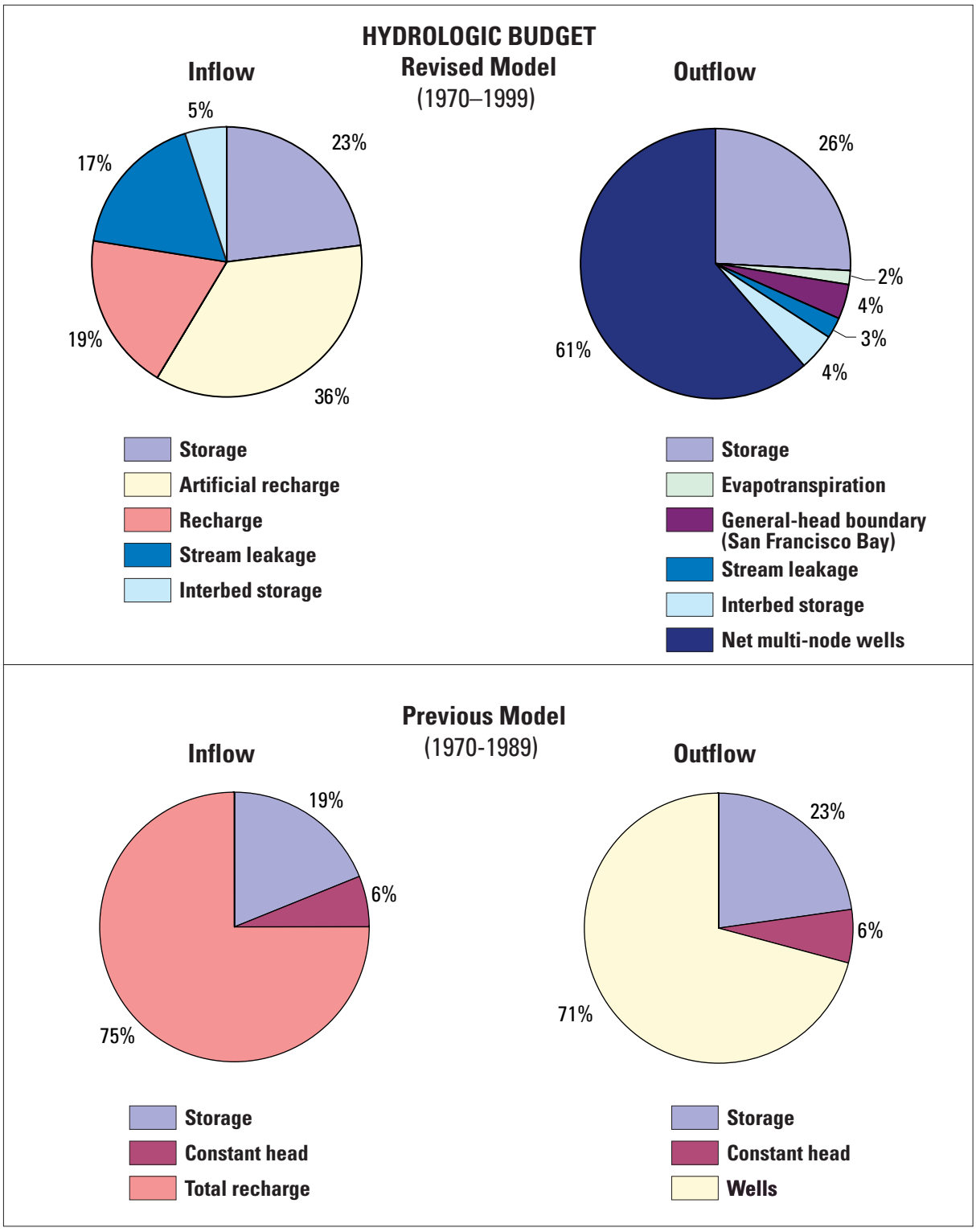

Figure 20. (A) percentages of components of the hydrologic budget for the previous model for the period 1970–89 and the revised model for the period 1970–99, Santa Clara Valley, California, and (B) inflow and outflow components through time for the period 1970–99, Santa Clara Valley, California.

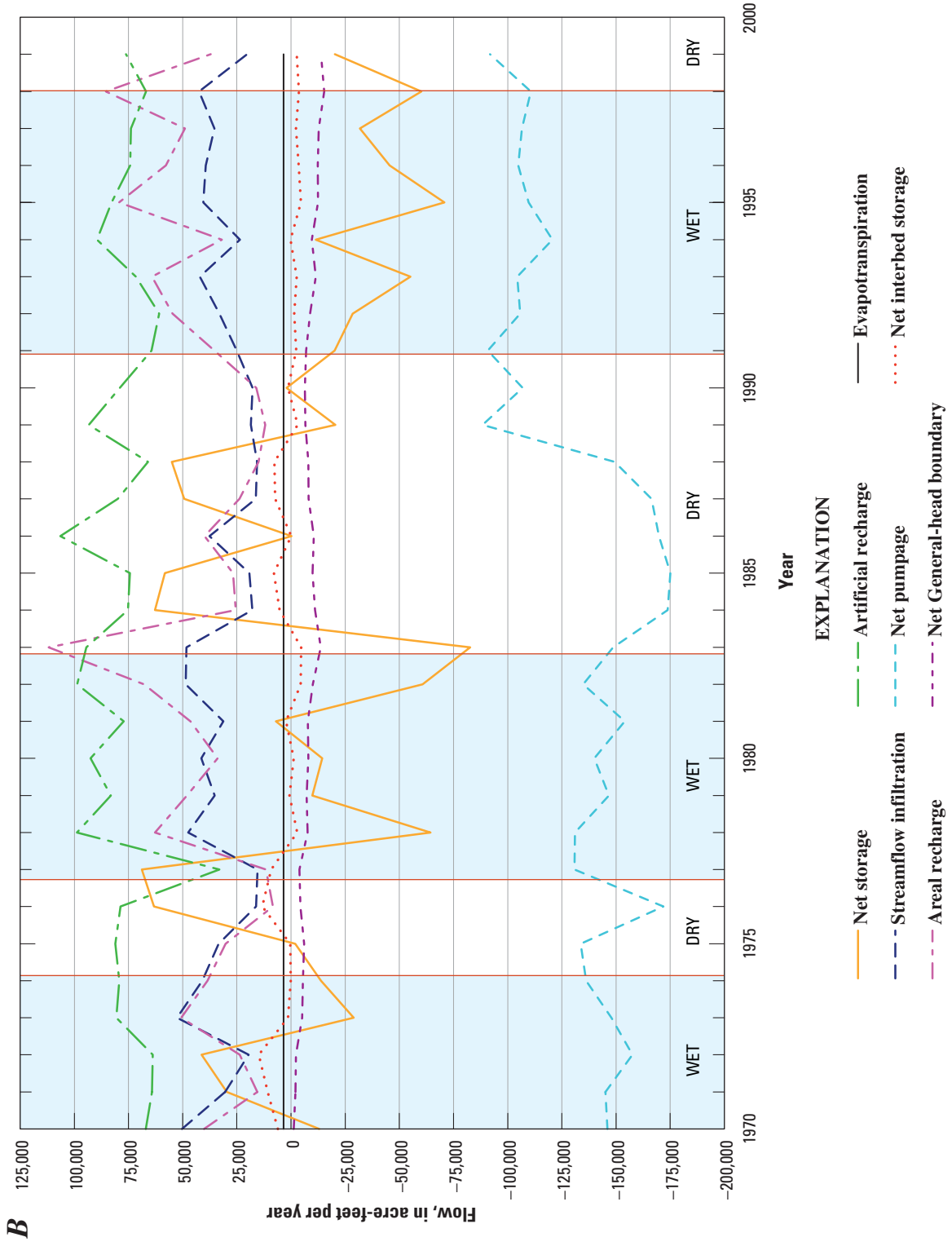

Figure 20. —Continued.

Several elements of the revised model remain uncertain and will require additional investigation to improve the accuracy of the simulation of the ground-water and surface-water flow and simulation of regional subsidence. The increased accuracy will allow SCVWD to address more detailed management questions related to the operation of artificial-recharge facilities, minimization of subsidence, increase in ground-water pumpage, or reduction in pumping of ground water high in nitrate or other contaminants. The largest uncertainties are related to model layering, smaller inflows and outflows, and selected hydrologic features and properties.

The representation of sedimentary layering and distribution of facies within the related model layers needs to be improved before the model is suitable for simulating the flow and distribution of artificial recharge using solute-transport or particle-tracking simulations. The current model-layering remains, in part, uncertain on the basis of model layers that were derived from a combination of well-screen distributions and lithologic layering. The redefinition of the sequence of stratigraphic layering would refine the geologically controlled flow paths in the ground-water flow system, and is part of ongoing research by the USGS.

Some of the smaller inflows and outflows remain uncertain and may affect the accuracy of the model locally. The model could be improved by including more detailed estimates of the extent of leakage from water transmission lines, the nature of inflow and outflow that could affect seawater intrusion along the San Francisco Bay, and the distribution of gaining and losing streamflow reaches that are related to natural runoff events or application of artificial recharge. Distributed valley-floor recharge could be estimated with more detail and could distinguish between a combination of natural recharge from precipitation and artificial recharge from urban anthropogenic effects such as leaky water distribution systems, urban irrigation and concentrated urban runoff, or leaky sewer pipes.

Hydrologic features that remain uncertain include the location of some fault segments, critical-head distributions, and selected hydraulic properties. The exact location of the New Cascade Fault remains uncertain and is the subject of continued investigations by the USGS and the SCVWD. The distribution of critical heads remains uncertain and will be potentially better defined through inclusion of estimates from consolidation tests of cores obtained from the completion of the new monitoring-well sites. The uncertainty in critical heads is greatest along the southwestern and western parts of the basin where the model overestimation of subsidence may be the result of overestimating initial critical heads for 1970 (fig. 18). Selected hydraulic properties that remain uncertain include horizontal hydraulic conductivities related to a potential coarse-grained stream-channel facies farther north along Coyote Creek towards the San Francisco Bay that may be in alignment with the InSAR deformation pattern. These extensions of the deformation that are apparent from the InSAR images may be related to coarse-grained facies of the ancestral drainage along Coyote Creek and Guadalupe River (Schmidt, 2002). Additional estimates of horizontal hydraulic conductivity could be obtained from slug tests at the new monitoring-well sites. Finally, the distribution of streambed conductances could be better defined through the application of seepage-run studies and more detailed classification of streambed sediments.

Summary and Conclusions

The Santa Clara Valley is a long, narrow trough extending about 35 mi southeast from the southern end of San Francisco Bay. Ground water from the regional alluvial-aquifer system is a major source of water in the Santa Clara Valley, which has been the site of intensive agricultural and urban development throughout the 20th century. The related ground-water development resulted in ground-water-level declines of more than 200 ft and has induced as much as 12.7 ft of land subsidence between the early 1900s and the mid-1960s. Since the 1960s, Santa Clara Valley Water District has imported surface water to meet growing demands and reduce dependence on ground-water supplies. The use of imported water and implementation of artificial recharge has resulted in the sustained recovery of the ground-water flow system throughout many parts of the Santa Clara Valley. Management of the ground-water resources is facilitated by the development of a regional ground-water/surface-water flow model that simulates the flow of ground water and surface water, changes in ground-water storage, and related effects such as potential land subsidence.

A revised numerical ground-water/surface-water flow model of the Santa Clara Valley was developed as part of a cooperative investigation with Santa Clara Valley Water District. The flow model was developed to better define the geohydrologic framework of the regional flow system and to better delineate the supply and demand components that affect the inflows to and outflows from the regional ground-water flow system. Development of the model included revisions to the previous ground-water flow model that upgraded the temporal and spatial discretization, added source-specific inflows and outflows, simulated additional flow features such as land subsidence and multi-aquifer wellbore flow, and extended the period of simulation through September 1999. The transient-state model was calibrated to historical surface-water and ground-water flows for the period 1970–99 and to historical subsidence for the period 1983–99.

The regional ground-water flow system consists of multiple aquifers that compose upper- and lower-aquifer systems. The upper-aquifer system is further divided into a confined region that is roughly coincident with the combined extent of the bay muds and an unconfined region that occurs between the confining beds and the surrounding mountains. Ground-water inflow occurs as natural recharge in the form of areal infiltration of precipitation and streamflow infiltration along stream channels. Ground-water inflow also occurs as artificial recharge from infiltration of imported water at recharge ponds, and from leakage along selected transmission pipelines. Ground-water outflow occurs as evapotranspiration, stream base flow, discharge through pumpage from wells, and subsurface flow to the San Francisco Bay.

The geohydrologic framework of the regional ground-water flow system was subdivided into six model layers for the simulation of developed ground-water flow conditions. The upper-aquifer system is composed of Holocene and Pleistocene-age deposits. The lower-aquifer system is composed of early Pleistocene and Pliocene-age deposits. In addition to the hydrostratigraphic layering, the model is bounded below and along the mountain fronts by relatively impermeable bedrock. The regional aquifer systems are also dissected by several laterally extensive faults that may form at least partial barriers to the horizontal flow of ground water.

The spatial and temporal extent of the ground-water flow model was extended relative to previous models. While the layering and coverage over the San Francisco Bay region remain similar to components of the previous models, the model now covers the entire Santa Clara Valley, including the Evergreen subregion that was not previously simulated. The temporal discretization is now monthly, and the historical simulation was extended to the period 1970–99. The spatial discretization also was "regularized" to square cells 1,000 ft per side throughout the model grid.

The hydraulic properties were redefined on the basis of cell-based lithologic properties that were delineated on the basis of aggregate thicknesses of coarse-grained, fine-grained, and mixed textural categories. The textural categories were used to estimate the horizontal and vertical hydraulic conductivities, and aquifer storage properties. The estimation of aquitard and confining-layer storage properties also was based on the cell-based aggregated thickness of fine-grained deposits and was used to simulate elastic and inelastic land subsidence.

The simulated inflows and outflows for the Santa Clara Valley Model included monthly specified flows and head-dependent flows. Specified inflows included valley-floor recharge as the areally distributed infiltration of a portion of monthly precipitation, artificial recharge from infiltration of imported water at infiltration ponds and along selected stream channels, and leakage from selected transmission pipelines. Specified streamflows were routed through all of the gaged and ungaged creeks and rivers, which results in head-dependent streamflow infiltration. Intrawellbore flow resulted in head-dependent interlayer inflows and outflows through pumped and nonpumped wells. A small amount of head-dependent inflow also occurs along the coastal boundary with the San Francisco Bay and may represent underflow or leakage from the Bay. Head-dependent outflows were simulated as ground-water pumpage; evapotranspiration along the stream channels; stream base flow; and outflow along the coastal boundary with the San Francisco Bay, which may represent underflow or leakage to the Bay.

The model was upgraded to MF2K and was calibrated to fit historical ground-water levels, streamflow, and land subsidence for the period 1970–99. The revised model slightly overestimates measured water levels with an average error of –7.34 ft. The streamflow generally shows a good match on gaged creeks and rivers for flows greater than 1.2 ft^3/s. The revised model also fits the measured compression and compaction at the two extensometer sites located near San Jose within 16 to 27 percent and near Sunnyvale within 3 percent of the maximum measured seasonal deformation for the deepest extensometers, respectively.

The slightly increased total ground-water inflow and outflow of about 225,500 acre-ft/yr is comparable with the previous model 207,200 acre-ft/yr for the period 1970–89 and is comparable to the simulated total inflow and outflow of about 205,300 acre-ft/yr for the period 1970–99. Overall the simulated net change in storage increased by about 189,500 acre-ft/yr for the entire period of simulation, which represents about one and a half years of the 1970–99 average pumping. The changes in ground-water flow and storage generally reflect the major climate cycles and the additional importation of water by SCVWD, with the basin in recovery since the drought of the late 1980s and early 1990s. The rates of recharge of about 155,300 acre-ft/yr for the previous model and 147,800 acre-ft/yr for the revised model are similar for the period 1970–89. The average total recharge rate from natural and artificial recharge and from streamflow infiltration for the revised model for the entire simulation period of 1970–99 was about 157,100 acre-ft/yr, which represents about 59 percent of the inflow to the ground-water flow system. This rate of inflow is comparable to the average rate of artificial recharge of about 77,600 acre-ft/yr, which also represents about 30 percent of the inflow to the ground-water flow system. Similarly, rates of pumpage of about 146,900 acre-ft/yr for the previous model and 147,000 acre-ft/yr for the revised model are comparable for the period 1970–89. The average pumpage rate is somewhat less for the entire 29.75-year simulation period, averaging about 133,400 acre-ft/yr. The average pumpage represents about 69 percent of the outflow from the ground-water flow system. Most of the simulated recharge infiltrates and flows through the uppermost layers (i.e. model layers 1 and 3) of the aquifer system. Most of the water that flows to the deeper model layers is occurring through wellbores, with wellbore flow representing 19 percent of the total ground-water inflow between model layers.

References Cited

Anderson, S.R., and Hanson, R.T., 1987, Relation of aquifer compaction to Cenozoic depositional environments in the Tucson basin, Arizona, *in* Abstracts with Programs: Geological Society of America Annual Meeting and Exposition, Phoenix, Arizona, October 1987, 573 p.

Bartugno, E.J., McJunkin, R.D., and Wagner, D.L., 1991, Map showing recency of faulting, San Francisco–San Jose quadrangle, 1:250,000: California Department of Conservation, Division of Mines and Geology, Regional Geologic Map Series, Map 5A, Sheet 5.

California Department of Water Resources, 1967, Evaluation of ground water resources, South Bay, appendix A—Geology: Bulletin 118-1, 153 p.

_____ 1975, Evaluation of groundwater resources, south San Francisco Bay, Volume III, northern Santa Clara County area: Bulletin No. 118-1[variously paged].

California History Center, 1981, Water in the Santa Clara Valley—a history: Seonaid McArthur, ed., California History Center, De Anza College, Local History Studies, v. 27,
155 p.

Catchings, R.D., and Goldman, M.R., Gandhok, G., Rymer, M.J., and Underwood, D.H., 2000, Seismic imaging evidence for faulting across the northwestern projection of the Silver Creek Fault, San Jose, California: U.S. Geological Survey Open-File Report 00-125, 29 p.

CH2M Hill, 1991, Santa Clara Valley groundwater model project, Hydrogeological interpretation and numerical flow model: Draft technical memorandum, prepared for City of San Jose and Santa Clara Valley Water District, 35 p.

_____ 1992a, Santa Clara Valley groundwater model project, GIS data base and utility program documentation: Prepared for City of San Jose and Santa Clara Valley Water District [variously paged].

_____ 1992b, Basinwide groundwater flow model: Draft technical memorandum, prepared for City of San Jose and Santa Clara Water District [variously paged].

D'Agnese, F.A., O'Brien, G.M., Faunt, C.C., Belcher, W.R., and San Juan, Carma, 2002, A Three-dimensional numerical model of predevelopment conditions in the Death Valley regional, ground-water flow system, Nevada and California: U.S. Geological Survey Water-Resources Investigations Report 02-4102, 114 p.

Fio, J.L., and Leighton, D.A., 1995, Geohydrologic framework, historical development of the ground-water system, and general hydrologic and water-quality conditions in 1990, South San Francisco Bay and Peninsula area, California: U.S. Geological Survey Open-File Report 94-357, 46 p.

Friebel, M.F., Freeman, L.A., Smithson, J.R., Webster, M.D., Anderson, S.W., and Pope, G.L., 2002, Water resources data, California water year 2001: U.S. Geological Survey Water-Data Report CA-01-2, v. 2, 450 p.

Galloway, D.L., Jones, D.R., Ingebritsen, S.E., 2000, Measuring land subsidence from space: U.S. Geological Survey Fact Sheet 051-00, 4 p.

Halford, K.J., and Hanson, R.T., 2002, User's guide for the drawdown-limited, multi-node well (MNW) package for the U.S. Geological Survey's modular three-dimensional finite-difference ground-water flow model, versions MODFLOW-96 and MODFLOW-2000: U.S. Geological Survey Open-File Report 02-293, 33 p.

Halford, K.J., and Hanson, R.T., 2003, Effects of simulating multi-node wells on model calibration, interpretation, and prediction results—Modflow and more 2003: Understanding through modeling—Conference Proceedings, International Ground Water Modeling Center, Golden, Colorado, September 16–19, 2003, p. 70–73.

Hanson, R.T., 1989, Aquifer-system compaction, Tucson basin and Avra Valley, Arizona: U.S. Geological Survey Water-Resources Investigations Report 88-4172, 69 p.

Hanson, R.T., Anderson, S.R., and Pool, D.R., 1990, Simulation of ground-water flow and potential subsidence, Avra Valley, Arizona: U.S. Geological Survey Water-Resources Investigations Report 93-4196, 47 p.

Hanson, R.T., and Benedict, J.F., 1994, Simulation of ground-water flow and potential subsidence, upper Santa Cruz Basin, Arizona: U.S. Geological Survey Water-Resources Investigations Report 93-4196, 47 p.

Hanson, R.T., and Leake, S.A., 1998, Documentation for HYDMOD, A program for time-series data from the U.S. Geological Survey's modular three-dimensional finite-difference ground-water flow model: U.S. Geological Survey Water-Resources Investigations Report 98-564, 57 p.

Hanson, R.T., Li, Zhen., and Faunt, C. C., 2003, Application of the multi-node well package to the simulation of regional-aquifer systems in the Santa Clara Valley, California—MODFLOW and More 2003: Understanding through Modeling—Conference Proceedings, International Ground Water Modeling Center, Golden, Colorado, September 16–19, 2003, p. 74–78.

Hanson, R.T., Martin, P., and Koczot, K.M., 2002a, Simulation of ground-water/surface-water flow in the Santa Clara–Calleguas Basin, Ventura County, California: U.S. Geological Survey Water-Resources Investigations Report 02- 4136, 214 p.

Hanson, R.T., Newhouse, M.W., Wentworth, C.M., Williams, C.F., Noce, T.E., and Bennett, M.J., 2002b, Santa Clara Valley Water District multi-aquifer monitoring-well site, Coyote Creek Outdoor Classroom, San Jose, California: U.S. Geological Survey Open-File Report 02-369, 4 p.

Harbaugh, A.W., Banta, E.R., Hill, M.C., and Anderman, E.R., 2000a, MODFLOW-2000, the U.S. Geological Survey modular ground-water model-user guide to observation, sensitivity, and parameter-estimation processes and three post-processing programs: U.S. Geological Survey Open-File Report 00-184, 209 p.

Harbaugh, A.W., Banta, E.R., Hill, M.C., and McDonald, M.G., 2000b, MODFLOW-2000, the U.S. Geological Survey modular ground-water model—user guide to modularization concepts and the ground-water flow process: U.S. Geological Survey Open-File Report 00-92, 121 p.

Harbaugh, A.W., and McDonald M.G., 1996, User's documentation for MODFLOW-96, an update to the U.S. Geological Survey modular finite-difference ground-water flow model: U.S. Geological Survey Open-File Report 96-485, 56 p.

Helm, D.C., 1975, One-dimensional simulation of compaction near Pixley, California, 1. constant parameters: Water Resources Research, v. 11, no. 3, p. 465–478.

_____ 1977, Estimating parameters of compacting fine-grained interbeds within a confined aquifer system by a one-dimensional simulation of field observations: International Association of Hydrological Sciences, International Symposium on Land Subsidence, 2d, Anaheim, California, December 1976, Publication 121, p.145–156.

_____1978, Field verification of a one-dimensional mathematical model for transient compaction and expansion of a confined aquifer system, *in* Verification of mathematical and physical models of hydraulic engineering: American Society of Civil Engineers, Proceedings of Specialty Conference, College Park, Maryland, p. 189–195.

Hevesi, J.A., Flint, A.L., and Flint, L.E., 2002, Preliminary estimates of spatially distributed net infiltration and recharge for the Death Valley region, Nevada–California: U.S. Geological Survey Water-Resources Investigations Report 02-4010, 36 p.

Hitchcock, C.S., and Kelson, K.I., 1999, Growth of late Quaternary folds in southwest Santa Clara valley, San Francisco Bay area, California—Implications of triggered slip for seismic hazard and earthquake recurrence: Geology, v. 27, no. 5, p. 391–394.

Hitchcock, C.S., Kelson, K.I., and Thompson, S.C., 1994, Geomorphic investigations of deformation along the northeastern margin of the Santa Cruz Mountains: U.S. Geological Survey Open File Report 94-187, map scale 1:24,000.

Holzer, T.L., 1981, Preconsolidation stress of aquifer systems in areas of induced land subsidence: Water Resources Research, v. 17, no. 3, p. 693–704.

Hsieh, P.A., and Freckleton, J.R., 1993, Documentation of a computer program to simulate horizontal-flow barriers using the U.S. Geological Survey's modular three-dimensional finite- difference ground-water flow model: U.S. Geological Survey Open-File Report 92-477, 32 p.

Ireland, R.L., Poland, J.F., and Riley, F.S., 1984, Land subsidence in the San Joaquin Valley, California, as of 1980: U.S. Geological Survey Professional Paper 437-I, 93 p.

Iwamura, T.I., 1980, Saltwater intrusion in the Santa Clara County Baylands area, California: Santa Clara Valley Water District Report, 115 p.

_____ 1995, Hydrogeology of the Santa Clara and Coyote Valleys ground water basins, California, *in* Sangines, E.S., Anderson, D.A., and Busing, A.V., eds., Recent geologic studies of the San Francisco Bay area: Pacific Section of the Society of Economic Paleontologists and Mineralogists, v. 76, p. 173–192.

Izbicki, J.A., Christensen, A.H., and Hanson, R.T., 1999, U.S. Geological Survey combined well-bore flow and depth-dependent water sampler: U.S. Geological Survey Fact Sheet 196-99, 2 p.

Jachens, R.C., Wentworth, C.M., Gautier, D.L., and Pack, S., 2001, 3-D geologic maps and visualization—A new approach to the geology of the Santa Clara (Silicon) Valley, California: U.S. Geological Survey Open-File Report 01-223, 10 p.

Jachens, R.C., Wentworth, C.M., Graymer, R.W., McLaughlin, R.J., and Chuang, F.C., 2002, A 40-km-long concealed basin suggests large offset on the Silver Creek fault, Santa Clara Valley, California: Geological Society of America Abstracts with Programs, v. 34, no. 5, p. A99.

Jaimes, Luis, C., 1998, Groundwater elevation monitoring network, Santa Clara Valley groundwater basin: Santa Clara Valley Water District 1998, 35 p.

Jennings, C.W., 1985, An explanatory text to accompany the 1:750,000 scale fault and geologic maps of California: California Department of Conservation, Division of Mines and Geology, Bulletin 201, 197 p.

_____ 1994, Fault activity map of California and adjacent areas, with locations and ages of recent volcanic eruptions: California Department of Conservation, Division of Mines and Geology, Bulletin 201, 92 p.

Johnson, N.M., 1995a, Characterization of alluvial hydrostratigraphy with indicator semivariograms: Water Resources Research, v. 31, no. 12, p. 3217–3227.

_____ 1995b, Deterministic and stochastic approaches for evaluating multiple scales of Santa Clara Valley hydrostratigraphy, *in* Sangines, E.M., Anderson, D.W., and Buising, A.B., eds., 1995, Recent geologic studies in the San Francisco Bay area: Pacific Section of the Society of Economic Paleontologists and Mineralogists, v. 76, p. 193–208.

Johnson, N.M., and Dreiss, S.J., 1989, Hydrostratigraphic interpretation using indicator geostatistics: Water Resources Research, v. 25, no.12, p. 2501–2510.

Koltermann, C.E., and Gorelick, S.M., 1992, Paleoclimatic signature in terrestrial flood deposits: Science, v. 256, p. 1775–1781.

Knudsen, K.L., Sowers, J.M., Witter, R.C., Wentworth, C.M., Helley, E.J., Nicholson, R.S., Wright, H.M., and Brown, K.M., 2000, Preliminary maps of Quaternary deposits and liquefaction susceptibility, nine-county San Francisco Bay region, California— a digital database: U.S. Geological Survey Open File Report 00-444, version 1.

Leake, S.A., and Prudic, D.E., 1991, Documentation of a computer program to simulate aquifer-system compaction using the modular finite-difference ground-water flow model: U.S. Geological Survey Techniques of Water-Resources Investigations, book 6, chap. A2, 68 p.

Leighton, D.A., Fio, J.L., and Metzger, L.F., 1994, Database of well and areal data, South San Francisco Bay and Peninsula area, California: U.S. Geological Survey Water-Resources Investigations Report 94-4151, 47 p.

Majumdar, Hiren, Gomez, M.J., McGarry, T.L., and Haines, D.A., 1977, District groundwater recharge facilities: Santa Clara Valley Water District 1977, 110 p.

Mantua, N., and Steven H., 2002, The Pacific Decadal Oscillation: Journal of Oceanography, v. 58, no.1, p. 35–44.

McDonald, M. G., 1986, Development of a multi-aquifer well option for a modular groundwater flow model, *in* Khanbilvardi, R.M., and Fillos, J., eds., Groundwater hydrology, contamination, and remediation: Washington, D.C., Scientific Publications, p. 383–398.

McDonald, M.G., and Harbaugh, A.W., 1988, A modular three-dimensional finite-difference ground-water flow model: Techniques of Water-Resources Investigations of the U.S. Geological Survey, book 6, chap. A1, 586 p.

Metzger, L.F., 2002, Streamflow gains and losses along San Francisquito Creek and characterization of surface-water and ground-water quality, southern San Mateo and northern Santa Clara Counties, California, 1996–97: U.S. Geological Survey Water-Resources Investigations Report 02-4078, 49 p.

Muir, K.S., and Coplen, T.B., 1981, Tracing ground-water movement by using the stable isotopes of oxygen and hydrogen, upper Penitencia Creek alluvial fan, Santa Clara Valley, California: U.S. Geological Survey Water-Supply Paper 2075, 18 p.

Oliver, H.W., 1990, Preliminary ground-water-quality data and the extent of the ground-water basin from drill-hole, seismic, and gravity data in the Palo Alto 7.5' quadrangle, California: U.S. Geological Survey Open-File Report 90-74, maps at scale 1:24,000.

Page, B.E., 1993, Geologic map of the Stanford lands and vicinity: Stanford Geological Survey, Palo Alto, California, Stanford University.

Pampeyan, E.H., 1970, Geologic map of the Palo Alto 7-1/2-minute quadrangle, San Mateo and Santa Clara Counties, California: U.S. Geological Survey Open-File Map, scale 1:12,000.

_____ 1979, Preliminary map showing recency of faulting in coastal north-central California: U.S. Geological Survey Miscellaneous Field Studies Map MF-1070, scale 1:250,000.

_____ 1993, Geologic map of the Palo Alto and part of the Redwood Point 7-1/2' quadrangles, San Mateo and Santa Clara Counties, California: U.S. Geological Survey Miscellaneous Investigation Series Map I-2371, scale 1:24,000.

Poland, J.F., 1971, Land subsidence in the Santa Clara Valley, Alameda, San Mateo, and Santa Clara Counties, California: U.S. Geological Survey Open-File Report, Map Scale 1:125,000 [This precedes the time when open files were assigned numbers. Also released within jacket labeled "San Francisco Bay Region Environment and Resources Planning Study Technical Report 2."]

Poland, J.F., and Ireland, R.L., 1988, Land subsidence in the Santa Clara Valley, California, as of 1982: U.S. Geological Survey Professional Paper 497-F, 61 p.

Prudic, D.E., 1989, Documentation of a computer program to simulate stream-aquifer relations using a modular, finite-difference, ground-water flow model: U.S. Geological Survey Open-File Report 88-729, 113 p.

Reichard, E.G., and Bredehoeft, J.D., 1984, An engineering economic analysis of a program for artificial groundwater recharge: Water Resources Bulletin, v. 20, no. 6, p. 929–939.

Reichard, E.G., Land, M., Crawford, S.W., Johnson, T., Everett, R.R., Kulshan, T.V., Ponti, D.J., Halford, K.J., Johnson, T.A., Paybins, K.S., and Nishikawa, T., 2003, Geohydrology, geochemistry, and ground-water simulation-optimization of the central and west coast basins, Los Angeles County, California: U.S. Geological Survey Water-Resources Investigations Report 03-4065, 184 p.

Schmidt, D.A., 2002, The kinematics of faults in the San Francisco Bay area inferred from geodetic and seismic data: unpublished Ph.D. dissertation, University of California at Berkeley, 200 p.

Stamos, C. L., Martin, P., Nishikawa, T., and Cox, B.F., 2001, Simulation of ground-water flow in the Mojave River Basin, California: U.S. Geological Survey Water-Resources Investigations Report 01-4002, 129 p.

Stanley, R.G., Jachens, R.C., Lillis, P.G., McLaughlin, R.J., Kvenvolden, K.A., Hostettler, F.D., McDougall, K.A., and Magoon, L.B., 2002, Subsurface and petroleum geology of the southwestern Santa Clara Valley ("Silicon Valley"), California: U.S. Geological Survey Professional Paper 1663, 55 p.

Tolman, C.F., and Poland J.F., 1940, Ground-water, salt-water infiltration, and ground-surface recession in Santa Clara Valley, Santa Clara County, California: Transactions of the American Geophysical Union Fall Conference, 1940, p. 23–35.

U. S. Census Bureau, 2003, http://quickfacts.census.gov/qfd/states/06/06085.html, accessed July 8, 2003.

Wagner, D.L., Bortugno, K.J., and McJunkin, R.D., 1990, Geologic map of the San Francisco–San Jose quadrangle: California Department of Conservation, Division of Mines and Geology, Regional Geologic Map Series, Map No. 5A, 5 sheets.

Wentworth C.M., 1993, General distribution of geologic materials in the San Francisco Bay region, California— a digital map database: U.S. Geological Survey Open File Report 93-693, 10 p.

_____ 1997, General distribution of geologic materials in the San Francisco Bay region, California—a digital map database: U.S. Geological Survey Open-File Report 97-744.

Wentworth, C.M., Blake, M.C., Jr., McLaughlin, R.J., and Graymer, R.W., 1998, Preliminary geologic map of the San Jose 30 X 60-minute quadrangle, California— a digital database: U.S. Geological Survey Open-File Report 98-795.

Wentworth, C.M., Hanson, R.T., Jachens, R.C., Langenheim, V.E., McLaughlin, R.J., Phelps, Geoffrey, Simpson, R.W., Stanley, R.G., and Williams, R.A., 2003a, Varied evidence for a blind thrust beneath the southwestern Santa Clara (Silicon) Valley, California: Geological Society of America, National Conference Abstracts with Programs, November 2–5, Seattle, Washington, p. 74.

Wentworth, C.M., Hanson, R.T., Newhouse, Mark, Jachens, R.C., Mankinen, E.A., Phelps, Geoffrey, Tinsley, J.C., Williams, C.F., Williams, R.A., Andersen, D.W., and Metzger, E.P., 2003b, Stratigraphy and hydrogeology of the Santa Clara Valley, San Francisco Bay region, California—a progress report: American Association of Petroleum Geologists, Pacific Section, Conference Program and Abstracts, May 19–24, Long Beach, California, p. 94.

Williams, R.A., Stephenson, W.J., Wentworth, C.M., Odum, J.K., Hanson, R.T., and Jachens, R.C., 2002, Definition of the Silver Creek Fault and Evergreen Basin sediments from seismic reflection data, San Jose, California: Transactions of the American Geophysical Union Fall Conference, December 2002, v. 83, no. 47.

Wilson, A.M., 1993, Evaluation of pumping strategies for managing land subsidence in the Santa Clara Valley, California: unpublished Master's thesis for Department of Applied Earth Sciences, Palo Alto, California, Stanford University, 90 p.

Zimmerman, D.A., Hanson, R.T., and Davis, P.A., 1991, A comparison of parameter estimation and sensitivity analysis techniques and their impact on the uncertainty in ground water flow model predictions: U.S. Nuclear Regulatory Commission NUREG/CR-5522 (Sandia National Laboratories SAND90-0128) [variously paged].